Development of an In-line Near-Infrared Spectrometer and a Near-Infrared Imaging Device and Their Application to Pharmaceutical Analysis

A Thesis for the Degree

of

Doctor of Engineering

Submitted to

School of Science and Technology

Kwansei Gakuin University by

Kodai Murayama

in October 2017

Contents

List of Abbreviations

AD: analog to digital

AOTF: acousto-optic tunable filter

API: active pharmaceutical ingredient

AsA: ascorbic acid

DR: diffuse reflectance

D-NIRs: distributed near-infrared spectrometer

DIF: direct interface

FDA: food and drug administration

FIF: fiber interface

FOV: field of view

FT: Fourier transformation

HPMC: hydroxypropyl cellulose

IC: integrated circuit

ICH: international conference on harmonization of technical requirement

InGaAs: indium gallium arsenide

LV: latent variable

MCC: microcrystalline cellulose

Mg-St: stearic acid magnesium salt

Mid-IR: mid-infrared

NEP: noise equivalent power

NIR: near-infrared

PAT: process analytical technology

PCA: principal component analysis

PCMW: perturbation-correlation moving window

PLSR: partial least squares regression

PD: photodiode

PDA: photodiode array

P-NIRs: polychromator near-infrared spectrometer

QbD: quality by design

RMS: root mean square

RMSECV: root-mean-square-error of cross-validation

RMSEP: root means squared error of prediction

SD: standard deviation

SNR: signal to noise ratio

Tr: transmission

2DCOS: two-dimensional correlation spectroscopy

UV: ultraviolet

Vis: visible

General Introduction

In the production of a large number of pharmaceuticals, continuous quality assurance has become a major issue. In 2004, the US Food and Drug Administration (FDA) proposed the Process Analytical Technology (PAT) with the aim of improving the development efficiency, quality, and productivity of pharmaceutical products.[1] With this proposal, the introduction of systems/analyzers has advanced in the pharmaceutical manufacturing line. Figure 1 shows the conceptual diagram of PAT. In the PAT for pharmaceutical product manufacturing, clarifying the variable factors for the analysis and quality control of the manufacturing process, understanding the primary factors, and process improvement by feeding back the obtained results to the manufacturing process, are desired. For this purpose, an analyzer capable of real-time measurement is required.[1-5] Further, for providing high quality pharmaceutical products in a stable and efficient manner, the concept of QbD (Quality by Design) has attracted attention. In the "Pharmaceutical development guidelines Q8" (R2) presented by the International Conference on Harmonization of Technical requirement (ICH), QbD is defined as a systematic approach to development that begins with predefined objectives and emphasizes product and process understanding and process control, based on sound science and quality risk management. Based on these guidelines, introduction of

analyzers into the process lines is actively being studied.[6-7]

The in-line analysis tool is an essential technique to understand the formulation process and forms the core of PAT for implementing a new quality control system for pharmaceutical products. Since the in-line analysis tools can rapidly analyze without any impact on the manufacturing process, they have the advantage of obtaining a lot of high quality information for understanding the manufacturing process.[1-3] Spectroscopic techniques are one of the most effective methods of PAT in pharmaceutical processes.[2,4,8,9] Representative spectroscopic techniques for industrial process analysis are an ultraviolet-visible (UV-Vis) spectroscopy, mid-Infrared (mid-IR) spectroscopy, Raman spectroscopy and Near-Infrared (NIR) spectroscopy.[2] UV-Vis spectroscopy is effective for extracting qualitative and quantitative information regarding the contents of tablets.[10] Mid-IR spectroscopy, NIR spectroscopy and Raman spectroscopy are effective for API concentration analysis, detection of intramolecular and intermolecular interactions, and evaluation of physical and chemical characteristics. It is also effective for evaluation of pharmaceutical blends and granulation processes.[11-13] In particular, NIR spectroscopic analysis technology is promising as an in-line analysis tool and many studies and practical implementation are progressing. Because of NIR spectroscopy enables non-destructive, non-contact and rapid analysis

by a diffuse reflection method of pharmaceutical formulation. This feature is difficult to achieve with other spectroscopy. In addition, with the purpose of evaluating and analyzing the variations in component concentration distribution and non-uniformity of the final product or the target of the process, the developments in imaging devices are progressing.[8,9] In particular, the NIR imaging device has become an important tool for understanding the quality characteristics defined in the QbD approach.[14-17]

NIR spectroscopy is one of the analytical methods capable of rapid analysis using light in the wavelength range of 800 to 2500 nm. There are four main characteristics of NIR spectroscopy. First is to be able to observe the absorption spectrum derived from the fundamental vibration overtones and combination modes of the molecular vibrations of the functional groups (O-H, C-H, N-H) that contain hydrogen atoms. In addition, on the short wavelength region of NIR, absorption spectrum of electronic transition of molecules is observed. Second is to be able to analyze without choosing the state of the sample, namely solid, liquid or gas. The third is to be able to perform non-destructive analysis without requiring pretreatment of the sample. In particular, the state of the pharmaceutical sample is often the state of the powder. Therefore, NIR spectroscopy can be analyzed by using diffuse reflection method, which is advantageous for non-destructive measurement of powder. The diffuse reflection method is one of

reflection methods. The diffuse reflection method is a method of measuring reflected light that has been absorbed by repeating reflection, refraction transmission, scattering, etc. of NIR light inside the sample and then again outside the sample. The fourth is to be able to perform contactless remote analysis using glass or optical fibers.[8,18]

Some of the representative spectroscopic methods of the NIR spectroscopic device are the Fourier transformation (FT) method, monochromator method, laser scan method, polychromator method and so on. Table 1 shows the features of each spectroscopic method. In the FT method, the spectrum is measured by Fourier transform of the optical interference signal obtained by moving in parallel a reflecting element such as a mirror and continuously changing the optical path length with the reference light.[19] By providing a wavelength reference mechanism inside the spectroscopic device, long wavelength measurement accuracy can be achieved. Further, in principle, it has the superiority of optical throughput. However, since it has a movable mechanism of the optical element, there are a few demerits such as long measurement time and susceptibility to vibrations, but in recent years, it is widely being used in the field of spectroscopic analysis. In the monochromator method, spectra are obtained by filtering specific wavelengths using diffraction gratings or acousto-optic elements.[20] In the monochromator method, wavelength scanning is performed by changing the angle of

the diffraction grating or the ultrasonic frequency of the acousto-optic device. Due to the high filtering effect of diffraction grating, high dynamic range and high wavelength resolution can be achieved. However, since specific wavelengths are cut out and measured, there are demerits such as long measuring time, large size, and susceptibility to vibrations. Laser scanning type (wavelength scanning type) is a method in which the light intensity from the sample is measured while scanning the wavelength of the irradiating light.[21] Since laser light is used, high wavelength resolution and high dynamic range characteristics can be easily obtained. On the other hand, since the measurement wavelength range is limited by the oscillation range of the laser, it is expensive, as it needs many laser light sources for measuring a wide-band. In polychromator method, wavelength dispersion of NIR light is carried out using diffraction grating or the like and the spectral region is simultaneously detected by a multi-channel detector. Since polychromator method has high light utilization efficiency and it can be configured without mechanically movable parts, it has features such as high resistance to vibration and easy miniaturization.[21] However, it is not as easy for the number of channels in the detector to increase the wavelength resolution compared to the other methods in order to determine the wavelength resolution.[21,22]

Since the in-line analysis of the formulation process is often in bulk such as powder,

the spectroscopic method should be capable of detecting diffuse reflected light. Further, since the manufacturing process must be monitored in real time, functions such as high speed, compactness, and maintainability are required.[2] From this point of view, if in-line NIR spectrometer take into consideration the contents of the features in Table 1, the polychromator type that has no mechanical driving part, can be considered suitable.[2,21] However, as described above, polychromator type spectroscopic device has the problem of low wavelength resolution.

In this paper, in order to realize a high-sensitivity Photo Diode Array (PDA), it was developed a world-class high-density 640-element PDA detector and a charge amplifier Integrated Circuit (IC). Using the PDA sensor that combines the high-density PDA and high-sensitivity IC, a polychromator type NIR spectrometer was developed that has high-speed and high wavelength resolution characteristics.[23] Since this polychromator-type NIR spectrometer possesses a high speed that can acquire a weak diffuse reflection spectrum in 10 msec or less, and a high wavelength resolution of 1.25 nm or less, it can achieve all the functions of an in-line analysis tool. Figure 2 shows the developed in-line NIR spectrometer. Figure 2 (a) shows the fiber interface type NIR spectrometer, Figure 2 (b) shows the diffuse reflectance optical fiber probe, and Figure

2 (c) shows the spectro-engine of polychromator type NIR spectrometer. The fiber interface type NIR spectrometer is used with the diffuse reflectance optical fiber probe. Further, by combining the polychromator type NIR spectrometer and the mirror scanning optical system, a portable NIR imaging device was developed that can be used onsite. Figure 3 shows the developed portable NIR imaging device and the in-line NIR spectrometer. The portable NIR imaging device is used by connecting the in-line NIR spectrometer with optical fiber. The conventional NIR imaging devices are a microscope-type FT-NIR imaging device with motorized XY stage.[14] Although the conventional NIR imaging device based on FT-NIR is excellent sensitivity and wavelength resolution, it has a problem of large size and slow measurement speed. However, the developed portable NIR imaging device is 18 cm × 20 cm × 22 cm in size, approximately 2 kg in weight and small enough to carry with one hand.[24-26] In addition, the portable NIR imaging device can acquire NIR imaging data composed of 10000 NIR spectra in approximately 15 minutes and has high speed of tenth times or more compared with the conventional FT-NIR type NIR imaging devices. Figure 4 shows the diagram of the function necessary for NIR imaging devices. Our portable NIR imaging device succeeded in offering the totally new function of portability to NIR imaging device. Using this in-line NIR spectrometer and NIR imaging device, the in-line

monitoring of the pharmaceutical product manufacturing process, tablet penetration analysis, and homogeneity of mixed samples and tablets were investigated.[23-28]

In Chapter 1, in order to realize a compact, high resolution, high sensitivity, high speed polychromator type NIR spectrometer (P-NIRs), the world-class high-density and high-sensitivity array detector was developed.[23] As P-NIRs use the newly developed 640-element PDA detector, they show an improved wavelength resolution and high sensitivity. Since the existing NIR spectrometers have PDA detectors having up to 512 elements, their maximum wavelength resolution is 1.56 nm. However, the newly developed PDA detector has made it possible to reach a wavelength resolution of 1.25 nm or less. Further, by using the PDA detector in conjunction with the newly developed charge amplifier array, measurement time has been shortened to about one 100th (from 1 sec to less than 10 msec). A high-performance prototype model was developed through mechanical investigation and prototyping of the remote DR detection mechanism necessary for the in-line monitoring of pharmaceutical processes, introduction of high-speed data processing, and addition of functions such as wireless interfaces. And a high-speed NIR spectrometer was developed for in-line use and validated its performance. In PAT, since the timely quality parameters and functional

properties of pharmaceutical products have to be monitored during the manufacturing process, high-speed P-NIRs are the extremely suitable NIR spectroscopes. Furthermore, due to its small size, it can be very easily installed in various pharmaceutical process lines. By measuring the DR-NIR spectra of D-mannitol and talc powders, P-NIRs were confirmed the achievement of high speed, high sensitivity, and high resolution. Further, P-NIRs was succeeded in the in-line monitoring of the mixed state of the powder samples using P-NIRs.

In Chapter 2, the feasibility of analysis of API inside the bi-layer tablets was investigated on the millisecond timescale using NIR spectroscopy.[27] In this experiment, the newly developed P-NIRs that can enable rapid spectral measurement of tablets were used. In the transmission measurement of tablets, since the transmitted light is extremely weak, measurement is difficult. However, since the NIR spectra of bi-layer tablets gave DR- and Tr-NIR spectra at 500 and 400 msec respectively. Comparison of the NIR spectrum with its second derivative showed that NIR spectrum was specific and selective with respect to the variations in ascorbic acid (AsA) concentration. Verification results and regression vectors demonstrated that the PLSR model enables the estimation of AsA concentration in bi-layer tablets. It was confirmed that the Tr-NIR

method was quite robust with respect to the orientation of the tablet. Therefore, this study is one-step towards the realization of real-time release test as it enables the transmission measurement of bi-layer tablets in less than a second.

In Chapter 3, the application of new portable NIR imaging device (D-NIR) in the dissolution process of tablets for the needs of PAT and/or QbD is reported.[25] In the conventional NIR imaging devices, since the NIR imaging is acquired while operating the sample, there are limitations on the speed and device size in acquiring the solubility of the tablet. However, since D-NIRs have high speed as well as portability, they are suitable for visualizing the dissolution process of the tablets that change moment by moment. The NIR spectra were measured in the 1000 to 1600 nm region of the model sample tablet containing 20 wt% of AsA and 80 wt% of HPMC as API during the dissolution process for up to 300 minutes. In the second derivative spectrum of the sample tablet, the 1361 nm band could be clearly identified as the unique band of AsA. As expected, the color contrast in the tablet dissolution image had changed before the start and this result was significantly enhanced by using the peak height ratio based images. The understanding of the tablet dissolution process, such as the degree of penetration of water into the tablet, can be improved by NIR imaging. The results

obtained in this study demonstrate that NIR imaging that uses the spectral variations such as band intensity variation and peak-height ratio variation at 1361 nm is a powerful tool for the evaluation of the tablet dissolution process.

In Chapter 4, a new version of the NIR imaging device shown in Chapter 3 was developed.[26] The new version achieved a high signal-to-noise ratio and high speed. The SNR of the new version is 10 times that of the old version and the measurement speed of the new version has improved to 7 times the old version. By using the new version, the blending monitoring was performed the in-line evaluation of the heterogeneity during the blending process and succeeded in determining the endpoint of homogeneous mixing. To evaluate the uniformity of mixed samples using the NIR imaging device, offline analysis at the laboratory was common. However, with the new version of NIR imaging device, it has become possible to perform at-line analysis at the site of the mixing process. In this experiment, using an in-line NIR spectrometer, continuous monitoring of the mixing process and NIR imaging spectra of the mixed samples were measured at different times. NIR imaging revealed that the AsA distribution in the blended sample varies over time. It was confirmed that a mixing time of 8 minutes was sufficient for homogeneous mixing. This study demonstrated that NIR imaging is

extremely useful for the further understanding of the results of in-line monitoring of the blending process.

In Chapter 5, in order to facilitate the development of probe design and in-line type NIR spectrometer, an optical fiber switching system was developed that can switch between spot size variable type DR probe and NIR imaging device (D-NIRs).[28] As an in-line analytical tool, the optimal design of a diffuse reflective probe is important in determining the spectral quality. However, the diffuse reflective probes are not designed considering the in-plane variations of powder samples. This switching system can acquire DR spectrum and NIR imaging data with one polychromator type NIR spectrometer (P-NIRs). Therefore, it was possible to evaluate the dispersibility and uniformity of the sample by NIR imaging and the quality of the spectral data obtained by DR probe. A model tablet containing 0 to 10% AsA was prepared as API and NIR spectrum in the 950 to 1700 nm region was measured using P-NIRs. The optical switching system provided with D-NIRs and P-NIRs was able to collect the DR spectrum and NIR imaging data rapidly, accurately, and automatically using the optical fiber-type switching module of the rotary mechanical parts. The NIR spectra of the model tablet samples were measured using spot sizes for the DR probe of ⌀1 and ⌀5

mm. The predicted concentration value of AsA was more accurate for ⌀5 mm than ⌀1 mm. In addition, the optimal spot size using NIR imaging data was estimated to be ⌀5 mm to ⌀7 mm. Therefore, the possibility of selecting a more suitable optical fiber probe by using a system that can switch between single point measurement type optical fiber probe and NIR imaging measurement is suggested.

In this paper, developed a high speed, highly sensitive in-line NIR spectrometer and portable NIR imaging device were clarified that the visualization of pharmaceutical manufacturing process can be realized. These results suggest that the in-line NIR spectrometer and NIR imaging device developed for the quality control of pharmaceutical manufacturing process are useful analysis tools. The developed in-line NIR spectrometer and NIR imaging device are expected to be applied to chemical processes, paper production processes, film production processes, food production processes, agriculture, and healthcare in addition to pharmaceutical manufacturing processes. Furthermore, the developed high-density, high-sensitivity PDA detector can be expected to be applied to other spectroscopic methods (for example, application to Raman spectroscopy apparatus).

References

1. U.S. Food Drug AdministrationDA, *Guidance for Industry, PAT: A Framework for Innovative Pharmaceutical Development, Manufacturing, and Quality Assurance* (U.S. Food and Drug Administration, Maryland, 2004).
2. Bakeev, K. A. (Ed.). (2010). Process analytical technology: spectroscopic tools and implementation strategies for the chemical and pharmaceutical industries. *John Wiley & Sons.*, p.13-38.
3. Cogdill, R. P., Knight, T. P., Anderson, C. A., & Drennen, J. K. (2007). The financial returns on investments in process analytical technology and lean manufacturing: benchmarks and case study. *Journal of Pharmaceutical Innovation*, 2(1-2), 38-50.
4. Workman Jr, J. (1995). A review of process near infrared spectroscopy: 1980–1994. *Journal of near infrared spectroscopy*, 1(4), 221-245.
5. Scott, B., & Wilcock, A. (2006). Process analytical technology in the pharmaceutical industry: a toolkit for continuous improvement. *PDA journal of pharmaceutical science and technology*, 60(1), 17-53.
6. International Conference on Harmonisation of Technical Requirements for Registration of Pharmaceuticals for Human Use, *ICH Harmonised Tripartite Guideline, Pharmaceutical Development Q8(R2)*, 2009.

7. Kourti, T., & Davis, B. (2012). The business benefits of quality by design (QbD). *Pharm Eng*, 32(4), 1-10.

8. Y. Ozaki and T. Amari. (2000): Near-Infrared Spectroscopy in Chemical Process Analysis. *Sheffield Academic Press*, p.53-92.

9. Hassell, D. C., & Bowman, E. M. (1998). Process analytical chemistry for spectroscopists. *Applied Spectroscopy*, 52(1), 18A-29A.

10. Behera, S., Ghanty, S., Ahmad, F., Santra, S., & Banerjee, S. (2012). UV-visible spectrophotometric method development and validation of assay of paracetamol tablet formulation. *Journal Analytical and Bioanalalytical Techniques*, 3(6), 2-6.

11. Wartewig, S., & Neubert, R. H. (2005). Pharmaceutical applications of Mid-IR and Raman spectroscopy. *Advanced drug delivery reviews*, 57(8), 1144-1170.

12. T.R.M De Beer, C. Bodsonb, B. Dejaegher, B. Walczak, P. Vercruyssea, A. Burggraevea, A. Lemos, L. Delattre, Y. Vander Heyden, J.P. Remone, C. Vervaet, W.R.G. Baeyens (2008). Raman spectroscopy as a process analytical technology (PAT) tool for the in-line monitoring and understanding of a powder blending process. *Journal of pharmaceutical and biomedical analysis*, 48(3), 772-779.

13. Vergote, G. J., De Beer, T. R. M., Vervaet, C., Remon, J. P., Baeyens, W. R. G., Diericx, N., & Verpoort, F. (2004). In-line monitoring of a pharmaceutical blending

process using FT-Raman spectroscopy. *European Journal of Pharmaceutical Sciences*, 21(4), 479-485.

14. Šašić, S., & Ozaki, Y. (Eds.). (2011). Raman, infrared, and near-infrared chemical imaging. *John Wiley & Sons*.
15. Reich, G. (2005). Near-infrared spectroscopy and imaging: basic principles and pharmaceutical applications. *Advanced drug delivery reviews*, 57(8), 1109-1143.
16. Awa, K., Okumura, T., Shinzawa, H., Otsuka, M., & Ozaki, Y. (2008). Self-modeling curve resolution (SMCR) analysis of near-infrared (NIR) imaging data of pharmaceutical tablets. *analytica chimica acta*, 619(1), 81-86.
17. Shinzawa, H., Awa, K., & Ozaki, Y. (2012). Compression effect on sustained-release and water absorption properties of cellulose tablets studied by heterospectral two-dimensional (2D) correlation analysis. *Analytical Methods*, 4(6), 1530-1537.
18. Threlfall, T. L. & Chalmers, J. M. (Eds.). (2002) Handbook of Vibrational Spectroscopy, vol. 5. *John Wiley & Sons.*, p.423–435.
19. Andrews, D. L. (Ed.). (2009) Encyclopedia of Applied Spectroscopy, *John Wiley & Sons.*, p.872-886.
20. Threlfall, T. L. & Chalmers, J. M. (Eds.). (2002) Handbook of Vibrational

Spectroscopy, vol. 1. *John Wiley & Sons.*, p.383–392.

21. Threlfall, T. L. & Chalmers, J. M. (Eds.). (2002) Handbook of Vibrational Spectroscopy, vol. 1. *John Wiley & Sons.*, p.393–417.

22. Ozaki, Y. (2012). Near-infrared spectroscopy—its versatility in analytical chemistry. *Analytical Sciences*, 28(6), 545-563.

23. Murayama, K., Genkawa, T., Ishikawa, D., Komiyama, M., & Ozaki, Y. (2013). A polychromator-type near-infrared spectrometer with a high-sensitivity and high-resolution photodiode array detector for pharmaceutical process monitoring on the millisecond time scale. *Review of Scientific Instruments*, 84(2), 023104.

24. Ishikawa, D., Shinzawa, H., Genkawa, T., Kazarian, S. G., & Ozaki, Y. (2014). Recent Progress of Near-Infrared (NIR) Imaging—Development of Novel Instruments and Their Applicability for Practical Situations—. *Analytical Sciences*, 30(1), 143-150.

25. Ishikawa, D., Murayama, K., Awa, K., Genkawa, T., Komiyama, M., Kazarian, S. G., & Ozaki, Y. (2013). Application of a newly developed portable NIR imaging device to monitor the dissolution process of tablets. *Analytical and bioanalytical chemistry*, 405(29), 9401-9409.

26. Murayama, K., Ishikawa, D., Genkawa, T., Sugino, H., Komiyama, M., & Ozaki, Y.

(2015). Image Monitoring of Pharmaceutical Blending Processes and the Determination of an End Point by Using a Portable Near-Infrared Imaging Device Based on a Polychromator-Type Near-Infrared Spectrometer with a High-speed and High-Resolution Photo Diode Array Detector. *Molecules*, 20(3), 4007-4019.

27. Ishikawa, D., Genkawa, T., Murayama, K., Komiyama, M., & Ozaki, Y. (2014). Feasibility study of diffuse reflectance and transmittance near infrared spectroscopy for rapid analysis of ascorbic acid concentration in bilayer tablets using a high-speed polychromator-type spectrometer. *Journal of Near Infrared Spectroscopy*, 22(3), 189-198.
28. Murayama, K., Ishikawa, D., Genkawa, T., & Ozaki, Y. (2017). An application for the quantitative analysis of pharmaceutical tablets using a rapid switching system between a near-infrared spectrometer and a portable near-infrared imaging system equipped with fiber optics. to submitted *Applied Spectroscopy*

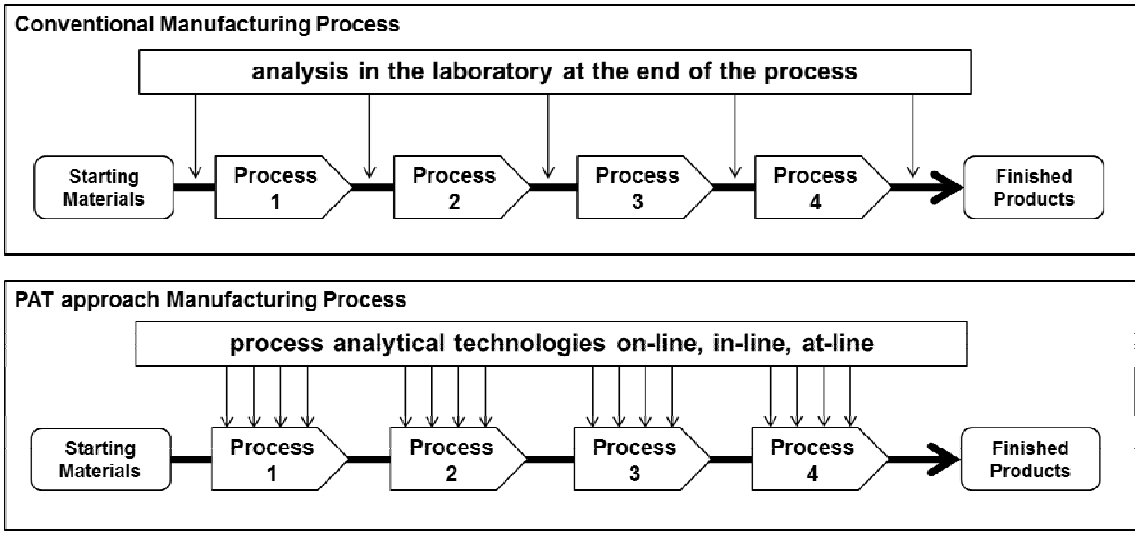

Figure 1 Diagram of conventional and PAT approach manufacturing process

Table 1　Table of the features of each spectroscopic method

	Fourier-transform	Poly-chromator	Mono-chromator	AOTF	Laser-scan
Scan speed	△	◎	△	○	◎
Spectral range	◎	○	◎	○	×
Spectral accuracy	◎	○	○	○	○
Spectral resolution	◎	△(○)	◎	△	◎◎
Signal dynamic-range	○～△	○	◎	○～△	◎
Device dimension	○～△	◎	△	○	◎
Optical efficiency	◎	◎	△	×	◎
Robustness	△	◎	△	◎	◎

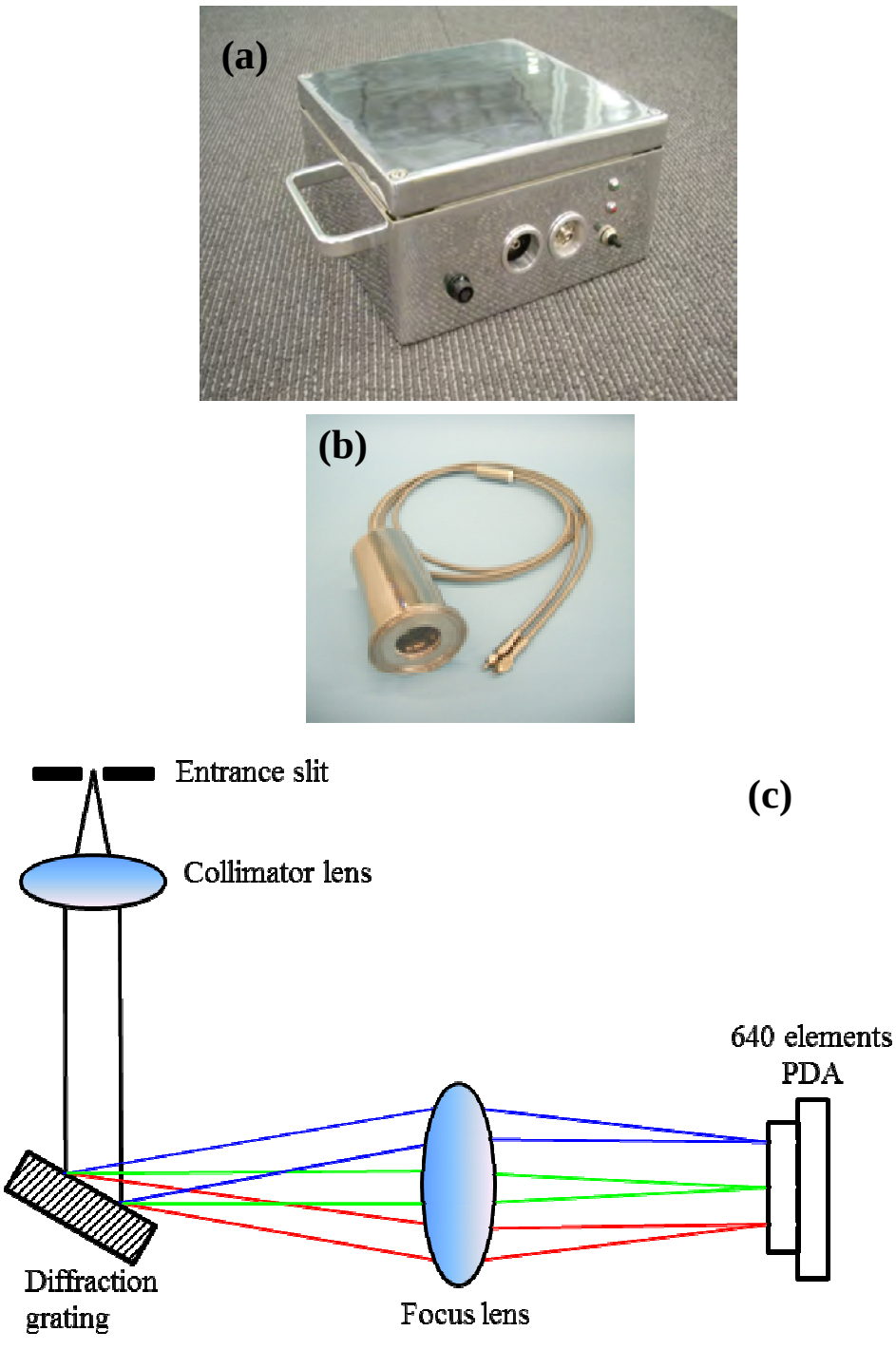

Figure 2 (a) In-line type NIR spectrometer, (b) diffuse reflectance optical fiber probe and (c) spectro-engine of P-NIRs

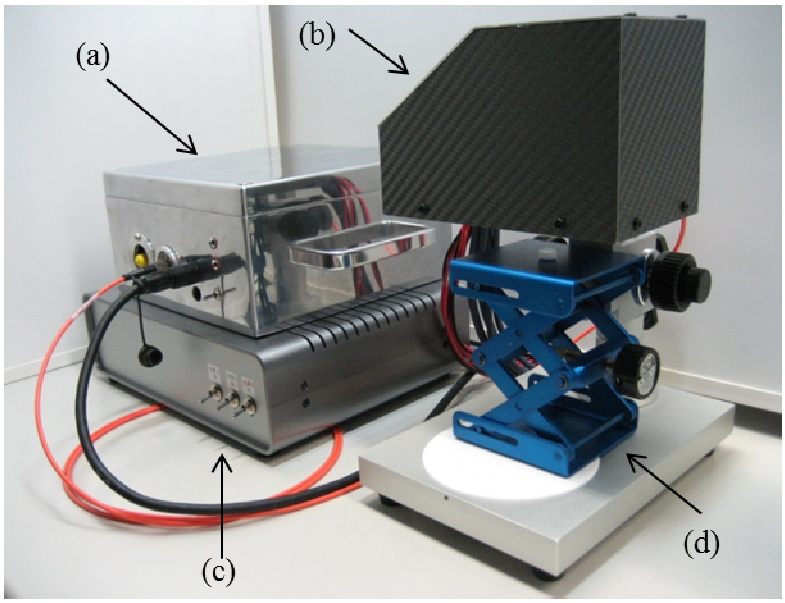

Figure 3 Portable NIR imaging device and in-line NIR spectrometer: (a) in-line type NIR spectrometer, (b) portable NIR imaging device, (c) control box for NIR imaging device and (d) sample stage

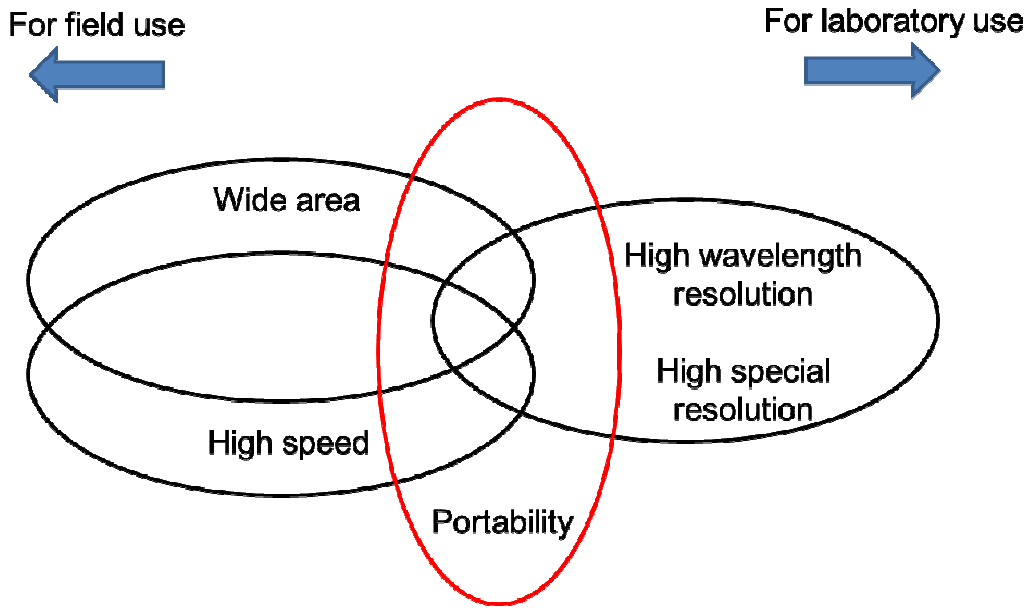

Figure 4　The diagram of the function necessary to NIR imaging devices

Chapter 1

A Polychromator-Type Near-Infrared Spectrometer with a High-Sensitivity and High-Resolution Photodiode Array Detector for Pharmaceutical Process Monitoring on the Millisecond Time Scale

Abstract

In the fine chemicals industry, particularly in the pharmaceutical industry, advanced sensing technologies have recently begun being incorporated into the process line in order to improve safety and quality in accordance with PAT. For estimating the quality of powders without preparation during drug formulation, near-infrared (NIR) spectroscopy has been considered the most promising sensing approach. In this study, a compact polychromator-type NIR spectrometer equipped with a photodiode (PD) array detector was developed. This detector is consisting of 640 InGaAs-PD elements with 20 μm pitch. Some high-specification spectrometers which use InGaAs-PD with 512 elements have a wavelength resolution of about 1.56 nm when covering 900–1700 nm range. On the other hand, the newly developed detector, having the PD with one of the world's highest density, enables wavelength resolution of below 1.25 nm. Moreover, thanks to the combination with a highly-integrated charge amplifier array circuit, measurement speed of the detector is higher by two orders than that of existing PD array detectors. The developed spectrometer is small (120 mm × 220 mm × 200 mm) and light (6 kg), and it contains various key devices including the high-density and high-sensitivity PD array detector, NIR technology and spectroscopy technology for a spectroscopic analyzer that has the required detection mechanism and high sensitivity for powder measurement, as

well as a high-speed measuring function for blenders. Moreover, the characteristics of the developed NIR spectrometer were evaluated, and the measurement of powder samples confirmed that it has high functionality.

1. Introduction

In the pharmaceutical industry, at a worldwide level, the development and approval of new drugs is increasingly being governed by common regulations. In this scenario, there has emerged the need for a quality assurance method with a strong scientific basis. To satisfy this need, the U. S. Food and Drug Administration proposed process analytical technology (PAT) for the design, analysis, and control of pharmaceutical manufacturing processes through the timely measurement of the critical process parameters that affect the final product quality. This technique is expected to replace conventional validation techniques and realize improved manufacturing efficiency and quality control of pharmaceuticals.[1–4]

PAT is used to analyze the manufacturing process, determine the factors essential for understanding the manufacturing process, and clarify variable factors that affect quality control. At the same time, it is important to improve the manufacturing process based on the results of PAT. From these viewpoint, real-time measurement is essential. Toward this end, spectroscopy, in particular, near-infrared (NIR) spectroscopy, has attracted considerable interest because it affords several advantages such as noncontact and nondestructive measurements and availability of remote detection by optical fiber.[5–10]

The Fourier transform method is widely used in NIR spectrometers; this method

obtains the spectrum by the Fourier transform of interference signal data acquired while changing the optical path length.[7] It needs a wavelength standard, and therefore, it has very high wavelength accuracy. Moreover, in principle, it has superior optical throughput. Finally, various improvements have recently been made to the drive mechanism of the variable optical length, data processing, and so on. The monochromator-type spectroscopic method is also widely used in NIR spectrometers; this method is a wavelength dispersion method.[8] In this method, the wavelength is continuously swept by changing the angle of the diffraction grating. The advantages of this method are the high dynamic range and high wavelength resolution. However, it does have some disadvantages, such as the long measurement time, large size, and lack of robustness owing to the wavelength being swept mechanically. The laser-scanning-type method is used to sweep the emission wavelength by varying the current or the external cavity. Although the measurement wavelength area is limited to the range of laser emission, this method has advantageous features such as high dynamic range and high wavelength resolution. In this method, multiple lasers with different emission wavelength regions are required to cover the measured NIR wavelength region. The method which uses a polychromator employs a spatial wavelength dispersion device, and it enables detection over a wavelength region by using a multichannel detector. Unlike in the

monochromator-type method, this method simultaneously detects multiple beams over a wavelength region. The number of channels in the multichannel detector determines the wavelength resolution. This method has advantageous features such as high-speed measurement, robustness, and compactness owing to the non-mechanical moving architecture.[9]

These methods involve specific advantages and disadvantages, and it is necessary to select one that is most suitable for use as an in-line analyzer. Generally speaking, this PAT application requires features such as high-speed measurement, compact size, and maintainability (if possible, maintenance-free). The polychromator-type method provides these features; however, its wavelength resolution is inferior to that of other methods. If the wavelength resolution of this method could be improved, it would become the best method for in-line spectroscopy. To improve the wavelength resolution of this method, it is necessary to increase the pixel number of the photodiode array (PDA);[10] the pixel number of PDA also determines the PDA device size. The spectrometer size increases in proportional to the PDA device size. In other words, both wavelength resolution improvement and device miniaturization can be achieved by increasing the pixel number and density of PDA.

In the present study, we have developed a new PDA detector that combines a

high-density array with a charge-amplifier-array-type integrated circuit (IC). It holds PDA with one of the world's highest density (20-μm pitch) and unusual high speed (~10 ms). This novel detector has allowed us to improve the wavelength resolution and detection sensitivity of the polychromator-type NIR spectrometer (P-NIRs). We have designed a new P-NIRs using this PDA as well as an improved optical probe to improve the sensitivity. The wavelength resolution and sensitivity of the P-NIRs were evaluated through the measurement of a powder sample, and its applicability to an in-line monitoring process was examined through the measurement of a powder mixture process.

2. Development of High-density and High-sensitivity PDA Detector

2.1 High-density PDA

The detector consists of a high-density PDA containing 640 elements with 20μm pitch. InGaAs photodiodes with a wavelength sensitivity of 900–1700 nm (photoreceptive sensitivity: 0.8 at 1550 nm) are used. The wavelength resolution of the NIR spectrometer which uses the new PDA with 640 elements is 60% higher than that of a conventional high-specification NIR spectrometer that has a PDA with 256 elements. If a measurement wavelength region is 900–1700 nm, the wavelength resolution is 3.1 nm for a spectrometer with a PDA having 256 elements while it is 1.25

nm for that with the 640 elements. Figure 1-1 shows a diagram of a part of the newly developed PDA. This is a PN-junction-type PDA. The substrate structure of the photodiode is formed by growing an InGaAs optical absorption layer on an InP-based substrate by epitaxial growth and then growing an InP cap layer on the InGaAs optical absorption layer. Moreover, an InP buffer layer is formed between the InP substrate and the InGaAs photoabsorption layer. An SiO_2 mask pattern is formed in order to form the 640-element PDA with 20 μm pitch and 10 μm photoreceptive width on the substrate. Zn is diffused into the obtained substrate to form a high-density PN-junction-type PDA. The PDA converts the energy of incident light into a photocurrent. The photocurrent is output to the outside with a metallic pad. The PDA may suffer from fluctuations in the current output owing to light energy entering between two adjacent PDs. To prevent these fluctuations and to improve sensitivity, an optical cover material was placed between adjacent PDs.[11-13] Figure 1-1 shows a chart of the electrode pattern of the PDA. The 640 elements in the PDA are divided into two sets of 320 elements based on whether the pixel number is even or odd. Moreover, the bonding pads are arranged in a staggered manner with a two-step arrangement. In this manner, the array density could be increased.

2.2 Charge Amplifier Array Silicon Integrated Circuit

A charge-amplifier-array-type Si-IC that amplifies the photocurrent converted by the 640-element PDA was also newly developed. Figure 1-2 shows a block diagram of the charge-amplifier-array-type Si-IC. It consists of a 320-element charge amplifier array that is highly integrated to match with a PDA with world top class density, a sample hold circuit, a shift register circuit, and a timing generator circuit. A photocurrent from the photodiodes charges the integral capacitor, and the electric charge is converted into a voltage by the charge amplifier. The output voltage can be calculated by Eq. (1).

$$V_s = \frac{(I_s + I_d) \cdot T_c}{C_f} \qquad (1)$$

where, V_s [V], I_s [A], I_d [A], T_c [s], and C_f [F] indicate the output voltage, signal current, dark current, charge time, and integral capacitance, respectively.

The charge amplifier can maintain a high dynamic range by having, and selecting two integral capacitors (that have value of 0.5 pF and 10 pF). All elements of the charge amplifier array work completely at the same time by the clock synchronous method that is controlled by the timing generator circuit. The charge time is controlled based on the external input pulse width. The signal of each element after charging was completed is held by the sample hold circuit, following which each signal is read one-by-one by the

shift register circuit at high speed. The bonding pad arrangement of the charge-amplifier-array type Si-IC is the same as that of the PDA.

Existing PDAs individually acquire the photocurrent signal converted by each element by using an external amplifier, and therefore, they require a measurement time of sub-seconds to detect the signal level. In contrast, the newly developed PDA acquires the photocurrent signal converted by each element simultaneously using the charge-amplifier-array-type Si-IC, and therefore, it requires a measurement time of less than 10 ms.

2.3 Photodiode Array Detector

Figure 1-3 shows the newly developed photodiode array sensor. An AlN substrate was selected owing to its good heat conduction and other features. At its center, it contains 640 InGaAs photodiode elements with 20-μm pitch, which we believe to be the highest density reported thus far in the world, on both sides of the substrate, and the newly developed charge-amplifier-array-type Si-IC is mounted on top of this. The substrate is mounted on a ceramic package via a thermoelectric cooler and is sealed with a cap with a sapphire window after filling with N_2.

To evaluate the sensitivity and speed of the PDA, the noise characteristics were

evaluated. The light receiving surface was shaded, and 100 measurements were carried out with an operation temperature of 25 °C, charge time of 10 ms, and integral capacitance of 0.5 pF. The root mean square noise voltage (V_{rms}) of each pixel was calculated from the measured data, and the root mean square noise current (I_{rms}) of each pixel was calculated by Eq. (1). Figure 1-4 shows a plot of the root mean square noise current of each pixel. The root mean square noise current of each pixel in the PDA was less than 0.03 pA. Moreover, the noise equivalent power (NEP) was calculated by Eq. (2).

$$\mathrm{NEP} = \frac{I_{rms}}{S} \qquad (2)$$

where, the photoreceptive sensitivity S is 0.8 A/W at 1550 nm. In all pixels, NEP was less than 0.0375 pW, demonstrating that the newly developed PDA can detect even a feeble light.

3. Design of NIR Spectrometer

3.1 Development of Polychromator-type NIR Spectrometer

In the present study, we developed two types of P-NIRs: one with an optical fiber interface (FIF) model with a diffuse reflectance (DR) optical fiber probe for remote measurement, and the other with a direct interface (DIF) model with a built-in DR optical fiber probe. Figures 1-5 and 1-6 show the FIF and DIF, respectively. Both

P-NIRs consists of a polychromator equipped with a PDA detector, an internal optical source (halogen lamp, power consumption 5 W), an 18-bit analog to digital (AD) convertor for signal conversion and CPU, a data interface, a power supply (battery and external source), and a DR optical fiber probe. The optical fiber for irradiating light is connected with a built-in optical source, and the optical fiber for receiving light diffuse-reflected from a sample is connected with the spectrometer. Figure 1-7 shows a schematic diagram of the P-NIRs spectroscopy system, and Table 1-1 summarises the specifications of this system. A halogen lamp is used to irradiate the samples with NIR light through the optical fiber. The optical fiber comprises a bundle of ~100 optical fibers with a core diameter of 190 μm. The DR light enters the spectrometer through the optical fiber, and it is dispersed by the diffraction grating device. The dispersed light is irradiated on the PDA by a condensing lens. The PDA output is converted by the 18-bit AD converter and the CPU carries out calculation processes such as the averaging on it. Thereafter, the data sent to a control computer as spectrum data.

The targeted measurement performance of the P-NIRs is inspection of the process line in 10 ms. Toward this end, the P-NIRs employs a high-speed AD converter (1×10^6 samples/s), a digital signal processor, and parallel processing of data. Separately, the P-NIRs has functions such as the wireless data interface, battery operation, and external

synchronous sampling of data. The P-NIRs is controlled by a control computer through a serial or a wireless communication protocol. The P-NIRs receives instructions (control commands) from the control computer, and executes the spectral measurement, process data, and transfer data. The absorption spectrum is displayed and saved on the control computer.

3.2 Spectro-engine of P-NIRs

Figure 1-8 shows the spectro-engine of P-NIRs. The light diffuse reflected from a sample is collimated by the collimator lens, and collimated light enters the diffraction grating. The light is diffracted into beams of each wavelength. The light is focused onto the pixels of the PDA by using a focusing lens in conjunction with a mirror. The intensity of the beams of each wavelength is detected by the PDA, and the spectral data are obtained through signal processing.

3.3 Diffuse Reflectance Optical Fiber Probe for High Sensitivity

In the present study, a DR optical fiber probe was also newly developed for convenient and sensitive spectral measurement. This optical fiber probe consists of the condensing lens and the optical fiber bundle. The lens condenses the irradiating light and

the light diffuse-reflected from the sample. By changing the focusing distance of the condensing lens, one can flexibly vary the working distance between the probe and the sample. The optical fiber bundle is an assembly of optical fibers that transmits the irradiating and diffuse reflection lights. The optical fiber bundle is bunched together at one end, and it is separated into the optical fibers for the irradiating light and the optical fiber for the diffuse reflection light at the other end.

The irradiating light intensity increases as the caliber of optical fiber increases, and the detection property improves, on one hand it also leads to an increase in the mechanical fragility. The optical fiber bundle was selected and the composition was examined, to achieve a certain mechanical strength, a sufficient light intensity and a high optical wavelength resolution. One of the best solution to achieve this is the combination of the multimode fiber for detection and a large number of high numerical aperture, small diameter, optical fibers for irradiation. About 100 optical fibers of its guiding diameter of 200mm allowed us to realize a certain mechanical strength, adequate diameter and a high efficiency.

A DIF model spectrometer was developed that has a built-in DR probe shown in Fig. 6, for the direct installation to a rotation blender the DIF model has a three-axis accelerometer to detect its posture, wireless data interface and lithium ion batteries.

4. Experimental

4.1 Evaluation of Wavelength Resolution

To demonstrate importance of the wavelength resolution and detection sensitivity of P-NIRs, the DR-NIR spectra of talc ($Mg_3Si_4O_4(OH)_2$, Kanto Chemical Co., Inc.) was measured by using the DR optical fiber probe (FIF model). The distance between the probe and the talc powder was approximately 50 mm, the sampling time was 30 ms, and averaged spectrum calculated from 10 spectra was obtained; the total acquisition time for one spectrum was 0.3 s. Moreover, a halogen lamp (5 W) was used as the light source.

The NIR spectra generally have two major drawbacks: band overlaps are severe and the baseline fluctuation of the spectra is often considerable. The second-derivative pretreatment of the spectra is essential for overcoming these problems. If the wavelength resolution of an obtained NIR spectrum is low, it is difficult to separate overlapping bands because the spectrum is distorted. Therefore, the band separation result by the second-derivative pretreatment is also affected by the wavelength resolution. Thus, we have assumed that one can evaluate the wavelength resolution by calculating the second derivative of the spectrum.

To evaluate the wavelength resolution of P-NIRs, that of the NIR spectrum obtained with a 1 nm wavelength resolution was decreased to 5 and 10 nm by the simple moving average method. These spectra were subjected to the second-derivative treatment by the Savitzky-Golay method (smoothing point: 11 point).[14]

4.2 Blending Monitoring Test

To evaluate the high speed performance of P-NIRs, we measured the dynamic mixture spectra of talc and D-mannitol ($HOCH_2(CHOH)_4CH_2OH$, Kanto Chemical Co., Inc.) during rotation mixing with the DIF model of P-NIRs. Monitoring powder blending process by using NIR spectroscopy has been investigated,[15-17] because it is highly desired to detect the homogeneity of mixed powder. The outline of the blending test setup is shown in Figure 1-9. When DR method is used to measure a spectrum, it is highly desirable to keep an irradiation distance constant, however powder under mixing always moves and the irradiation distance changes largely during spectral measurement. Therefore, high speed is highly requested for the NIR spectral measurement in blending process.

The 2-L glass bottle is connected with the clump ferrule of the DIF model of P-NIRs. The center of rotation is in the connected part, and the rotation speed is 12 rpm. First, a

300 g of talc was put into the glass bottle, and then, a 700 g of D-mannitol was added on the talc sample. When P-NIRs is in the bottom position the mixture sample in the bottle reaches the optical window (sapphire), so this timing is adopted as a measurement point. The spectral measurement is performed by detecting the measuring points by the built-in three-axis accelerometer during rotation. The sampling time was 30 ms, and averaged spectrum calculated from 30 spectra was obtained; the total acquisition time for one spectrum was 0.9 s. The light source is a halogen lamp of only 5 W.

5. Results and Discussion

5.1 Change in Spectral Shape in the Second Derivative Spectra with Difference in Wavelength Resolution

Figure 1-10 shows the second-derivative spectra of talc with wavelength resolution of 1, 5, and 10 nm. It yields a sharp peak at 1392 nm owing to the first overtone stretching mode of the OH group.[18] The second-derivative spectrum with 1-nm wavelength resolution measured by P-NIRs shows a narrow band shape, but the second-derivative spectrum with 5 nm and 10 nm wavelength resolution show a broad band shape. Moreover, in the second-derivative spectrum with 10 nm wavelength resolution, the peak intensity decreased to one half of that of obtained with 1-nm wavelength resolution.

It has been found that the low wavelength resolution exerts a large influence on the band separation performance. Thus, it has been confirmed that high wavelength resolution is very effective for the band separation in certain application. And, it has been shown that the wavelength resolution of the newly developed P-NIRs is sufficiently high. In general, NIR spectral measurements do not require as high a spectral resolution as that required by IR and Raman spectral measurements. However, in the case of pharmaceutical applications high wavelength resolution is needed because pharmaceutical industry requests high precision analysis and high precision discrimination of raw materials. Moreover, DR method often needs a pretreatment such as second derivative, where wavelength resolution controls analysis performance as shown in Figure 1-10. Therefore, NIR spectrometers for PAT should have high wavelength resolution, and P-NIRs is equipped with a high wavelength resolution required for PAT application.

5.2 Blending Process Monitoring Test of the Modeling Tablet

Figure 1-11 shows some DR-NIR spectra of the D-mannitol and talc mixture, measured during rotation mixing. Because of high speed of P-NIRs, we could obtain spectral data at each rotation. The spectrum at 0 s reflects D-mannitol only, and the

bands at 1495 and 1580 nm are owing to the first overtones of the OH and CH stretching vibration modes. As spectral variations during rotation mixing, both the change in spectral shape and the baseline drift were observed. In general, baseline drift in DR-NIR spectra during powder mixing is mainly caused by the mean particle size and surface condition. Therefore, it is considered that the baseline fluctuation reflects change in the mean particle size of mixture powder at the irradiated area.

Figure 1-12 shows the second-derivative of the spectra shown in Figure 11. These spectra were subjected to the second-derivative treatment by the Savitzky-Golay method (smoothing point: 31 point). In the original spectra baseline changed largely, while in the second-derivative spectra were observed relative intensity changes between the band at 1392 nm due to talc and those at 1495, 1580 nm arising from D-mannitol. After the mixing for 200 s, the variation of the baseline of the original spectra converged. Also, the variation of second-derivative of 1392, 1495 and 1580 nm converged.

Figure 1-13 shows a plot of a 5 point moving block standard deviation of peak intensities at 1392, 1495, and 1580 nm in the second-derivative spectra versus time. During the initial stage of mixing, the power sample in the bottle is inhomogeneous, and therefore, the spectra, in which bands mainly due to either D-mannitol or talc are dominant, are detected at every measurement, causing a high standard deviation value.

As mixing proceeds, the sample becomes homogeneous; then, the spectra of the mixtures of D-mannitol and talc as the mixing ratio are detected, and thus, the variation of absorbance decreases, yielding a low standard deviation value. The results shown in Fig. 13 that the standard deviation gives a constant value of 200 s after the start of rotation mixing. Thus, it is very likely that the sample in the bottle becomes homogeneous after 200 s. The sample homogeneity was confirmed by an existing method carried out for a sample taken from a bottle by offline measurement, and it is found that the developed P-NIRs enables in-line monitoring of mixing samples. These results demonstrate that this P-NIRs has high speed and sufficiently compact for realizing in-line monitoring in pharmaceutical processes.

6. Conclusion

We have developed one of the world's highest density and high-sensitivity array detector to realize a compact, high-resolution, high-sensitivity, and high-speed polychromator-type NIR spectrometer. The P-NIRs shows improved wavelength resolution and high sensitivity by the use of the newly developed PDA detector with 640 elements. Existing NIR spectrometers have PDA detector with at most 512 elements, and thus their wavelength resolution is at best 1.56 nm. However, the developed novel

PDA detector has allowed one to reach wavelength resolution of 1.25 nm or even better. Moreover, the combined use of the PDA detector with the developed charge-amplifier array has shortened the measurement time from ca. 3 s to below 10 ms.

Through a mechanical investigation and prototyping of a remote DR detection mechanism required for in-line monitoring of the pharmaceutical process, introduction of high-speed data processing, and addition of functions such as a wireless interface, we have developed a prototype model of a high-speed spectrometer for in-line use and confirmed its performance. In PAT, where one must monitor timely quality parameters and functional properties of pharmaceuticals during their manufacturing process, P-NIRs having high speed is a very suitable NIR spectrometer. Moreover, because of its small size, it is very easy to set it up at various pharmaceutical process lines. We have confirmed that P-NIRs have achieved high speed, high sensitivity and high resolution by measuring the DR-NIR spectra of D-mannitol and talc in the powder state.. Moreover, we have shown that P-NIRs can be used to evaluate the homogeneity of the mixed powder samples through the in-line monitoring of the mixed states of the powder samples.

7. References

1. U.S. Food Drug AdministrationDA, *Guidance for Industry, PAT: A Framework for Innovative Pharmaceutical Development, Manufacturing, and Quality Assurance* (U.S. Food and Drug Administration, Maryland, 2004).
2. K. A. Bakeev, *Process Analytical Technology* (Blackwell publishing Ltd., Oxford, 2005), p.13-38.
3. Y. Ozaki and T. Amari, *Near-Infrared Spectroscopy in Chemical Process Analysis* (Sheffield Academic Press, Sheffield, 2000), p.53-95.
4. T. L. Threlfall and J. M. Chalmers, *Handbook of Vibrational Spectroscopy*, vol. 5 (John Wiley & Sons, New York, 2002), p.423–435.
5. U. Hoffmann and N. Zanier-Szydlowski, J. Near Infrared Spectrosc. **7**, 33 (1999).
6. Y. Wu, Y. Jin, Y. Li, D. Sun, X. Liu, and Y. Chen, Vib. Spectrosc. 58, 109 (2012).
7. Y. Ozaki and S. Morita, *Encyclopedia of Applied Spectroscopy* (John Wiley & Sons, Weinheim, 2009), p.872-886.
8. F. A. DeThomas and P. J. Brimmer, *Handbook of Vibrational Spectroscopy,* vol. 1 (John Wiley & Sons, New York, 2002), p.383–392.
9. E. W. Stark, *Handbook of Vibrational Spectroscopy,* vol. 1 (John Wiley & Sons, New York, 2002), p.393–417.

10. Y. Ozaki, Anal. Sci., **28**, 545 (2012).

11. K. Sakakibara, Y. Sanpei, and A. Miura, Japan Patent 4165785 (Aug. 8, 2008).

12. M. Wada, and K. Sakakibara, Japan Patent Kokai 2002-319696 (Oct. 31, 2002).

13. M. Komiyama, Y. Sanpei, A. Miura, K. Sakakibara, T. Yakihara, T. Fujita, S. Kobayashi, S. Oka and Y. Akasaka, USPatent 6,552,325 B1 (Apr. 22, 2003).

14. A. Savitky and M. J. E. Golay, Anal. Chem. **36**, 1627 (1964).

15. S. S. Sekulic, H. W. Ward, II, D. R. Brannegan, E. D. Stanley, C. L. Evans, S. T. Sciavolino, P. A. Hailey, and P. K. Aldridge, Anal. Chem. **68**, 509 (1996).

16. O. Berntsson, L. -G. Danielsson, B. Lagerholm, and S. Folestad, Powder Technol. **123**, 185 (2002).

17. Y. Roggo, P. Chalus, L. Maurer, C. Lema-Martinez, A. Edmond, and N. Jent, J. Pharmaceut. Biomed. Anal. **44**, 683 (2007).

18. S. Petit, A. Decarreau, F. Martin, and R. Buchet, Phys. Chem. Miner. **31**, 585 (2004).

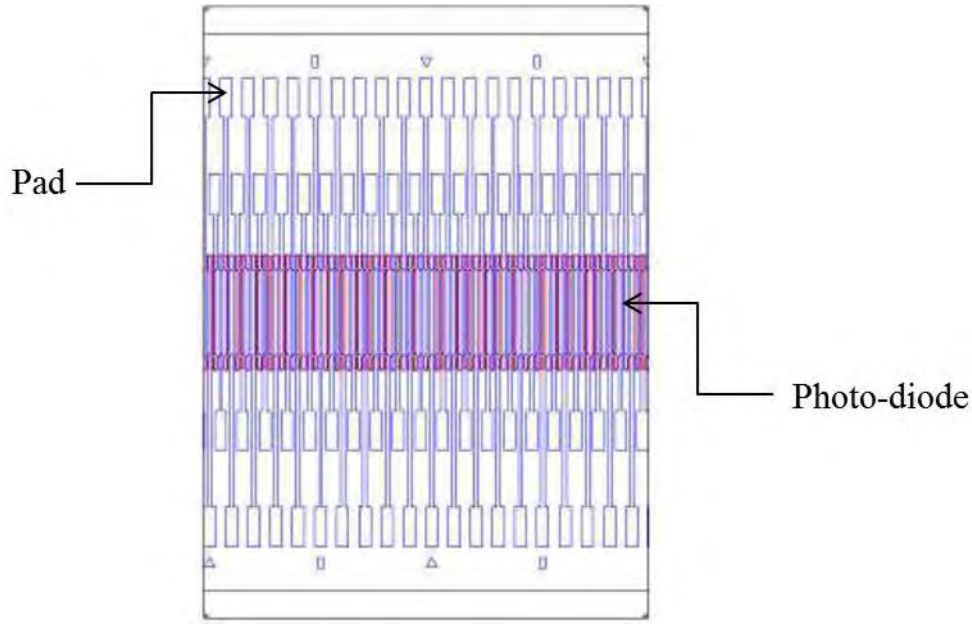

Figure 1-1 Part of the 640-element PDA.

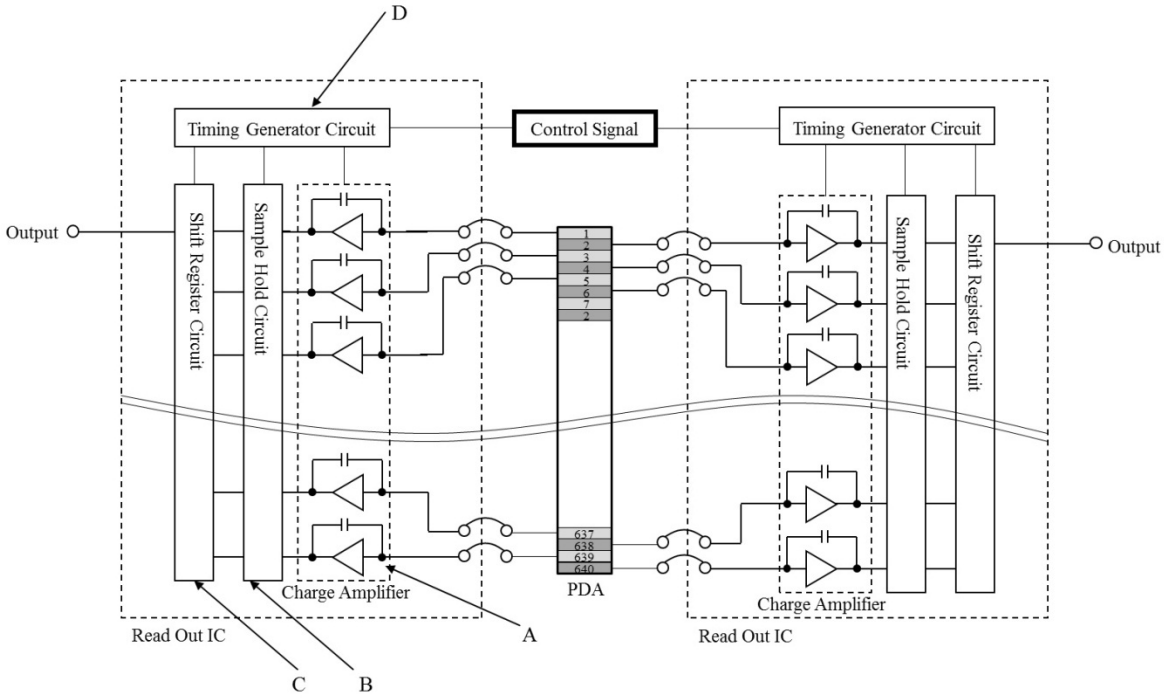

Figure 1-2 Block diagram of PDA: (A) 320-element charge amplifier array, (B) sample hold circuit, (C) shift registor circuit, and (D) timing generator circuit. Two ROICs and one PDA are assembled by the wire bonding method.

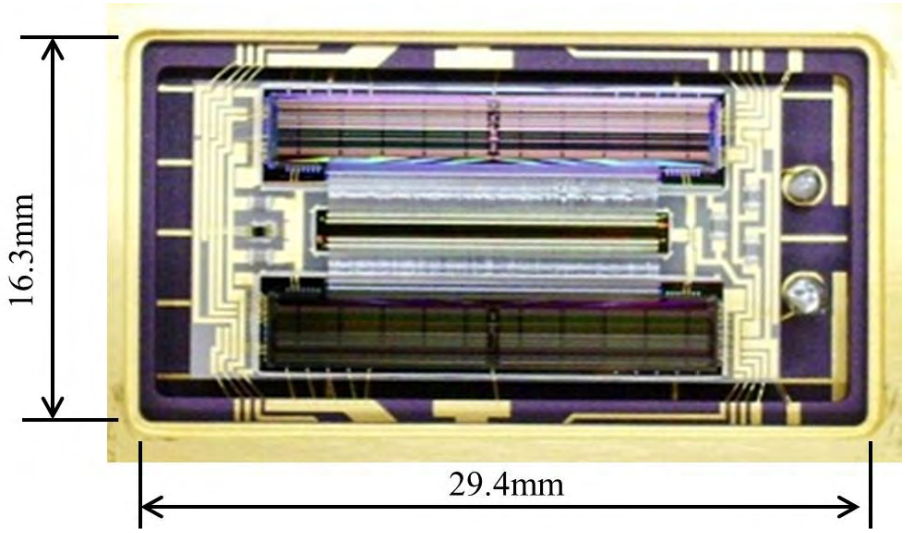

Figure 1-3　Outline view of photodiode array sensor.

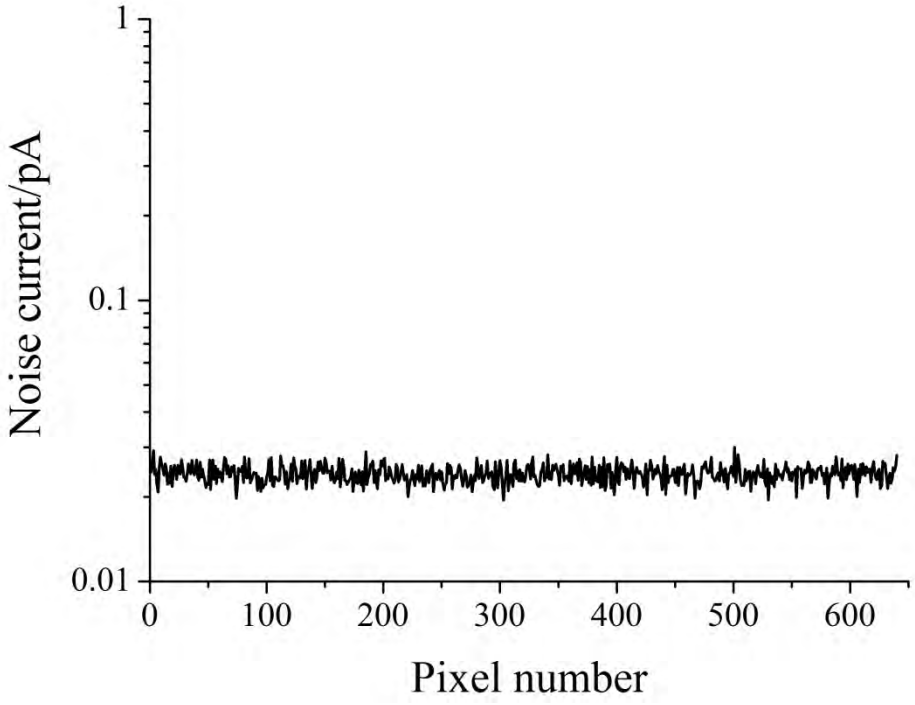

Figure 1-4　Plot of root mean square noise current of each pixel.

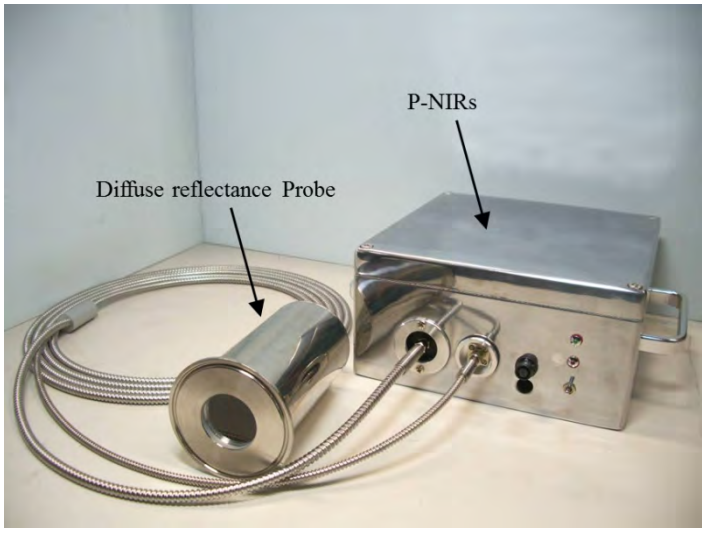

Figure 1-5 Fiber interface model of P-NIRs equipped with diffuse reflectance probe.

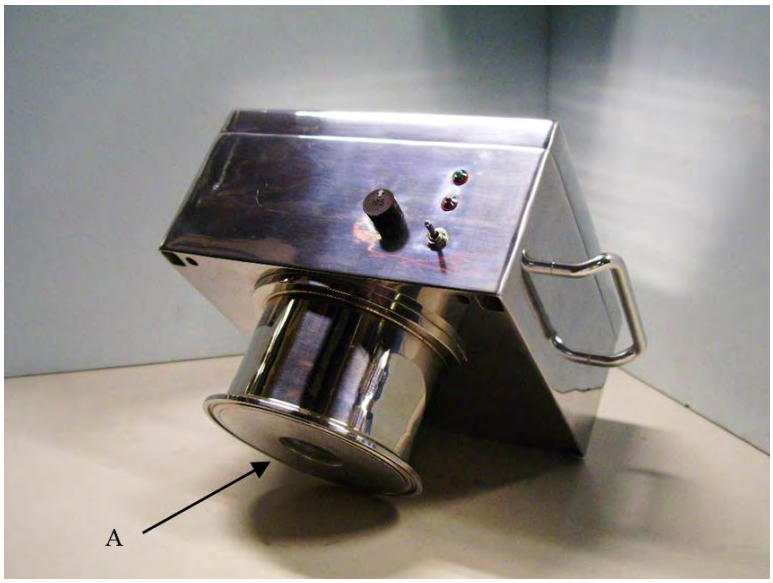

Figure 1-6 Direct interface model of P-NIRs. (A) Optical window through which the irradiating and the diffuse reflected light are transmitted.

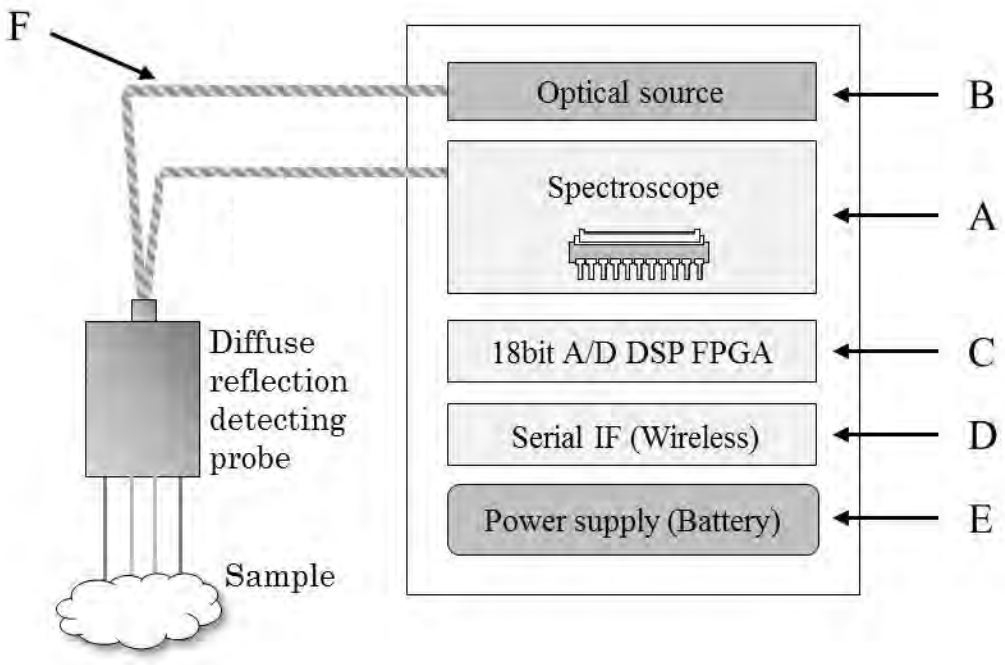

Figure 1-7 Spectroscopic analyzer configuration: (A) spectroscope with a PDA detector, (B) internal optical source, (C) 18-bit analog/digital convertor for signal conversion and CPU, (D) data interface, (E) power supply (battery and external source), and (F) optical fiber probe.

Table 1-1 Specification of P-NIRs

Item	Fiber-Interface model	Direct-Interface model
Spectral range	900 – 1700 nm	
Wavelength resolution	1.25 nm	
Wavelength accuracy	< 0.1 nm	
Absorbance noise level	< 0.1 mAbs.	
Sampling time	Min. 1 ms/spectrum	
Measurement interval	Min. 10 ms	
Number of PD elements	640 elements	
Optical interface	Optical fiber input	Direct: through an optical window
Data interface	Serial communication: RS232C, USB Wireless LAN: 802.11b	
Size	120 mm×220 mm×200 mm	160 mm×220 mm×200 mm
Weight	< 6 kg	< 7 kg
Power supply	AC / DC, battery Typ. 15 W	
Operating temperature	+5 – 45ºC	
Operating humidity	5 – 90 %RH	

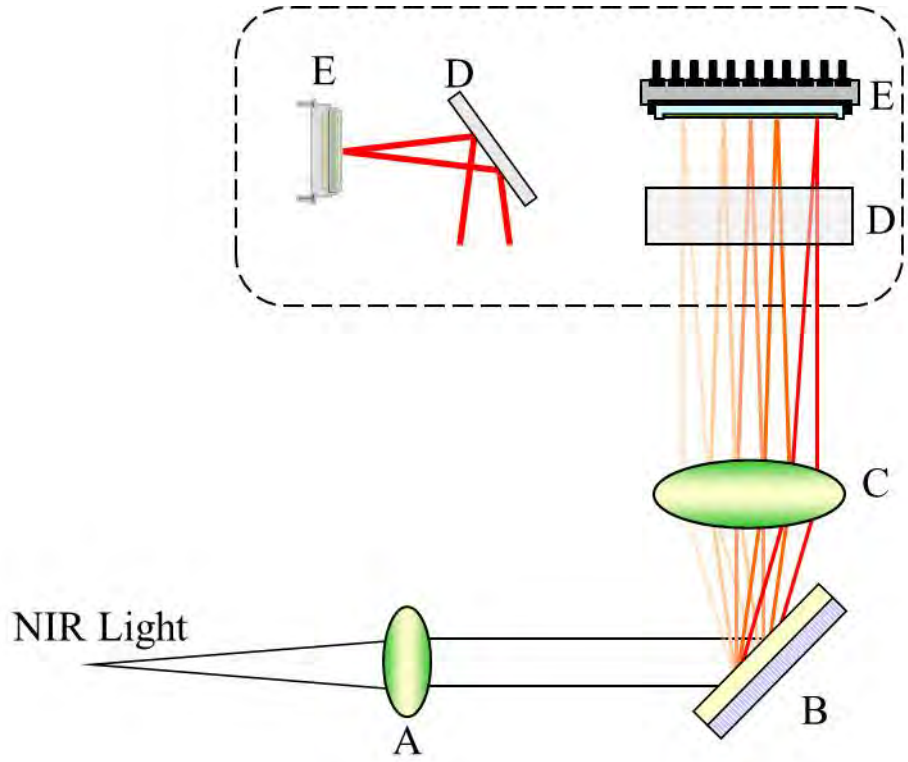

Figure 1-8 Spectro-engine of P-NIRs: (A) collimator lens, (B) diffraction grating, (C) focusing lens, (D) mirror, and (E) 640-element PDA.

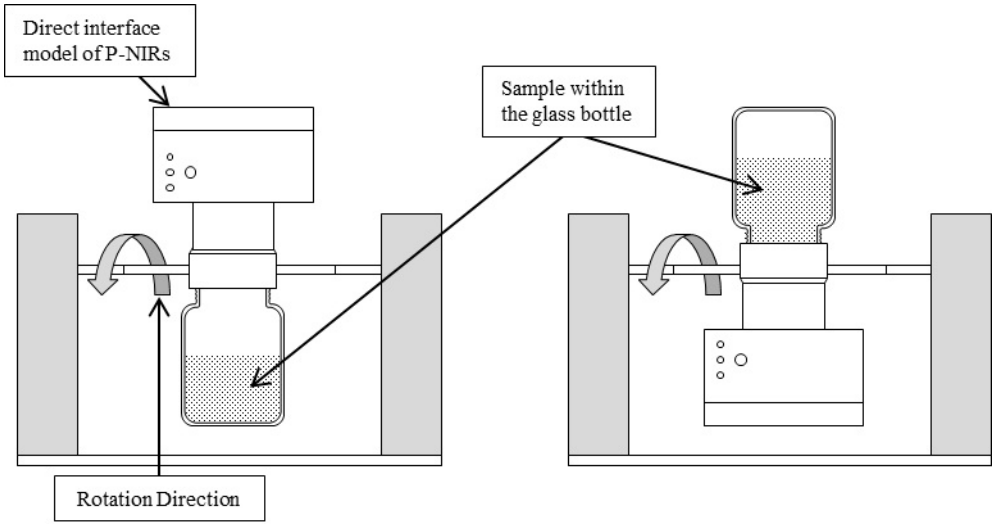

Figure 1-9 Blending test setup.

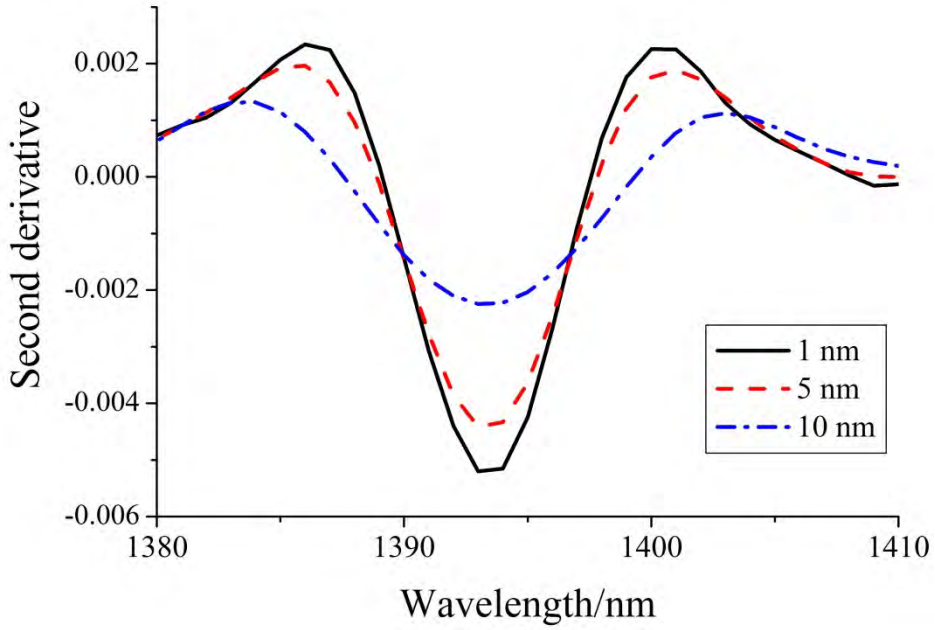

Figure 1-10 Second-derivative spectra of talc with different wavelength resolutions.

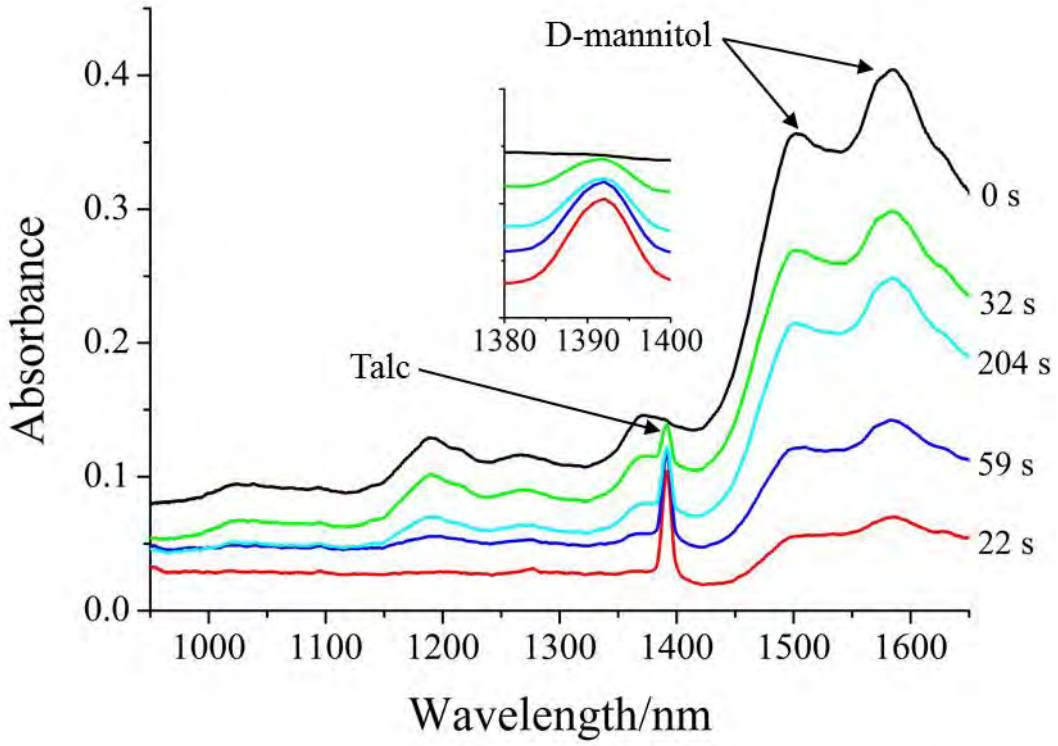

Figure 1-11 DR-NIR Spectra of the D-mannitol and talc during mixing.

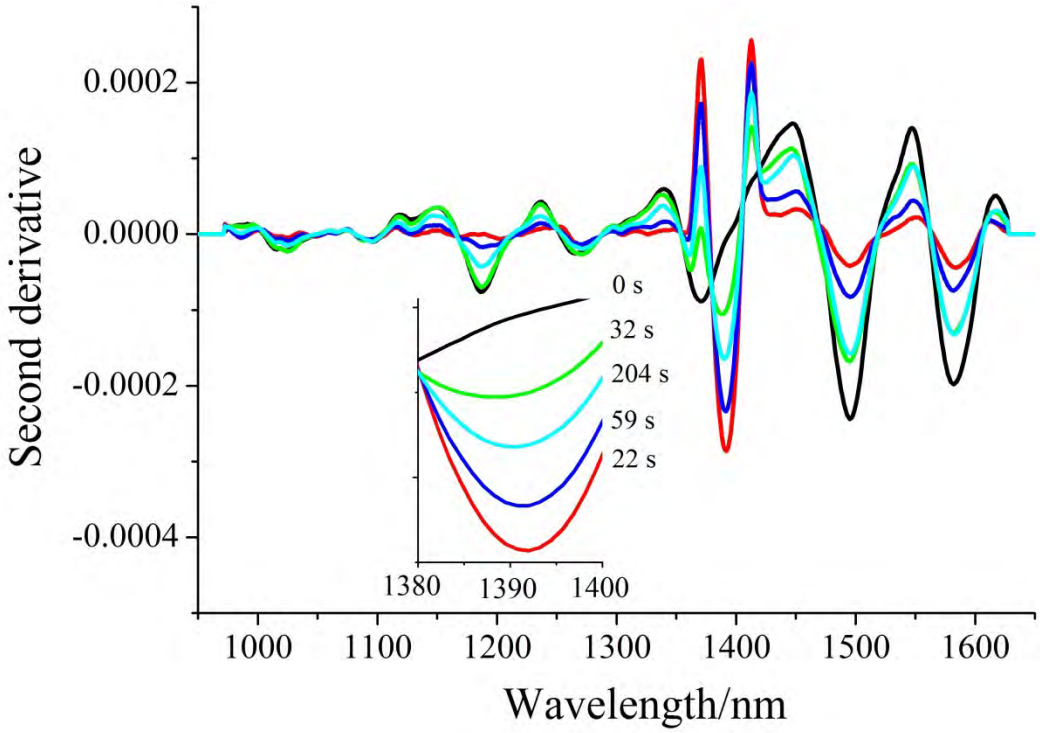

Figure 1-12 Second-derivative spectra of the D-mannitol and talc during mixing.

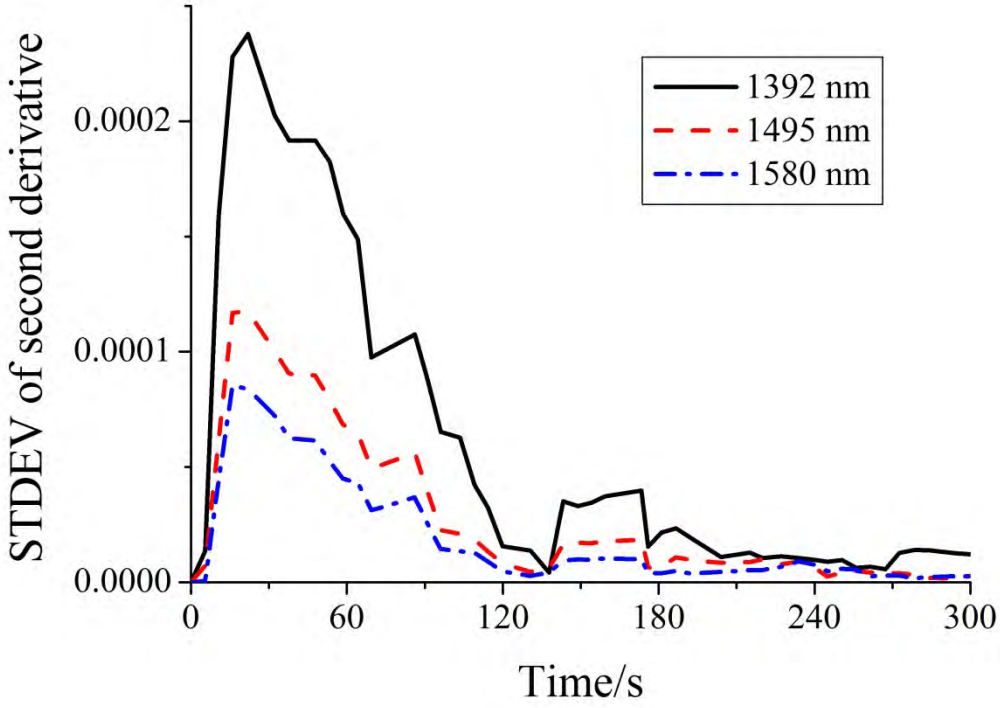

Figure 1-13 Plots for standard deviation of the second-derivative absorbance at 1392, 1495, and 1580 nm versus time.

Chapter 2

Feasibility Study of Diffuse Reflectance and Transmittance Near-Infrared Spectroscopy for Rapid Analysis of Ascorbic-Acid Concentration in Bilayer Tablets using High-speed Polychromator-type Spectrometer

Abstract

Feasibility of real-time release testing of bilayer tablets was investigated using near-infrared (NIR) spectroscopy. The newly developed polychromator-type NIR spectrometer was used to compare the diffuse reflectance (DR) and transmittance (Tr) NIR spectroscopic techniques. This spectrometer not only performs highly sensitive NIR measurements but also affords the NIR spectra of an intact tablet in a millisecond (ms)-time scale; i.e., 500 ms for the DR-NIR measurements and 400 ms for the Tr-NIR measurements. The bilayer tablets were prepared with the first layer comprising 0–10% ascorbic acid (AsA), 20% corn starch, 5% talc, 30% microcrystalline cellulose, and 45–35% lactose, and second layer comprising 20% corn starch, 5% talc, 30% microcrystalline cellulose, and 45% lactose; their DR- and Tr-NIR spectra were acquired from both the sides of the tablet. With the help of the obtained spectra, the feasibility of DR- and Tr-NIR spectroscopy for the quantitative analysis of AsA in the bilayer tablets was compared. The DR- and Tr-NIR spectra of the bilayer tablets and their second derivative spectra were studied. The AsA bands were not identified in the DR- and Tr-NIR spectra. However, the AsA bands at 995 and 1458 nm were observed in the second-derivative spectra. All the developed regression models predicted the AsA concentration and regression vectors indicated that the prediction was based on the AsA

bands. In addition, the model using the Tr-NIR spectra could predict the AsA concentration, even when the bilayer tablet was flipped.

1. Introduction

Since the introduction of process analytical technology (PAT) by the United States Food and Drug Administration,[1] near-infrared (NIR) spectroscopy has been attracting attention as a powerful PAT tool.[2-5] The advantages of NIR spectroscopy, such as nondestructive and in situ analysis and analysis using an optic fiber,[5] are suitable for the implementation of NIR measurements in industrial plants. Owing to the increased focus on NIR spectroscopy, novel and unique NIR spectrometers and their applications in PAT have been developed recently.[6-11] Genkawa et al. developed an online NIR and mid-infrared (online NIR/mid-IR) dual-region spectrometer, which enables the sequential acquisition of the NIR and mid-IR spectra (10,000–1200 cm^{-1}).[6] Monitoring of fermentation processes and band assignment of water and liquid oleic acid were performed with the online NIR/mid-IR spectrometer.[6,7] Murayama et al. developed a high-sensitivity and high-resolution photodiode array (PDA) detector and a high-speed polychromator-type NIR spectrometer (P-NIRs).[8] Ishikawa et al. combined an imaging unit with the P-NIRs for the development of a compact NIR-imaging device with high speed and high portability (D-NIRs).[9,10]

In this study, the rapid analysis of ascorbic acid (AsA) concentration in a bilayer tablet was investigated using P-NIRs. The P-NIRs was used to investigate the feasibility

of the real-time tablet release, namely 100% inspection, during the tablet-making process, which is one of the most important goals of PAT using NIR spectroscopy.

Extensive research has been conducted on the qualitative and quantitative analyses of active pharmaceutical ingredients (APIs) in intact tablets using NIR spectroscopy.[11-28] The advantages of diffuse reflectance (DR) and transmittance (Tr) spectral-acquisition methods were reported.[18-25] The advantages and disadvantages of both the methods are summarized as follows: The DR-NIR method is robust against sample positioning errors, which is advantageous for online NIR measurements. For the analysis of tablets, the DR-NIR spectra allows the utilization of a wide region of wavelength, while the spectral range with wavelengths greater than 1400 nm are unavailable in the Tr-NIR spectra. On the other hand, the Tr-NIR spectra reveal information about the entire tablet, whereas the DR-NIR spectra reveal information only about limited regions on the tablet surface. At low API concentrations, the prediction precision of the Tr-NIR method is better than that of the DR-NIR method.

Hence, the DR- or Tr-NIR method can be chosen based on the distribution of analytes in the tablet. For example, the DR-NIR method is desirable when the API is homogeneously distributed in the tablet. On the other hand, the Tr-NIR method may be applied when the API is heterogeneously distributed in the tablet such as a bilayer tablet.

A bilayer tablet can be used to achieve the following: 1) controlling the release rate of two APIs, and 2) separating two incompatible substances. Otsuka and Fukui measured the Tr- and DR-NIR spectra of bilayer tablets containing the polymorphic forms of carbamazepine.[27] They reported that the calibration models developed for the determination of polymorphic content based on the Tr-NIR spectra had a linear relationship unlike those based on the DR-NIR spectra. Ito et al. developed calibration models for acetaminophen and caffeine anhydrate contents in a bilayer tablet by using the Tr-NIR spectra.[28] They reported that the developed calibration models exhibited sufficient linearity and accuracy and that it was not necessary to keep the irradiated side of the tablet for Tr-NIR analysis.

As mentioned above, the analysis of tablets by NIR spectroscopy has been extensively researched. Most of the research was performed for laboratory use with the help of Fourier-transform and monochromator-type spectrometers;[12-16,18-21,23-28] in some cases, portable NIR spectrometers were used.[17,22] Generally, the spectra obtained from laboratory-use spectrometers have high signal-to-noise ratios (SNR). However, the laboratory-use spectrometers require larger spectral scanning times; consequently, the spectral measurement of a sample takes several seconds. However, for real-time tablet release testing, a high-speed NIR spectrometer, which enables the acquisition of Tr-NIR

spectra on a millisecond (ms)-time scale, is preferred. Because the absorptivity in the short-wave NIR region (900 nm – 1300 nm) is very low for most of the samples, the Tr-NIR spectrum of an intact tablet (up to 5-mm thick) can be obtained. However, compared to the DR-NIR method, longer exposure and scanning times are required for the Tr-NIR method to achieve an SNR similar to that of the DR-NIR method. For real-time release testing, reliable spectral acquisition on a ms-time scale is preferred. The P-NIRs was developed to achieve ms-spectral acquisition.[8] The P-NIRs is equipped with a novel PDA detector that combines a high-density array (640 InGaAs photodiodes with 20-μm pitch) and a charge amplifier array-type integrated circuit that covers the 900–1700-nm range with a point to point resolution of 1 nm. The noise level of the P-NIRs is less than 0.0001 absorbance units and the configurable measurement interval is 10 ms. With P-NIRs, it is possible to investigate the feasibility of real-time release testing of a tablet using the Tr-NIR spectroscopy and compare it with that of the DR-NIR spectroscopy.

In this study, the DR- and Tr-NIR spectra of the bilayer tablets were acquired on a ms-time scale (500 ms for DR-NIR and 400 ms for Tr-NIR spectra) by using the P-NIRs and partial least-squares regression (PLSR) for the development of the API concentration models. From the results of these regression models, the feasibility of

rapid analysis of APIs in a bilayer tablet was investigated. This study compares the DR- and Tr-NIR spectra of bilayer tablets obtained on a ms-time scale by using a portable NIR spectrometer. Thus, the present study is a step toward real-time release testing of bilayer tablets by NIR spectroscopy.

2. Materials and Methods

2.1 Sample Preparation

AsA (Kanto Chemical Co. Inc., Tokyo, Japan), lactose (Wako Pure Chemical Industries, Ltd., Osaka, Japan), talc (Kanto Chemical Co. Inc.), corn starch (Wako Pure Chemical Industries, Ltd., Osaka Japan), and microcrystalline cellulose (Merck KGaA, Darmstadt, Germany) were used to formulate the bilayer tablets. All the reagents used were of analytical grade. AsA was used instead of an actual API component in the present study.

2.2 Bilayer Tablet Preparation

The sample bilayer tablets were prepared by the pressure bonding method with a single-punch tableting machine (Handtab-100, Ichihashi Seiki Co. Ltd., Kyoto, Japan). The first layer of the tablet contained AsA (0–10% at 2% intervals) and the second layer

did not contain AsA. In addition to AsA, the first layer contained corn starch (20%), talc (5%), microcrystalline cellulose (30%), and lactose (45–35% according to the AsA concentration). Because the second layer did not contain AsA, the lactose concentration in the second layer was 45%.

Firstly, the powdered samples required for each layer were weighed separately in an analytical balance and were blended well in a plastic bag. Then, the powder for the first layer was set in the cavity of a tableting machine and was compressed with a rod under a gauge pressure of 10 MPa. Instead of measuring the tablet weight, the quantity of the blended powder was adjusted by setting the depth of the cavity so that the thickness of the first layer became 1.0 ± 0.1 mm. After confirming the thickness, the powder for the second layer was added on the first layer in the cavity of the tableting machine and was compressed under the same gauge pressure. The tablets with a thickness of 2.0 ± 0.1 mm, which is the typical thickness range for commercial tablets, were selected and 30 bilayer tablets (six AsA concentration levels, five tablets each) were prepared for the experiments.

2.3 NIR Spectrometer

Recently developed P-NIRs[8] was used for the spectral acquisition on a ms-time scale.

Two types of P-NIRs models are available: (i) an optical fiber interface model with a DR optical fiber probe, and (ii) a direct interface model with a built-in DR optical fiber probe. The optical fiber interface model was used in this study. Details of this spectrometer are described in a previous report.[8]

2.4 Spectral Data Acquisition

The NIR spectra of the 30 bilayer tablets were measured on both the sides (from the first to the second layer and from the second to the first layer) by the Tr- and DR-NIR methods. Figure 2-1 illustrates a schematic diagram of the spectral acquisition. A bilayer tablet was placed in the tablet holder and NIR light was irradiated from a halogen lamp (5 W) located 55 mm above the tablet. In the DR-NIR measurement, an optical detection probe was set at an angle of 20° to prevent the effect of specular reflection, and a DR standard (SRS-99-020, Labsphere, Inc., USA) was used as the background reflectance material. The sampling time for obtaining one spectrum was set as 50 ms and an average spectrum was calculated from 10 spectra; the total acquisition time for one tablet was 500 ms. In the Tr-NIR measurement, the optical detection probe was positioned directly beneath the tablet and NIR light transmitted through the tablet was measured. To measure the background spectrum, diffuse transmittance plates of 1-mm

thickness (ZDF-1000, Labsphere, Inc., USA) were stacked in pairs and used. The sampling time was 400 ms; averaging was not performed. In both the measurements, the NIR spectra in the 900–1700 nm region were measured with a point to point resolution of 1 nm. The optimal sampling times for each method were determined from preliminary experiments. In these experiments, the DR standard and diffuse transmittance plates were used and a sampling time that provided the maximum signal intensity without detector saturation was chosen. In addition, 10 spectra were averaged for the DR-NIR measurement so that the total acquisition time was almost the same as that of the Tr-NIR measurement for the comparison between DR-NIR and Tr-NIR spectra.

2.5 Spectral Data Analysis

The Unscrambler® X ver. 10.2 (CAMO software AS, Norway) was used for the pretreatment of spectra and PLSR modeling of AsA concentration. The AsA concentration in the tablets was calculated from the weight of AsA, which was obtained during tablet preparation. To minimize uncertainties in the tablet preparation, the mean spectrum calculated from the NIR spectra of five tablets with the same AsA concentration were used for the modeling. Firstly, the DR- and Tr-NIR measurements

were converted to the absorbance units, namely $\log_{10}$ (1/DR) or $\log_{10}$ (1/Tr). Then, the mean of the five spectra was calculated for each AsA concentration and the spectral regions for PLSR modeling were selected by referring to the band assignments of AsA: the 1400−1500-nm region for the DR-NIR spectra and the 950−1050-nm region for the Tr-NIR spectra (Figure 2-2). In these regions, the AsA bands arising from the second and first overtones of the O–H stretching vibration were observed at 995 and 1458 nm, respectively.[29] Subsequently, the obtained mean spectra were subjected to the Savitzky–Golay second-derivative treatment.[30] The window size of the second-derivative treatment was determined by referring to the appearance of the AsA bands at 995 and 1458 nm in the spectra of tablets, and a second-order polynomial was used, as shown in Table 2-1. After mean-centering the second-derivative spectra, the PLSR models based on the DR- and Tr-NIR spectra acquired from both sides of the tablet were constructed to determine the AsA concentration. The PLSR models were validated by the leave-one-out cross-validation method and the coefficient of determination (R^2) and root-mean-square-error of cross-validation (RMSECV) were calculated. In the present study, four PLSR models were constructed: DR 1, DR 2, Tr 1, and Tr 2. The DR 1 and DR 2 models were based on the DR-NIR spectra obtained by irradiating NIR light from the first and second layers, respectively, and the Tr 1 and Tr 2 models were based on the

Tr-NIR spectra obtained by irradiating NIR light from the first and second layers, respectively.

3. Results and Discussion

3.1 Comparison of NIR Spectra and Their Second Derivatives

To validate the performance of ms-spectral acquisition by P-NIRs and the necessity of band separation, the NIR spectra and their second derivatives obtained by the DR- and Tr-NIR methods were compared. Figure 2-3 depicts the DR-NIR spectra of the bilayer tablets with and without AsA obtained by irradiating NIR light from the first (Figure 2-3a) and second (Figure 2-3b) layers. Regardless of the light-irradiated side, it was difficult to identify an intensity change in the AsA band in the DR-NIR spectra because of band overlapping and baseline fluctuation. Similarly, no change in the AsA-band intensity was observed in the Tr-NIR spectra shown in Fig. 2-4. Compared to the DR-NIR spectra, the Tr-NIR spectra in the region shorter than 1400 nm are easily observed and the spectra in the region longer than 1400 nm are quite noisy. This decline in the SNR at the longer-wavelength region is not due to the P-NIRs or ms measurement, but it is an unavoidable problem in the Tr-NIR method when tablets with higher thickness are used. Similar results have been reported in other studies where the FT-type

and monochromator-type spectrometers and higher spectral-scanning times were adopted.[14,18,19,24,27]

Figure 2-5 shows the second-derivative DR-NIR spectra of the bilayer tablet and their expansion in the 1440–1480-nm region. The second-derivative spectra are spiky because of the high wavelength resolution of P-NIRs (1 nm) and noise enhancement by the derivation. However, an intensity change in the band at 1458 nm due to AsA is clearly observed. The intensity of this AsA band in the DR 2 spectrum (Figure 2-5b) is smaller than that in the DR 1 spectrum (Figure 2-5a), because DR light is attenuated during its passage through the first-layer side. The second-derivative Tr-NIR spectra of the bilayer tablet are shown in Figure 2-6. The band at 1458 nm is not observed because of the decline in the SNR in this wavelength region. Instead, a significant band-intensity change, which is related to the AsA concentration, is found at 995 nm. The amount of spectral variations with AsA concentration is similar between the spectra of Tr 1 and Tr 2. Unlike the DR-NIR method, the tablet side from which the light is irradiated need not be confirmed in the Tr-NIR method.

3.2 Comparison in PLSR Models

To identify the feasibility of rapid analysis of API in a bilayer tablet, validation

results of the PLSR modeling for AsA concentration in the first layer are evaluated. Table 2-1 summarizes the analysis conditions and cross-validation results of the PLSR models. All the PLSR models achieved an R^2 greater than 0.87 and RMSECV lesser than 1.6%. The models DR 1 and Tr 1, which used the spectra obtained by irradiating NIR light from the first-layer side, showed slightly better results than those using spectra obtained by irradiating the light from the second-layer side (models of DR 2 and Tr 2). As shown in Figure 2-7, the RMSECV decreases drastically with the first and second latent variables (LVs) and becomes almost constant after the second LV. These results indicate that all the constructed regression models describe changes in the AsA concentration with the first and second LVs based on the spectral change due to AsA and not noise signal. Therefore, the NIR spectroscopic technique combined with PLSR modeling enables the prediction of the API concentration in a bilayer tablet by using the NIR spectra obtained on a ms-time scale. To enable the practical use of this technique, further investigations are required for optimizing the spectral acquisition and analysis method conditions.

Regression vectors of the models were used to interpret the obtained PLSR models. Figure 2-8 shows the regression vectors of the PLSR models. In the regression vector of the DR 1 model (Figure 2-8a), the band at 1458 nm has the largest regression

coefficient; however, no prominent regression coefficient is obtained in that of the DR 2 model (Figure 2-8b). Hence, the DR 1 model is based on the intensity change of the AsA band at 1458 nm, whereas the DR 2 model is based on the intensity change of the AsA band as well as other components. Despite observing an intensity change with AsA concentration in the DR 2 spectra (Figure 2-5b), the DR 2 model is less accurate than the DR 1 model (Table 2-1). In contrast, the regression vectors of the models obtained using the Tr-NIR spectra indicate that the largest regression coefficient is obtained at the 995-nm band because of AsA (Figures 2-8c and 2-8d), and both the regression models are based on a change in the AsA concentration, which is similar to the DR 1 model. However, large positive coefficients were observed at 1473 and 1022 nm (Figures 2-8a and 2-8d), which probably result because of a decrease in the prediction accuracy of the DR 1 and Tr 2 models. Further investigations are required for improving the SNR of these bands.

Besides the feasibility of nondestructive measurement of API in a bilayer tablet, the advantages of the Tr-NIR method while turning over the bilayer tablet were investigated. Figure 2-9 shows the comparison of the predicted AsA concentrations with their actual values when the AsA concentrations were predicted by inserting the spectral data set of DR 2 to the DR 1 model or Tr 2 to the Tr 1 model. The AsA concentrations predicted by

using the Tr-NIR method are in agreement with the actual concentrations, whereas those predicted by using the DR-NIR method are lower than the actual concentrations. The maximum difference between the predicted and actual values is 5.3% for the tablet with 10% AsA. This result supports the results of previous studies that a Tr-NIR method is useful for the quantitative analysis of a bilayer tablet.[26,27] For the DR-NIR method, an identification algorithm such as Hotellings T^2 or F-Residuals will be advantageous in detecting the direction of the bilayer tablet to avoid orientation issues of the bilayer tablet when used in the actual production environment.

4. Conclusion

In this study, the feasibility of the analysis of API in a bilayer tablet on a ms-time scale using NIR spectroscopy was investigated. The newly developed P-NIRs, which enables the high-speed spectral measurement of an intact tablet, was used. The NIR spectra of the bilayer tablets were acquired by both th DR- and Tr-NIR methods at 500 and 400 ms to obtain the DR- and Tr-NIR spectra, respectively.

Comparison of the NIR spectra with their second-derivatives showed that the NIR spectra were specific and selective to variation in the AsA concentration. The validation results and regression vectors demonstrated that the PLSR models enabled the

prediction of the AsA concentration in the bilayer tablet. The Tr-NIR method was confirmed to be fairly robust for tablet orientation. Thus, the present study is a step toward the real-time release testing of bilayer tablets.

5. References

1. U.S. Food Drug Administration, Guidance for Industry, PAT: A Framework for Innovative Pharmaceutical Development, Manufacturing, and Quality Assurance (U.S. Food and Drug Administration, Maryland, 2004).
2. K.A. Bakeev, Process Analytical Technology (Blackwell publishing Ltd., Oxford, 2005), p.13-38.
3. Y. Ozaki and T. Amari, Near-Infrared Spectroscopy in Chemical Process Analysis (Sheffield Academic Press, Sheffield, 2000), p.53-95.
4. T.L. Threlfall and J. M. Chalmers, Handbook of Vibrational Spectroscopy, vol. 5 (John Wiley & Sons, New York, 2002), p.423–435.
5. Y. Ozaki, “Near-Infrared Spectroscopy –Its Versatility in Analytical Chemistry”, Anal. Sci. 28, 545 (2012).
6. T. Genkawa, M. Watari, T. Nishii and Y. Ozaki, “Development of a Near-Infrared/Mid-Infrared Dual-Region Spectrometer for Online Process Analysis”, Appl. Spectrosc. 66, 773 (2012).
7. T. Genkawa, M. Watari, T. Nishii, M. Suzuki and Y. Ozaki, “Two-Dimensional Heterospectral Correlation Analysis of Water and Liquid Oleic Acid using an Online Near-Infrared/Mid-Infrared Dual-Region Spectrometer”, Appl. Spectrosc. 67,

724 (2013).

8. K. Murayama, T. Genkawa, D. Ishikawa, M. Komiyama and Y. Ozaki, “A polychromator-type near-infrared spectrometer with a high-sensitivity and high-resolution photodiode array detector for pharmaceutical process monitoring on the millisecond time scale”, Rev. Sci. Instrum. 84, 023104 (2013)
9. D. Ishikawa, K. Murayama, T. Genkawa, K. Awa, M. Komiyama, Y. Ozaki, “Development of compact near-infrared imaging device with high-speed and portability for pharmaceutical process monitoring”, NIR News 23, 14–17, (2012).
10. D. Ishikawa, K. Murayama, T. Genkawa, K. Awa, M. Komiyama, K. Sergei and Y. Ozaki, “Application of a newly developed portable NIR imaging device to dissolution process monitoring of tablets”, Anal. Bioanal. Chem. in press, (2013).
11. A.C. Moffat, S. Assi and R.A. Watt, “Identifying counterfeit medicines using near infrared spectroscopy”, J. Near Infrared Spectrosc. 18, 1 (2010).
12. M. Laasonen, T. Harmia-Pulkkinen, C. Simard, M. Räsänen and H. Vuorela, “Development and validation of a near-infrared method for the quantitation of caffeine in intact single tablets”, Anal. Chem. 15, 754 (2003).
13. I. Jedvert, M. Josefson and F.W. Langkilde, “Quantification of an active substance in a tablet by NIR and Raman spectroscopy”, J. Near Infrared Spectrosc. 6, 279

(1998).

14. N.W. Broad, R.D. Jee, A.C. Moffat and M.R. Smith, “Application of transmission near-infrared spectroscopy to uniformity of content testing of intact steroid tablets”, Analyst 126, 2207 (2001).

15. G.E. Ritchie, R.W. Roller, E.W. Ciurczak, H. Mark, C. Tso and S.A. MacDonald, “Validation of a near-infrared transmission spectroscopic procedure. Part B: Application to alternate content uniformity and release assay methods for pharmaceutical solid dosage forms”, J. Pharm. Biomed. Anal. 29, 159 (2002).

16. M. Alcalà, J. León, J. Ropero, M. Blanco and R.J. Romañach, “Analysis of low content drug tablets by transmission near infrared spectroscopy: selection of calibration ranges according to multivariate detection and quantitation limits of PLS models”, J. Pharm. Sci. 97, 5318 (2008).

17. A.J. O'Neil, R.D. Jee, G. Lee, A. Charvill and A.C. Moffat, “Use of a portable near infrared spectrometer for the authentication of tablets and the detection of counterfeit versions”, J. Near Infrared Spectrosc. 16, 327 (2008).

18. J. Gottfries, H. Depui, M. Fransson, M. Jongeneelen, M. Josefson, F.W. Langkilde and D.T. Witte, “Vibrational spectrometry for the assessment of active substance in metoprolol tablets: a comparison between transmission and diffuse reflectance

near-infrared spectrometry", J. Pharm. Biomed. Anal. 14, 1495 (1996).

19. P. Merckle and K.-A. Kovar, "Assay of effervescent tablets by near-infrared spectroscopy in transmittance and reflectance mode: acetylsalicylic acid in mono and combination formulations", J. Pharm. Biomed. Anal. 17, 365 (1998).
20. S.S. Thosar, R.A. Forbess, N.K. Ebube, Y. Chen, R.L. Rubinovitz, M.S. Kemper, G.E. Reier, T.A. Wheatley and A.J. Shukla, "A comparison of reflectance and transmittance near-infrared spectroscopic techniques in determining drug content in intact tablets", Pharm. Dev. Technol. 6, 19 (2001).
21. R.C. Schneider and K.-A. Kovar, "Analysis of ecstasy tablets: comparison of reflectance and transmittance near infrared spectroscopy", Forensic Sci. Int. 134, 187 (2003).
22. R.P. Cogdill, C.A. Anderson, M. Delgado-Lopez, D. Molseed, R. Chisholm, R. Bolton, T. Herkert, A.M. Afnán and J.K. Drennen "Process analytical technology case study part I: Feasibility studies for quantitative near-infrared method development", AAPS PharmSciTech. 6, E262, (2005).
23. M. Otsuka, H. Tanabe, K. Osaki, K. Otsuka and Y. Ozaki, "Chemoinformetrical evaluation of dissolution property of indomethacin tablets by near-infrared spectroscopy, J. Pharm. Sci. 96, 788 (2007).

24. S.M. Short, R.P. Cogdill and C.A. Anderson, “Figures of merit comparison of reflectance and transmittance near-infrared methods for the prediction of constituent concentrations in pharmaceutical compacts”, J. Pharm. Innov. 3, 41 (2008).

25. M. Ito, T. Suzuki, S. Yada, A. Kusai, H. Nakagami, E. Yonemochi and K. Terada, “Development of a method for the determination of caffeine anhydrate in various designed intact tablets by near-infrared spectroscopy: A comparison between reflectance and transmittance technique”, J. Pharm. Biomed. Anal. 47, 819 (2008).

26. M. Iyer, H.R. Morris and J.K. Drennen, “Solid dosage form analysis by near infrared spectroscopy: comparison of reflectance and transmittance measurements including the determination of effective sample mass”, J. Near Infrared Spectrosc. 10, 233 (2002).

27. M. Otsuka and Y. Fukui, “Determination of carbamazepine polymorphic contents in double-layered tablets using transmittance- and reflectance-near-infrared spectroscopy involving chemometrics”, Drug Dev. Ind. Pharm. 36, 1404 (2010).

28. M. Ito, T. Suzuki, S. Yada, H. Nakagami, H. Teramoto, E. Yonemochi and K. Terada, “Development of a method for nondestructive NIR transmittance spectroscopic analysis of acetaminophen and caffeine anhydrate in intact bilayer tablets”, J. Pharm. Biomed. Anal. 53, 396 (2010).

29. H. Lui, B. Xiang and L. Qu, “Structure analysis of ascorbic acid using near-infrared spectroscopy and generalized two dimensional correlation spectroscopy”, J. Mol. Struct. 794, 12 (2006).

30. A. Savitzky and M.J.E. Golay, “Smoothing and differentiation of data by simplified least squares procedures”, Anal.Chem. 36, 1627 (1964).

Table 2-1. Analysis conditions and cross-validation results of PLS models

Model	Wavelength region (nm)	Window size of second-derivative	Number of LVs	R^2	RMSE (%)
DR 1	1400–1500	13	2	0.89	1.3
DR 2	1400–1500	13	2	0.87	1.6
Tr 1	950–1050	25	2	0.93	1.1
Tr 2	950–1050	25	2	0.88	1.4

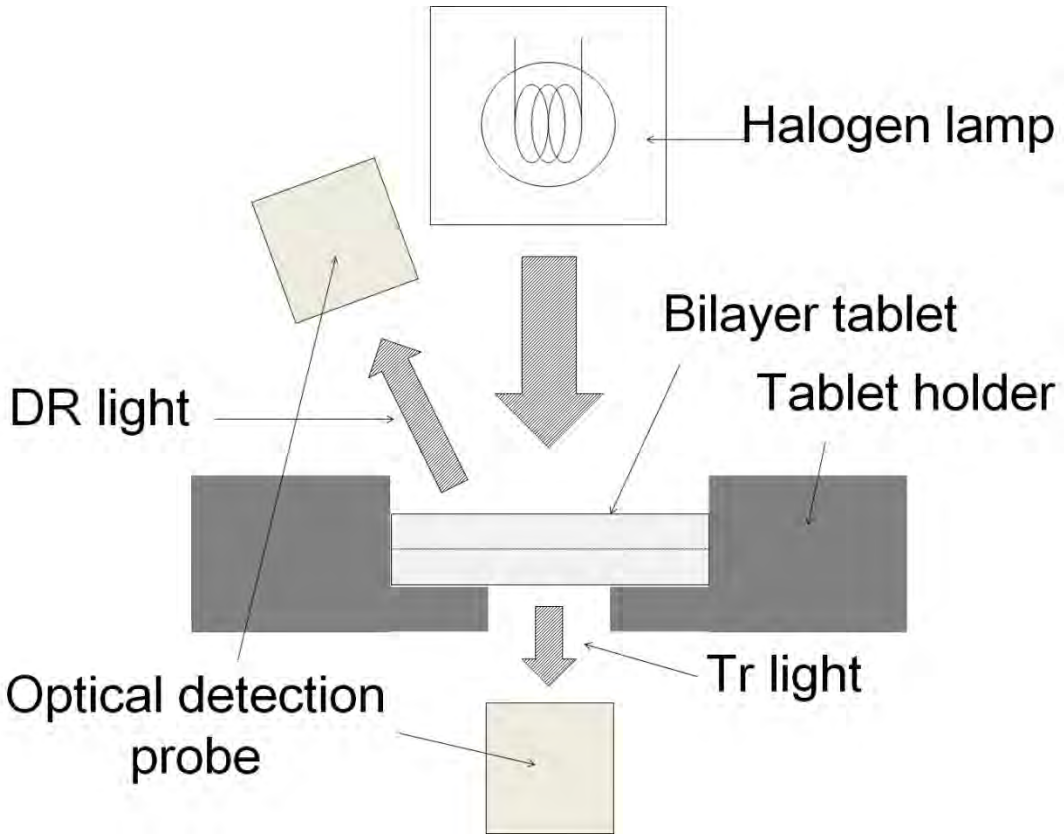

Figure 2-1. Schematic diagram of the spectral measurement system.

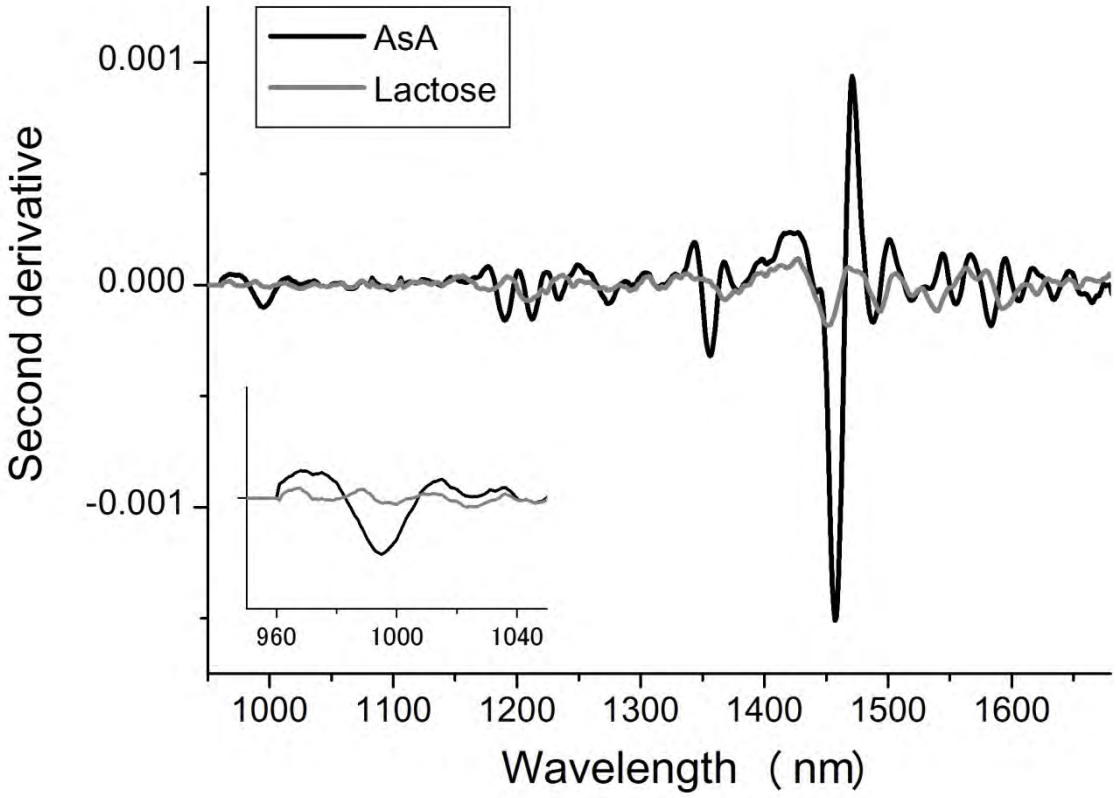

Figure 2-2. Second-derivative DR-NIR spectra of AsA and lactose powder samples.

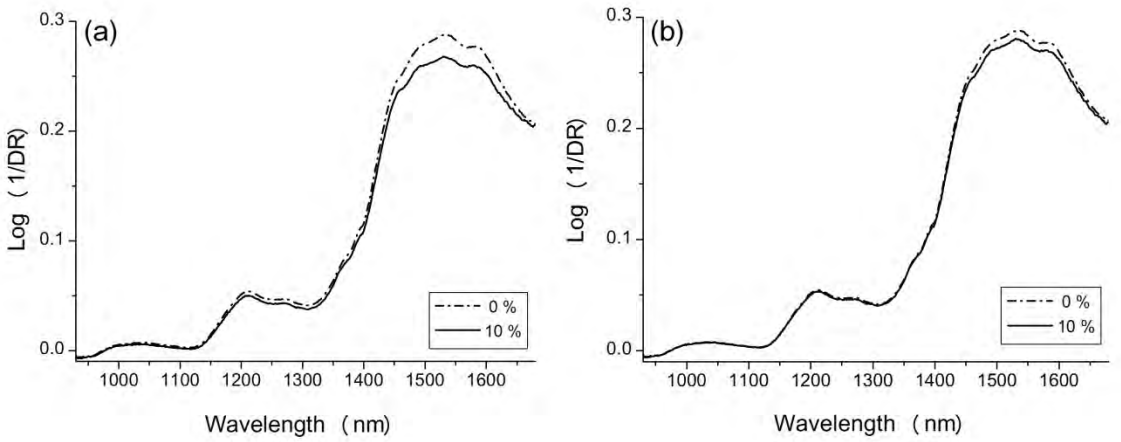

Figure 2-3. DR-NIR spectra of the bilayer tablets with and without AsA; spectra obtained by irradiating light from (a) the first and (b) second layer sides.

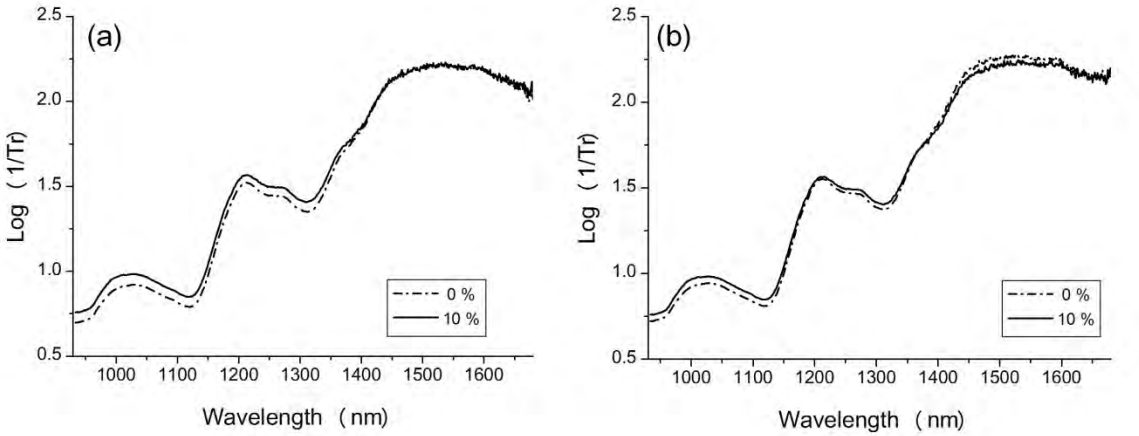

Figure 2-4. Tr-NIR spectra of the bilayer tablets with and without AsA; spectra obtained by irradiating light from (a) the first and (b) second layer sides.

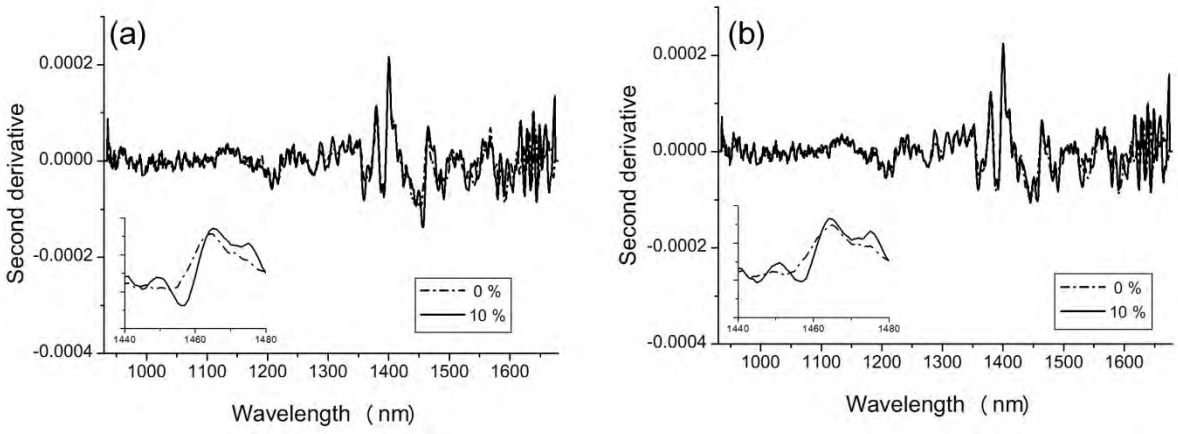

Figure 2-5. Second-derivative DR-NIR spectra of the bilayer tablets with and without AsA; spectra obtained by irradiating light from (a) the first and (b) second layer sides.

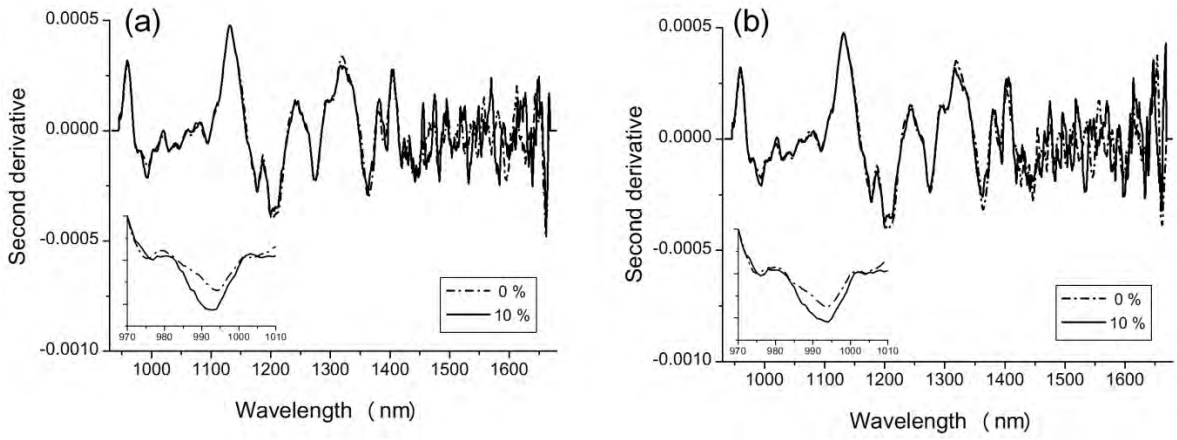

Figure 2-6. Second-derivative Tr-NIR spectra of the bilayer tablets with and without AsA; spectra obtained by irradiating light from (a) the first and (b) second layer sides.

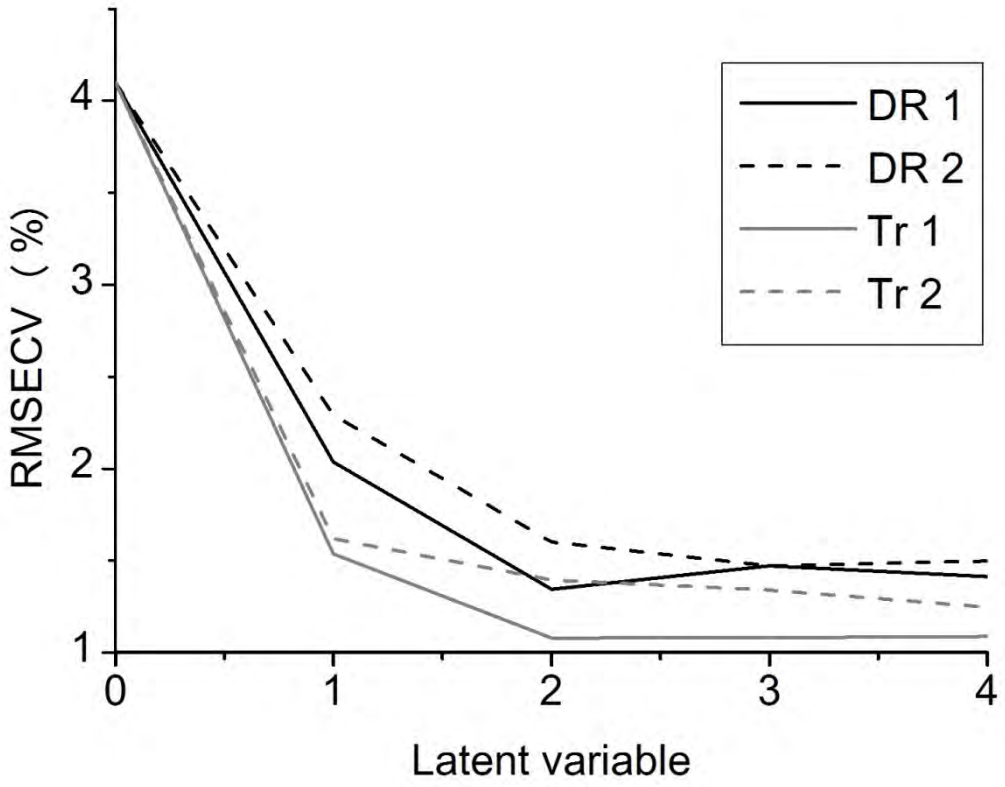

Figure 2-7. Relationship between the RMSECV and latent valriables.

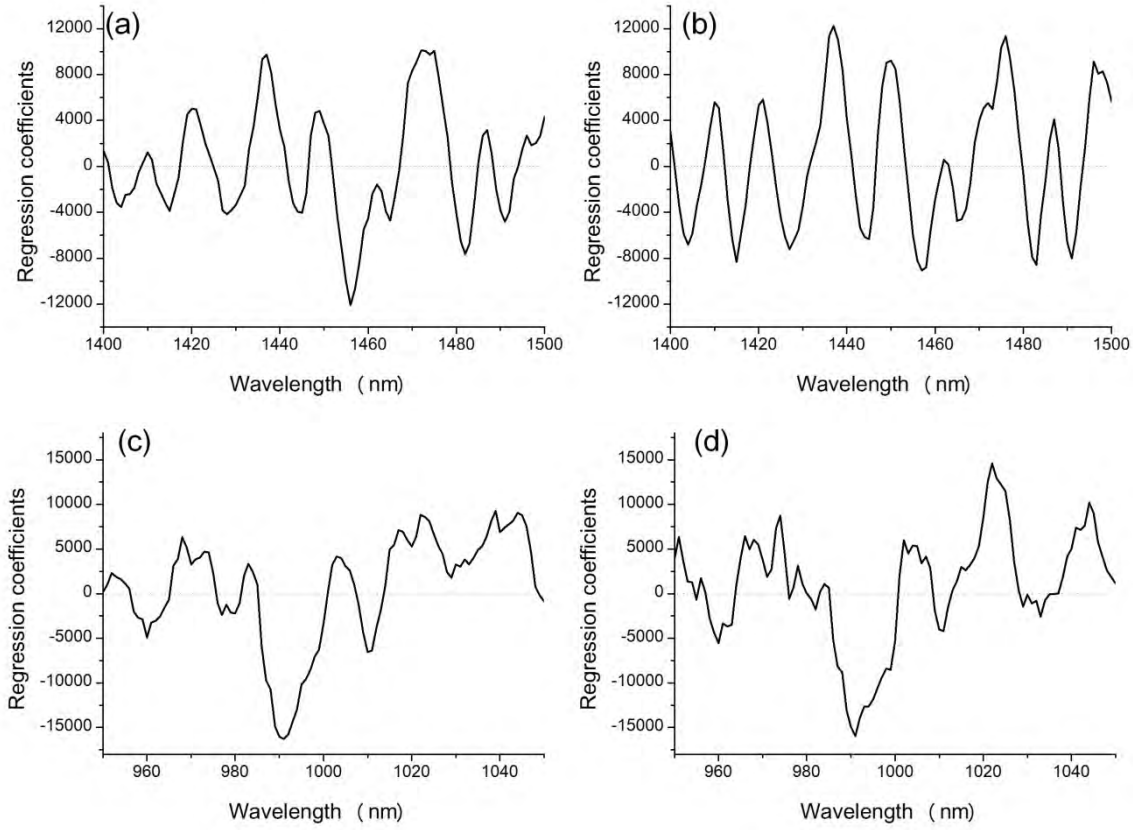

Figure 2-8 Regression vectors of PLS model; (a) DR 1 model, (b) DR 2 model, (c) Tr 1 model, and (d) Tr 2 model.

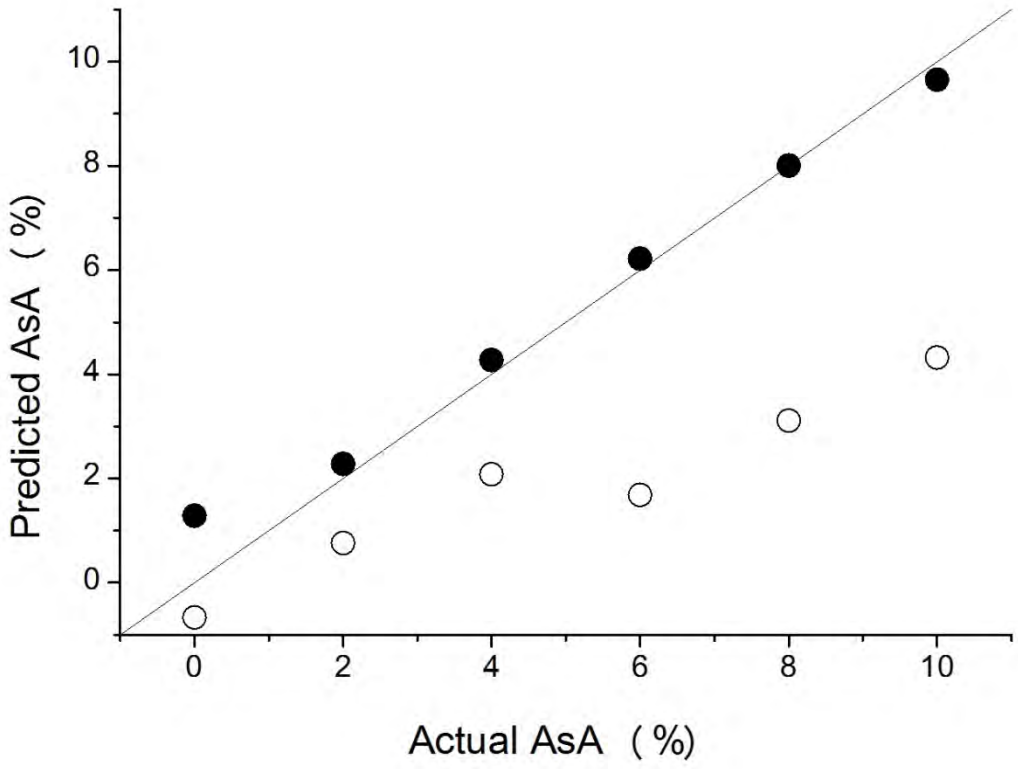

Figure 2-9 Comparison of predicted value of AsA concentration with actual value.

Chapter 3

Application of a Newly Developed Portable NIR Imaging Device to Dissolution Process Monitoring of Tablets

Abstract

We have recently developed a novel portable NIR imaging device (D-NIRs), which has high speed and high wavelength resolution. This NIR imaging approach has been developed by utilizing D-NIRs for studying the dissolution of a model tablet containing 20 % ascorbic acid (AsA) as an active pharmaceutical ingredient (API) and 80 % hydroxypropyl methylcellulose (HPMC), where the tablet is sealed by a special cell. Diffuse reflectance (DR) NIR spectra in the 1000 – 1600 nm region were measured during dissolution of the tablet. An unique band at around 1361 nm of AsA was identified by the second derivative spectra of tablet and used for an NIR imaging of distribution of AsA in it. Two-dimensional change of AsA concentration of the tablet due to water penetration is clearly shown by using the band-based image at 1361 nm of NIR spectra obtained with high speed. Moreover, it is significantly enhanced by using the intensity ratio of two bands at 1361 and 1354 nm corresponding to AsA and water absorption, respectively, showing the dissolution process. The imaging results suggest that the amount of AsA in the imaged area decreases with increasing water penetration. The proposed NIR imaging approach using the intensity of a specific band or the ratio of two bands combined with the developed portable NIR imaging instrument, is a potentially useful practical way to evaluate the tablet at every moment during

dissolution and to monitor the concentration distribution of each drug component in the tablet.

1. Introduction

Process analytical technology (PAT) is a system that controls quality during pharmaceutical manufacturing process.[1-4] The goal of PAT is to ensure final product quality. In-process quality control requires the non-contact, non-destructive, and high-speed techniques. Near-infrared (NIR) spectroscopy combined with chemometrics techniques satisfy these requirements and thus attract attention as a useful PAT tool.[5] Therefore, it has been widely applied to evaluate quantity and quality of tablets. For each pharmaceutical process such as blending, granulation, drying and coating, a number of publications have reported ways to predict quantity of components, evaluate particle size, show the distribution of mixed components, and so on.[5-12] To make PAT more realistic, it is highly desirable to develop NIR instruments with high speed and high wavelength resolution. Moreover, their portability is very important for overcoming the constraints of space in practical situations. Thus, many innovative NIR spectrometers, which satisfy the technical requirements such as high speed and high accuracy, have been developed.[13,14] Our research group has also provided a newly developed NIR spectrometer named P-NIRs.[15] 1 nm wavelength resolution measurement with high accuracy is possible by the developed detector of P-NIRs.[15,16] Thus, P-NIRs seems to be very suitable for various purposes of PAT.

As one of the approaches to product performance of pharmaceutical process, the idea of quality by design (QbD) has also been proposed.[17-19] For QbD of the oral medication, the monitoring and evaluation of the tablet dissolution process is very important. Conventional dissolution tests in vitro (USP – United States Pharmacopeia) have been performed to evaluate the release and dissolution of active pharmaceutical ingredient (API) from a dosage formulation. However, these dissolution tests are destructive, time-consuming, and only yield a total amount of dissolved drug for one tablet or several tablets. Moreover, it does not provide direct insight into the internal structure and the mechanism of drug release during the dissolution, such as water sorption and drug diffusion.

In recent years, therefore, a number of novel imaging approaches have been proposed to monitor the behavior of a pharmaceutical tablet during dissolution.[17-21] These new approaches specifically study tablet dissolution based on two or three-dimensional monitoring by several spectroscopic imaging such as visible (Vis) and FTIR spectroscopic imaging. Bettini, et al (2001) described the physical changes of a tablet upon water intake using visible photography.[17] However, visible images and images based on them are only surface sensitive, so that these data do not provide correct qualitative and quantitative insights. FTIR spectroscopic imaging with high quantitative

and chemical sensitivity is superior to visible imaging in many aspects.[18] FTIR imaging has also shown that obtaining information on the spatial distribution of components during dissolution over time is possible.[19] Therefore, Kazarian and Van der Weerd (2008) investigated differences in the release time between components during tablet dissolution by using both FTIR-ATR and visible images to assess the mechanism of tablet dissolution and drug release.[20,21]

For the NIR region, although Hattori and Otsuka (2011) reported an NIR study of an interaction during the penetration of water into a tablet using a combined method of two dimensional correlation spectroscopy (2DCOS) and perturbation-correlation moving window (PCMW) method,[22,23] they did not describe the characteristics of the 2D spectra during the dissolution. Development and application of NIR imaging based on polychromator type spectrometer for industrial situation is relatively slow compared with FTIR spectroscopic imaging, though NIR imaging has some advantages over FTIR imaging.[24,25] NIR imaging can use an optical fiber and non-contact mode, and it is very suitable for probing thick samples. Therefore, it is very likely that NIR imaging is powerful for distribution analysis of a tablet and monitoring of tablet dissolution, which is an application that can be studied with the development of NIR imaging. The NIR imaging has advantages for distribution monitoring in a tablet and NIR imaging devices

are widely used for laboratory based analysis.[25-29] The ability to visualize and the quantitative result for concentration with high accuracy during tablet dissolution were provided.[28,29] However, NIR imaging devices which are available in the practical situation are still under developing, so that the evaluation method of tablet dissolution with clear visualization has not been fully established. Especially, to our best knowledge, there has been no portable NIR imaging system as pharmaceutical industrial monitoring tool.

In the present paper, therefore, an application of a novel portable NIR imaging device (D-NIRs) to monitor the dissolution process of tablets is reported.[30] D-NIRs is a compact 151 mm × 93 mm × 120 mm portable NIR imaging instrument. It allows imaging with relatively high speed (in the case of 1 mm spatial resolution, 50 seconds speed per 100 pixel), high wavelength resolution (1 nm), and maximum spatial resolution (0.025 mm per pixel). This instrument is useful not only for PAT, but also for other various industrial applications. We demonstrate the potential of this instrument in monitoring dissolution processes of tablets. We can visualize a tablet dissolution process and probe proceeding variations in the concentrations of tablet components using a single wavelength based imaging or a ratio of intensities of two bands based imaging.

2. Materials and Methods

2.1 Sample

Powder samples of ascorbic acid (AsA, Kanto Chemical Co, Ltd., Tokyo, Japan) and hydroxypropyl methylcellulose (HPMC, Wako Pure Chemical Industries, Ltd., Osaka, Japan) were used as materials for analytical tablets. Both of the reagents used were of analytical grade. Chemical structures of AsA and HPMC are illustrated in Figure 3-1. In the present study, instead of an actual API component, AsA was defined as the API. The average particle sizes of AsA and HPMC were 300 and 80 μm, respectively.

The sample tablets composed of 20 w% AsA and 80 w% HPMC were prepared by pressure bonding method with a single punch tableting machine (Handtab-100, Ichihashi Seiki Co. Ltd., Kyoto, Japan). Thickness of each tablet was 1.0 mm ± 0.1 mm, and its diameter was ⌀ = 8 mm.

2.2 NIR Imaging Device

In the present study, a newly developed portable NIR imaging device (D-NIRs) for collection of NIR spectra was used. The design and performance of D-NIRs are reported in our previous article.[30] Although the maintenance space of D-NIRs including a NIR spectrometer (P-NIRs), an imaging unit and a power source unit is 250 mm × 100 mm × 120 mm, the portable imaging unit requires only 191 mm × 93 mm × 120 mm in space.

The optical system of D-NIRs depends on P-NIRs, which is equipped with a 640 elements high density photo diode detector and a charge amplifier.[15,16] It can obtain spectra in the 1000 – 1600 nm region with a 1 nm spectral resolution in just a few seconds. Moreover, P-NIRs has a high portability (250 mm × 100 mm × 120 mm), and thus, P-NIRs itself has a high efficiency for application of process monitoring.

The imaging unit of D-NIRs consists of light sources and a pair of Galvano-mirror (approximately 2 mm × 2 mm). D-NIRs uses three halogen lamps of 5 W to acquire the sufficient incident energy for the collection of high accuracy spectral data. Each incident light focuses on a sample, and DR light obtained from the sample reaches Galvano-mirrors. These mirrors move to the direction of x- and y-axis, respectively, by two motors, and then the two dimensional spectral imaging data in the whole spectral region between 1000 – 1600 nm are obtained by a line scanning system. Although the available maximum measurement area of D-NIRs is 10 mm × 10 mm, the focused area is 6 mm × 6 mm because of the constraint of the location of three lamps. However, the design based on the combination of lamps and mirrors not only contributes to the portability of D-NIRs but also enables high-speed data acquisition at approximately 50 sec/100 pixels (in the case of 1 mm spatial resolution). The maximum spatial resolution of D-NIRs achieves 0.025 mm/pixel due to the special mechanical design for focus.

2.3 Tablet Cell Design

The construction of a developed tablet cell is shown in Figure 3-2 (a). The cell consists of two cover metals (top and bottom) onto which transparent BaF_2 windows are fixed. A tablet is clamped between the two windows. It is surrounded by a Teflon spacer that is slightly thicker than the tablet, so that a sealed compartment is formed. Water is supplied from the top hole of the cell and reaches the side of tablet through the hole on the top window. As shown in Figure 3-2 (b), this cell is set on a sample stage of D-NIRs.

Figure 3-3 displays visible images of tablet dissolution measured at 0 and 300 min from the start of water supply. Because the top metal has Φ10 mm cavity area in the center part, two-dimensional NIR spectral image of the tablet can be acquired through the cavity using D-NIRs.

2.4 Measurement Conditions and Spectra Acquisition

DR spectra in the 1000 – 1600 nm region of each pixel in a tablet were obtained by D-NIRs. Each measurement was carried out with about 20 min interval, and a field of view (FOV) was 10 mm × 10 mm. A spatial resolution (pixel size) was determined to be

300 μm, which corresponded to the average particle size of AsA. The NIR spectra acquisition was started immediately after water had been supplied into the cell, and the spectra measurement was continued up to 300 min. The tablet cell was positioned in the direction of the D-NIR from the mirror of D-NIRs as shown in Figure 3-3 (b). A working distance of 55 mm between the tablet and D-NIRs was maintained throughout all spectral measurements. The charge time for each measurement was 30 msec, and 100 repetitions for each time were carried out to ensure adequate accuracy of the spectra obtained from the tablet.

2.5 Data analysis

The spectral data was collected with Image controller (ver. 10.16, Yokogawa, Co. Tokyo, Japan) software and transferred into files for the Unscrambler (ver. X: CAMO, AS, Trondheim Norway) software. The obtained DR spectra were converted to spectra with absorbance ($\log(1/D_{ref})$) values, where D_{ref} is the diffuse reflectance obtained from the sample.[31] This absorbance was calculated by based on Kubelka-Munk formation that describes about relation among absorbance, diffuse reflectance and scattering of incident light. To search for an informative spectral region and/or a specific band by the effect of band separation, these spectra were subjected to a second derivative procedure

(21 points), including Savitzky-Golay smoothing of 2nd order polynomial.[32] A two-dimensional spectroscopic image was obtained by plotting the 2nd derivative intensities located at 1361 nm in the two-dimensional plane.

3. Results and Discussion

3.1 NIR spectra of AsA and HPMC in powder forms

Figure 3-4 shows NIR spectra in the region of 1000 – 1600 nm of powdered AsA, HPMC and water subjected to baseline offset procedure of water. The water was purified by Ultrapure water system (PureLab/PureLite PRB-002A, ORGANO, Co., Tokyo, Japan). It was dropped on the micro slide grass, and its spectrum was measured, individually. The spectrum of water was obtained by applying shorter charge times than those of others to avoid the saturation of spectrum. A broad absorption band of water in the 1400 - 1550 nm region is assigned to the first overtone of OH stretching, combination of OH symmetric and antisymmetric stretching modes.[33] Although a band associated with the OH stretching mode also appears in the spectrum of HPMC, it is completely overlapped with the water band.[34] In addition, a small broad absorption in the region of 1100 – 1300 nm is assigned to the second overtones of CH stretching vibrations of HPMC.[35] On the other hand, narrow bands of AsA at around 1361 and 1451 nm may be due to the first overtones of stretching vibrations of free and

inter-molecular hydrogen-bonded OH groups, respectively.[36] A broad absorption in the 1150 – 1250 nm region of AsA may also be assigned to CH stretching vibrations.[36]

3.2 NIR spectra and their second derivative spectra of sample tablets during dissolution process

NIR spectra and their second derivative spectra of the tablet at a point of *X*: 4.5 mm, *Y*: 1.5 mm during dissolution process are shown in Figure 3-5 (a) and (b), respectively. For the location of this point, an example of NIR image developed by the intensity of the absorbance at 1361 nm is shown in Figure 3-5 (c). The absorbance of a broad band in the 1400 – 1600 nm region increases with the expansion of bandwidth (Figure 3-5). It is found from the second derivative spectra that three bands exist at 1451, 1432, and 1420 nm in this region. However, a major reason for the intensity increase is water absorption because it increases with elapsed time. A time-dependent change in the 1150 – 1300 nm region is not clear. Recognition of the band at around 1361 nm from the original spectra was not so easy, because it exists as a shoulder band. However, it is possible to identify it as an unique band of AsA from the second derivative spectra.

Figure 3-6 displays expanded second derivative spectra in the 1380 – 1330 nm region. In this region, it is important to note that two bands appear. One of them observed at a

shorter wavelength (1354 nm) probably depends on the water absorption because its intensity increased with the elapsed time. To avoid overlapping with the bands due to water and HPMC, the band at 1361 nm due to AsA is selected for imaging.

3.3 Single wavelength-based imaging

Figure 3-7 (a) plots the intensity at 1361 nm of the second derivative spectra at several different points in the tablet versus the dissolution time. For reference of these points, the NIR images mapped by absorbance at 1361 nm are shown in Figure 3-7 (b). At around the center part (*X*: 4.0 mm, Y: 4.0 mm), the intensity at 1361 nm is almost constant, but at other points a linear decrease in the intensity is observed for the whole dissolution time. If these observed linear responses would follow the Beer-Lambert law, the intensity change of the band at 1361 nm may correspond to the change in the AsA concentration in the tablet.

Figure 3-8 exhibits changes in the distribution of the band intensity at 1361 nm with the elapsed time. The image contrast is based on the intensity at 1361 nm, a higher intensity corresponding to darker blue. As expected, the color of the right and left bottom parts of inside had become brighter than the initial color before the tablet dissolution was started. The result, therefore, suggests that the AsA concentration

decreases linearly upon water penetration, a phenomenon which could not be observed by visible images.

However, the second derivative intensity of the tablet edge was approximately 0 or higher than 0, showing that the concentration of AsA does not change from the initial time. As mentioned above, the light sources of D-NIRs focus on the inside of around 6 mm × 6 mm, so that the intensity of the outside of the focused area of the tablet decreases.

3.4 Peak height ratio-based imaging

In Figure 3-9, images developed by the peak-height ratio of two bands at 1361 and 1354 nm are given. The intensity ratio of two bands (I1361/I1354) is associated with the dissolution process and can avoid the edge effect as discussed above. The difference in the contrast of the inside of tablet for the peak-height ratio based image (I1361/I1354) is clearly larger than that of the single wavelength based images (cf. Figure 3-8). Moreover, as expected, the edge effect that is dependent on the design of the light source locations of D-NIRs could be avoided; the contrast of the outside is obviously drowned. Hence, it is very likely that the peak-height ratio based imaging is more effective than the single wavelength based imaging. In that case, bands used for the

peak-height ratio calculation must clearly be understood by second derivative procedure as in the case of the present study.

The results thus obtained may provide a potentially useful practical way to evaluate the tablet at every moment during dissolution and to monitor the concentration distribution of each component in the tablet. Moreover, although the portability is not necessarily required for fundamental investigation of tablet, this feature of D-NIRs will allow not only dissolution monitoring but also the industrial application to the pharmaceutical process.

4. Conclusion

The paper has reported an application of a new portable NIR imaging device (D-NIRs) in relation to the dissolution process of the tablets for the requiments of PAT and/or QbD. NIR spectra in the 1000 – 1600 nm region of the model sample tablets containing 20 wt% AsA as an API and 80 wt% HPMC were measured during the dissolution process up to 300 min. A band at 1361 nm could clearly be identified in the second derivative spectra of the sample tablets as the unique band for AsA. As expected, the color contrast in the images of the tablet dissolution had changed before it was started, and this result was enhanced significantly by using peak height ratio-based

images. The understanding of tablet dissolution processes such as the degree of water penetration into a tablet can be advanced by NIR imaging.

The results obtained in this study have demonstrated that NIR imaging using spectral changes, such as the change in the band intensity at 1361 nm and the change in the peaks-height ratio, is a powerful tool for the evaluation of the dissolution process of a tablet. In the near future, we plan to measure NIR imaging under flow of water and to evaluate the improved D-NIRs which are equipped with the four halogen lamps for practical tablet dissolution applications.

5. References

1. Bakeev KA (2005) Process analytical technology-spectroscopic tools and implementation strategies for the chemical and pharmaceutical industries. Blackwell, London
2. Hinz CD (2006) Process analytical technologies in the pharmaceutical industry the FDA's PAT initiative. Anal Bioanal Chem 384: 1036-1042
3. International conference on harmonisation of technical requirements for registration of pharmaceuticals for human use (2009) ICH Harmonised Tripartite Guideline Pharmaceutical Development Q8 (R2)
4. Rathore SA, Bhambure R, Ghare V (2010) Process analytical technology (PAT) for biopharmaceutical products. Anal Bioanal Chem 398:137-154
5. Ozaki Y (2012) Near-infrared spectroscopy- Its versatility in analytical chemistry. Anal Sci 28: 545-562
6. Trafford AD, Jee RD, Moffat AC, Graham P (1999) A rapid quantitative assay of intact paracetamol tablets by reflectance near-infrared spectroscopy. Analyst 124: 163-167
7. Andersson M, Folestad S, Gottfries J, Johansson MO, Josefson M, Wahlund KG (2000) Quantitative analysis of film coating in a fluidized bed process by in-line

NIR spectrometry and multivariate batch calibration. Anal Chem 2099–2108

8. Rantanen J, Räsänen E, Tenhunen J, Lansakosli M, Mannermaa JP, Yliruusi J (2000) In-line moisture measurement during granulation with a four-wavelength near infrared sensor: an evaluation of particle size and binder effect. Eur J Pharm Biopharm 50: 271-276
9. Ufret C, Morris K (2001) Modering of powder blending using on-line near infrared measurements. Drug Dev Ind Pharm 27: 719-729
10. Li W, Worosila GD, Wang W, Mascaro T (2005) Determination of polymorphconversion of an active pharmaceutical ingredient in wet granulation using NIR calibration models generated from the premix blends. J Pharm Sci 94: 2800–2806
11. Roggo Y, Chalus P, Manurer L, Martinez CL, Edmond A, Jent N (2007) A review of near infrared spectroscopy and chemometrics in pharma ceutical technology. J Pharm Biomed Anal 44(3): 683-700
12. Kogermann K, Aaltonen J, Strachan CJ, Pollanen K, Heinamaki J, Yliruusi J, Rantanen J (2008) Establishing quantitative in-line analysis of multiple solid-state transformations during dehydration J Pharm Sci 97:4983–4999
13. Siesler HW, Ozaki Y, Kawata S, Heise HM (2002) Near-infrared spectroscopy

Wiley-VCH, Weinheim

14. Ozaki Y, Morita S (2009) Encyclopedia of applied spectroscopy Wiley-VCH, Weinheim

15. Komiyama M, Sanpei Y, Miura A, Sakakibara K, Yakihara T, Fujita T, Kobayashi S, Oka S, Akasaka Y (2003) US Patent 6,552,325 B1

16. Murayama K, Genkawa T, Ishikawa D, Komiyama M, Ozaki Y (2013) A polychromator-type near-infrared spectrometer with a high-sensitivity and high-resolution photodiode array detector for pharmaceutical process monitoring on the millisecond time scale. Rev Sci Instrum 84: 023104

17. Bettini R, Catellani PL, Santi P, Massimo G, Peppas PN, Colombo P (2001) Translocation of drug particles in HPMC matrix gel layer: effect of drug solubility and influence on release rate. J Control Release 70: 383–391

18. Gao P, Meury RH (1996) Swelling of hydroxypropyl methylcellulosematrix tablets. 1. Characterization of swelling using a novel optical imaging method. J Pharm Sci 85: 725–731

19. Kimber JA, Kazarian SG, Štěpánek F (2012) Formulation design space analysis for drug release from swelling polymer tablets. Powder Technology 236: 179–187

20. Van der Weerd J, Kazarian SG (2004) Combined approach of FTIR imaging and

conventional dissolution tests applied to drug release. J Control Release 98: 295–305

21. Kazarian SG, Van der Weerd J (2008) Simultaneous FTIR spectroscopic imaging and visible photography to monitor tablet dissolution and drug release. Pharma Research 25(4): 853-860
22. Otsuka M, Tanabe H, Osaki K, Otsuka K, Ozaki Y (2007) Chemoinformetrical evaluation of dissolution property of indomethacin tablets by near-infrared spectroscopy. J Pharm Sci 96: 788-801
23. Morita S, Shinzawa H, Noda I, Ozaki Y (2006) Perturbation-correlation moving-window two-dimansional correlation spectroscopy. Appl Spectrosc 60: 398-406
24. Šašić S, Ozaki Y (2009) Raman, Infrared, and Near-Infrared chemical imaging. Wiley, New York
25. Lewis NE, Schoppelrei J, Lee E (2004) Near-infrared chemical imaging and the PAT initiative-NIR-CI adds a completely new dimension to conventional NIR spectroscopy-. spectroscopy 19(4): 28-34
26. EL-Hagrasy AS, Morris HR, D'amico F, Lodder RA, Dernnen JK Ⅲ (2001) Near-infrared spectroscopy and imaging for the monitoring of powder blend

homogeneity. J Pharm Sci 90(9): 1298-1307

27. Amigo JM, Ravn C (2009) Direct quantification and distribution assessment of major and minor component in pharmaceutical tablets by NIR-chemical imaging. European J Pharm Sci 37(2):76-82

28. Lewis EN, Carroll JE, Clarke FM (2001) A near-infrared view of pharmaceutical formulation analysis. NIR News 12(3): 16-18

29. Awa K, Okumura T, Shinzawa H, Otsuka M, Ozaki Y (2008) Self-modeling curve resolution (SMCR) analysis of near-infrared (NIR) imaging data of pharmaceutical tablets. Anal Chem Acta 619:81-86

30. Ishikawa D, Murayama K, Genkawa T, Awa K, Komiyama M, Ozaki Y (2012) Development of compact near infrared imaging device with high-speed and portability for pharmaceutical process monitoring. NIR News 23(8): 14-17

31. Griffiths PR, Olinger MJ (2002) In: Chalmers JM, Griffiths PR (ed) Handbook of vibrational spectroscopy, vol.1. Wiley, New York

32. Savitzky A, Golay MJE (1964) Smoothing and differentiation of data by simplified least squares procedures. Anal Chem 36 (8): 1627–1639

33. Kasemsumran Y, Du P, Murayama K, Huehne M, Ozaki Y (2004) Near-infrared spectroscopic determination of human serum albumin,-globulin, and glucose in a

control serum solution with searching combination moving window partial least squares. Anal Chim Acta 512: 223-230

34. Sahoo S, Kanti C, Mishra CS, Naik S (2011) Analytical characterization of a gelling biodegradable polymer. Drug Invention Today 3(6): 78-82

35. Pérez-Ramos DJ, Findlay PW, Peck G, Morris RK (2005) Quantitative analysis of film coating in a pan coater based on in-line sensor measurements. AAPS Pharma Sci Tech 6(1): 127-136

36. Lui H, Xiang BR, Qu LB (2006) Structure analysis of ascorbic acid using near-infrared spectroscopy and generalized two-dimensional correlation spectroscopy Molecular Structure 794:12-17

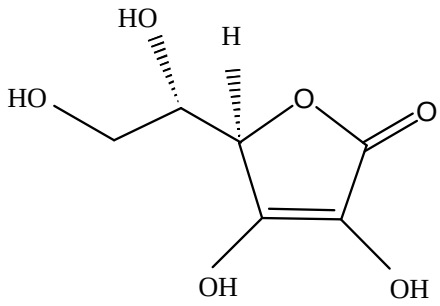

AsA ($C_6H_8O_6$)

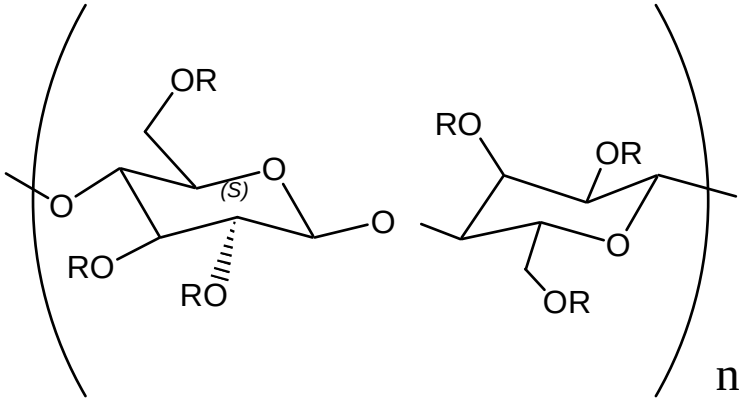

R=-H,-CH_3,-CH_2-CHOH-CH_3

HPMC

Figure 3-1 Chemical structures of ascorbic acid (AsA) and hydroxypropyl methylcellulose (HPMC)

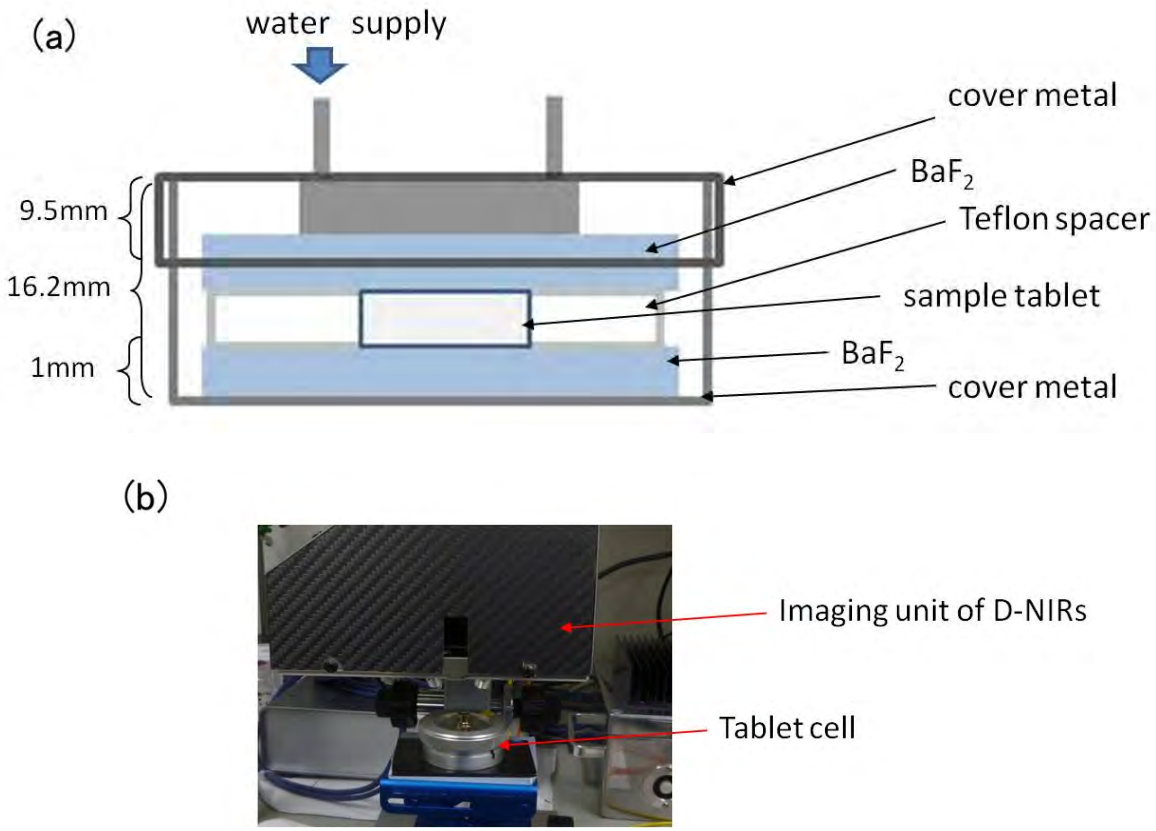

Figure 3-2 (a) A schematic diagram of the tablet cell, and (b) a photo the picture showing the arrangement of the tablet cell and D-NIRs.

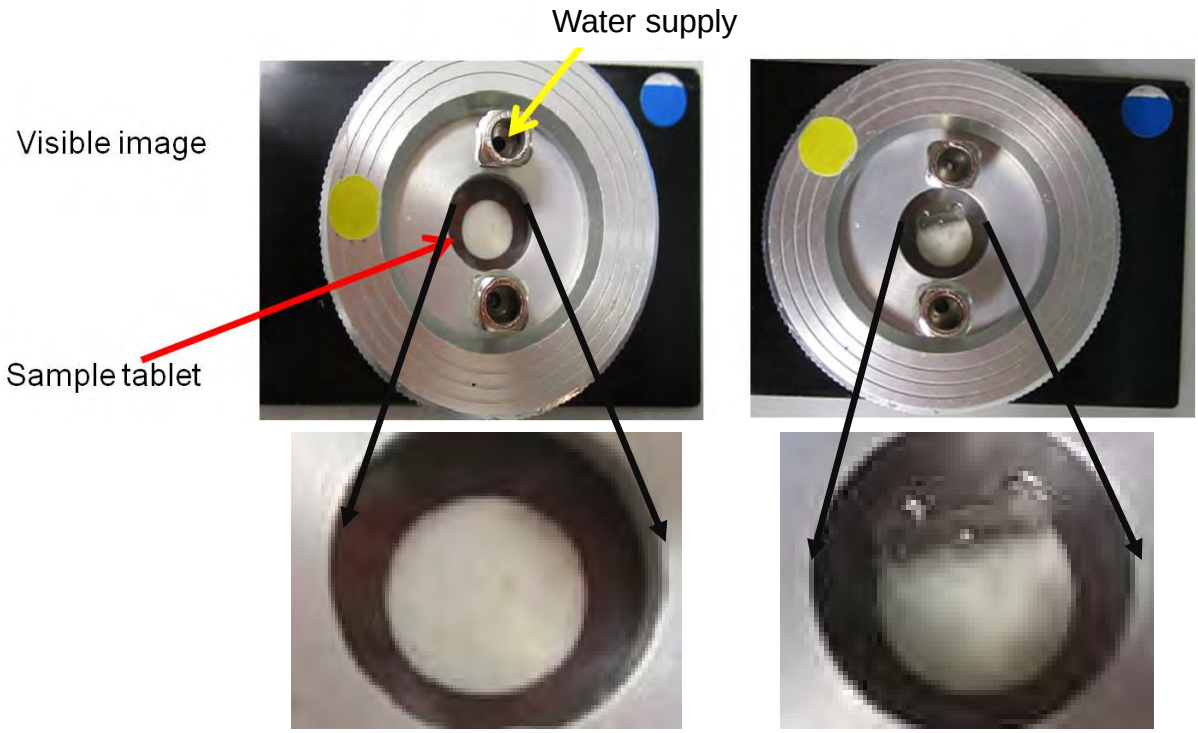

Figure 3-3 Visible images of tablet dissolution measured at 0 and 300 min from the start of water supply.

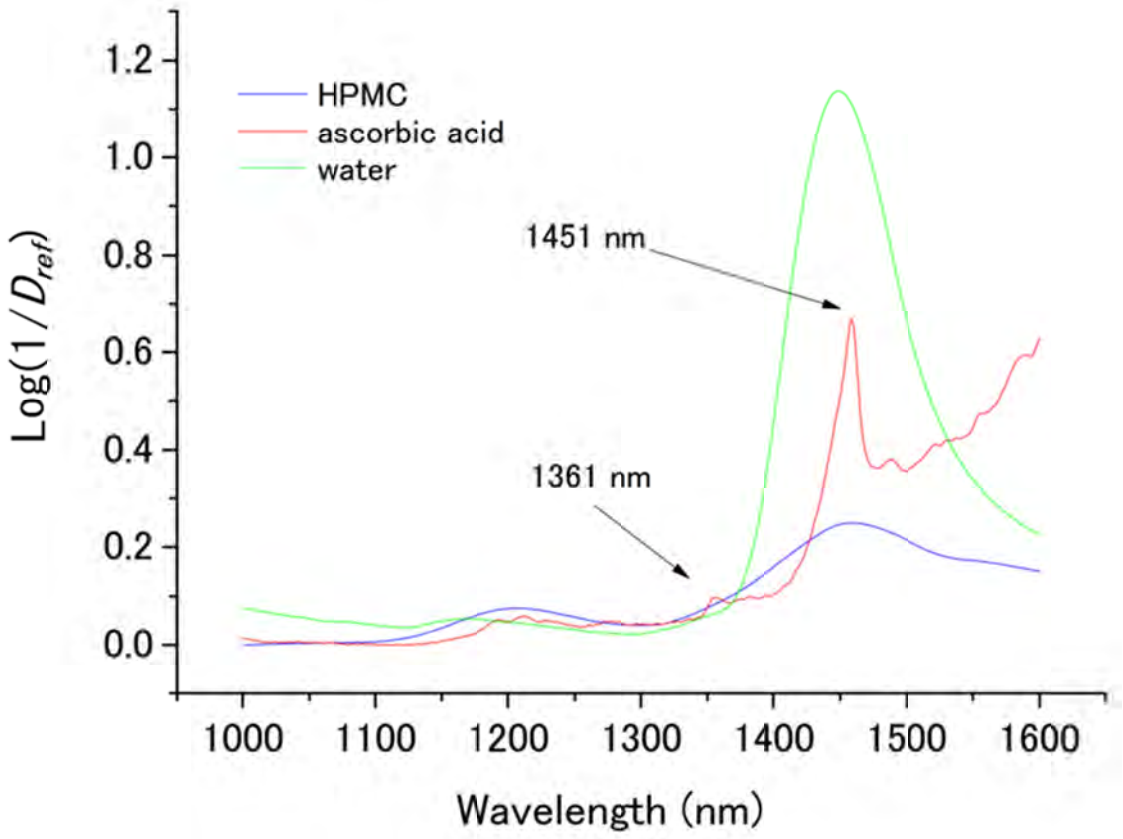

Figure 3-4 NIR spectra in the 1000 - 1600 nm region of AsA, HPMC powder and water.

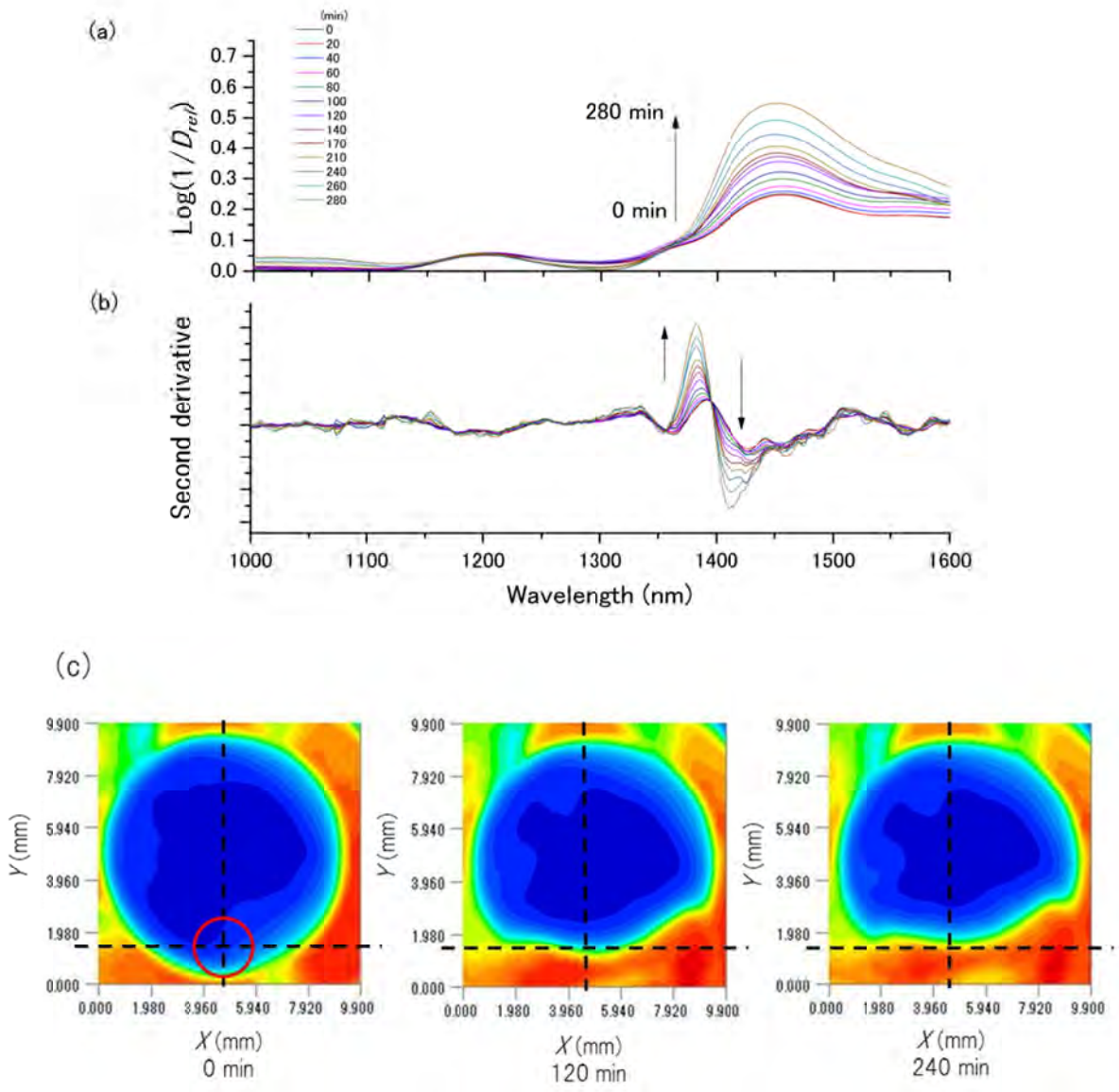

Figure 3-5 Time- dependent changes of (a) NIR spectra and (b) their second derivative spectra of the tablet dissolution process at a point of *X*: 4.5 mm, *Y*:1.5 mm. (c) NIR images of the point mapped at 0, 120, and 240 min by the absorbance of 1361 nm due to AsA.

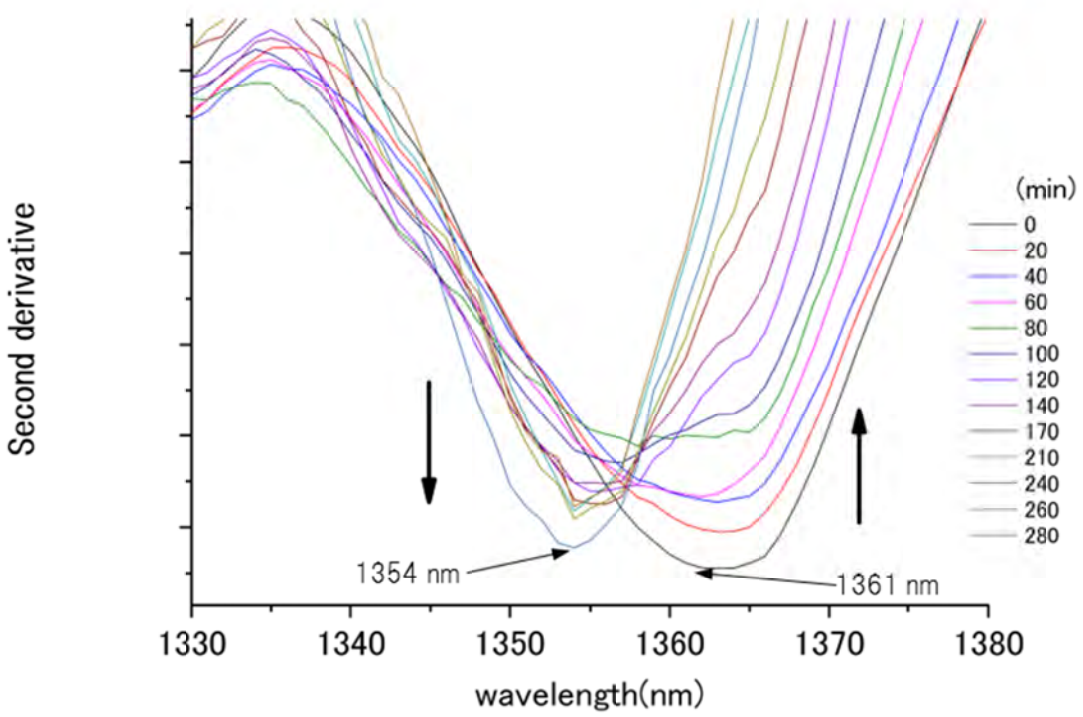

Figure 3-6 Time-dependent variations in enlarged second derivative spectra in the region of 1330 – 1380 nm of tablet dissolution process at the point of *X*: 4.5 mm, *Y*:1.5 mm with elapsed time

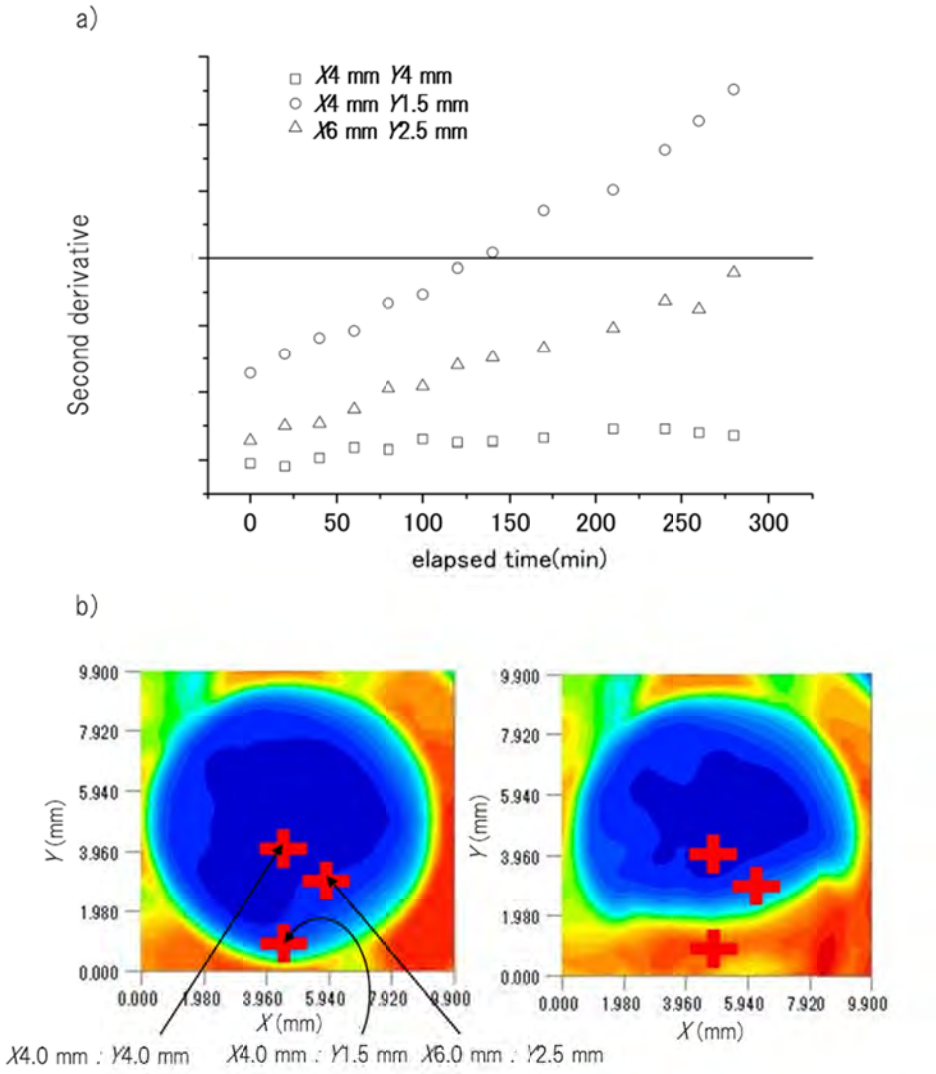

Figure 3-7 (a) Plots of the second derivative peak intensity at 1361 nm due to AsA in the second derivative spectra at several different points of *X*4.0 mm: *Y*4.0 mm, *X*4.0 mm: *Y*1.5 mm, and *X*6.0 mm: *Y*2.5 mm versus the elapsed time and (b) the images mapped at 0 and 240 min using the absorbance at 1361 nm.

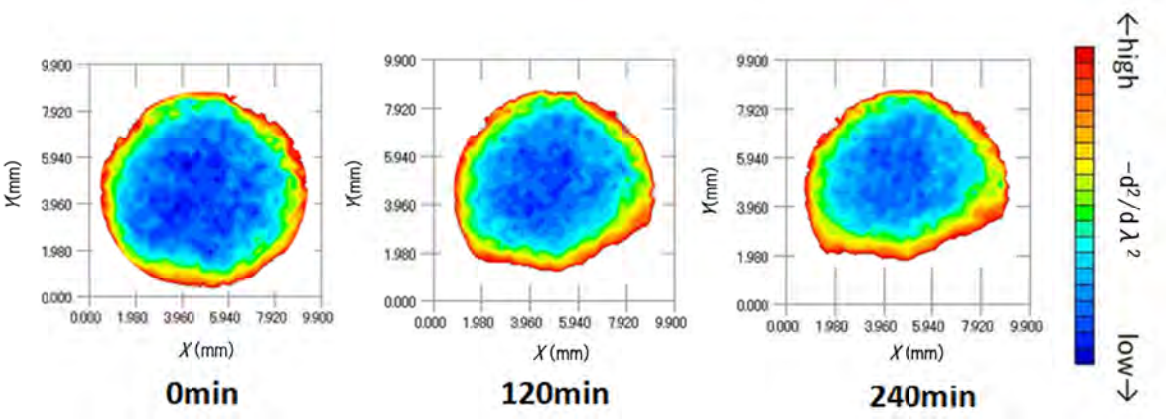

Figure 3-8 Changes in the single wavelength based-image of sample tablet dissolution process developed by using the second derivative intensity at 1361 nm due to AsA. These second derivative images were modified by arbitrary threshold to delete the color except the tablet part.

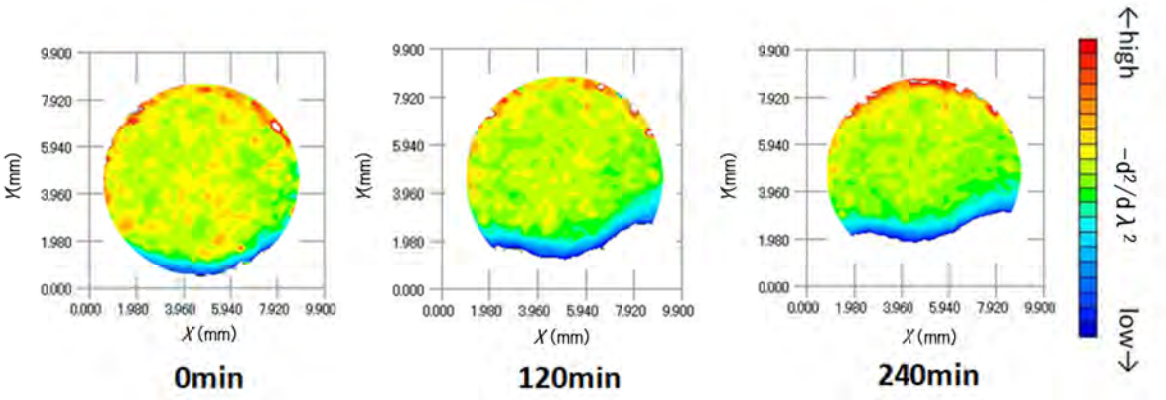

Figure 3-9 Changes in the peak-height ratio-based image of tablet dissolution developed by using the second derivative intensities at 1361 and 1354 nm due to AsA and water, respectively. These ratio images were modified by arbitrary threshold to delete the color except the tablet part.

Chapter 4

Image Monitoring of Pharmaceutical Blending Processes and the Determination of an End Point by Using a Portable Near-Infrared Imaging Device Based on a Polychromator-Type Near-Infrared Spectrometer with a High-speed and High-Resolution Photo Diode Array Detector

Abstract

In the present study a new version (ND-NIRs) of a polychromator-type near-infrared (NIR) spectrometer with a high-resolution photo diode array detector was developed, which a previously constructed (D-NIRs). The new version has four 5 W halogen lamps compared with the three lamps for the older version. The new version also has a condenser lens with a shorter focal point length. The increase in the number of the lamps and the shortening of the focal point of the condenser lens realize high signal-to-noise ratio and high-speed NIR imaging measurement. By using the ND-NIRs, the in-line monitoring of pharmaceutical blending was carried out and determined an end point of the blending process. Moreover, to determinate a more accurate end point, a NIR image of the blending sample was acquired by means of a portable NIR imaging device based on ND-NIRs. The imaging result has demonstrated that the mixing time of 8 minutes is enough for homogeneous mixing. In this way the present study has demonstrated that ND-NIRs and the imaging system based on a ND-NIRs hold considerable promise for process analysis.

1. Introduction

In modern pharmaceutical industries, the idea of new quality management has been proposed for the delivery of reliable pharmaceutical products. The idea is the quality by design (QbD) approach. QbD is an approach that clarifies the factors which significantly influence the quality properties of the medicine from the stage of the formulation design and the process design, and it carries out the quality control based on a scientific basis.[1] Process analytical technology (PAT) is used to analyze the manufacturing process, determine the factors essential for understanding the manufacturing process, and clarify variable factors that affect quality control.[2,3] PAT is positioned as a powerful technology to achieve the QbD approach. To evaluate the quality of an oral medication, the monitoring of component distribution including that of active pharmaceutical ingredient (API) is essential. It is well known that spectroscopic technology is attractive for the non-destructive monitoring of pharmaceutical tablets.[3-11] Evaluation methods for inhomogeneity in a tablet based on ultraviolet-visible (UV-Vis) spectroscopy and high performance liquid chromatography (HPLC) were developed about two decades ago.[10,11] However, the UV-Vis spectroscopy methods are usually based on destructive methods, so there are only a few reports on the use of UV-Vis spectroscopy in the quantitative analysis of tablet components. Recently

a number of research groups have been involved in the development of vibrational spectroscopy methods for PAT.[4-10] Near-infrared (NIR) spectroscopy in particular has attracted keen interest as a powerful PAT method since it has superior features for real time monitoring; it is a non-destructive and non-contact method.[4,12] Moreover, NIR can use optical fibers, allowing remote-sensing. Imaging techniques in the NIR region have also been developing.[13-19]

In previous studies has been involved in PAT studies through the development of new NIR instruments, particularly, imaging instruments.[15,19-21] We recently developed a distribution type NIR spectrometer (D-NIRs), which is an NIR imaging instrument based on a polychromator-type NIR spectrometer with a high sensitivity and high-resolution photodiode array detector. The portability of D-NIRs is superior. The size of the imaging unit is only 3 liter volume. D-NIRs enables high speed monitoring (25 ms/1 pixel) and high wavelength resolution (1.25 nm) of NIR imaging due to the newly developed InGaAs detector. The detector consists of a high-density PDA containing 640 elements with 20 μm pitch. InGaAs photodiodes with a wavelength sensitivity of 900-1700 nm (photoreceptive sensitivity: 0.8 at 1550 nm) are used.[20]

A NIR image obtained during the water dissolution process of a tablet demonstrated the potential of D-NIRs as a PAT tool.[19,22-24] Of course, NIR images of tablets measured

by using D-NIRs can clarify the distribution and the relative abundance of chemical components in the tablets.[15] It was successfully demosntrated that D-NIRs is an attractive tool for PAT and that it can be applied for QbD.

However, evaluation methods for pharmaceutical blending process based on NIR imaging are still under development, although the blending process can be monitored by NIR spectra[10,11,25] and it was reported that NIR imaging technique can be utilized for studying the effects of the particle sizes of chemical components on the blending process.[26] In addition, the end point of the blending process was determined by using a NIR imaging technique.[27] However, in this case it took long time to get an image and also the wavelength resolution was very low. Thus, it would be highly desirable to develop a NIR imaging system that enables both high speed and high wavelength resolution measurements in NIR imaging.

Quite recently, as a part of the present study we have built a new type of D-NIRs named ND-NIRs. The new type has four 5 W halogen lamps as light sources, that is, one more halogen lamp than the original type. In addition, in the scanning unit of ND-NIRs the focal length of the condenser lens is shortened to optimize the performance of the optical scanning system. The increase in the number of lamps together with the shortening of the focal length has enabled about seven times faster

imaging measurements compared with the original version. The purpose of the present study was to carry out the in-line monitoring of a pharmaceutical blending process and the determination of an end point of this blending process by using a ND-NIRs, polychromator-type NIR spectrometer with high speed and high wavelength resolution. Moreover, to determinate an accurate end point in a short time, a NIR image of the blending sample was acquired by means of a portable NIR imaging device based on ND-NIRs.

2. Experimental Section

2.1 New NIR Imaging Device (ND-NIRs)

A new version of D-NIRs (Yokogawa Electric Co., Tokyo, Japan) has been developed for the collection of NIR imaging spectra. Its imaging unit consists of galvanic mirrors, condenser lenses, a rectangular prism, a fiber-optic cable, and four halogen lamps as shown in Figures 4-1 and 4-2. There are two significant major differences between the original version (D-NIRs) and the new version (ND-NIRs). One is the number of lamps. The new version has four 5 W halogen lamps while the old version had only three. This increase in the number of lamps increased the light quantity significantly. Another important difference between the two versions is the length of the focal point of the condenser lens. The length has become significantly shorter in the new version (70 mm) compared with that in the old version (100 mm), greatly increasing the captured light

quantity. The aperture size of the condenser lens of the new version and the old version was same. The increase in the number of the lamps and shortening of the focal length of the condenser lens achieve high signal-to-noise ratio, enabling high-speed NIR imaging measurement. Figure 4-3 plots a root mean square (RMS) noise of D-NIRs and ND-NIRs at the high-light flux. The RMS noise evaluation test between D-NIRs and ND-NIRs that was carried out in accordance with the US Pharmacopeia.[28] The rms noise level of the old version is 0.5 mAbs/0.5 s, while that of the new version is 0.05 mAbs/0.5 s. The measurement speed of the new version (11 s/100 pixels) has become seven times higher compared with that of the original one (80 s/100 pixels).

It is also notable that the size of the new imaging unit is only 220 mm × 90 mm × 150 mm due to the contribution of these optimized elements in the imaging unit. The irradiation energy from the four halogen lamps reaches a sample, and the diffuse reflected light reaches the galvanic mirror. Finally, this signal is detected by a spectrometer named P-NIRs through the optical fiber. P-NIRs was also developed as a new spectrometer.[20] The high speed spectra mapping of 13 s per 25 mm^2 area of ND-NIRs is due to the P-NIRs. The superior futures of P-NIRs were reported in a previous paper.[20,21] The maximum scan area of ND-NIRs is 10 mm × 10 mm, and its spatial resolution (pixel size) is 25 μm.

2.2 Data Collection

The blending machine was rotated by 15 rpm in 15 min. The spectrometer, P-NIRs, was placed under this machine (Figure 4-4), and when the machine returned to the original position, the DR-NIR spectrum of blending powder was recorded by P-NIRs. The NIR spectra in the 950–1700 nm region were measured with a 1 nm interval, and they were converted to CSV format immediately. These spectral data were subjected to Savitzky-Golay (SG) smoothing and then to second derivative treatment with 19 point, and 2nd order.[30] Imaging measurements of DR-NIR spectra were carried out several times by using a ND-NIRs. DR-NIR spectra at each pixel were obtained by line scanning method, and the peak at 1458 nm due to the first overtone of OH stretching vibration of AsA identified by the point measurement was used for the NIR mapping.

2.3 Sample Preparation

Ascorbic acid (AsA), magnesium stearate and D-mannitol were purchased from Kanto Chemical Co., Inc. (Tokyo, Japan), and their powders were prepared for blending. These materials were introduced into a vessel type blending machine (Tsutsui Scientific Instruments Co., Ltd., Taito-ku, Japan). The outline of the blending test setup is shown

in Figure 4-4. To monitor the blending process, each material was added in the order D-mannitol, magnesium stearate and AsA. Finally, the prepared powder consisted of 88% (w/w) D-mannitol, 2% (w/w) magnesium stearate and 10% (w/w) AsA.

3. Results and Discussion

3.1 NIR Spectra of Ascorbic Acid, D-mannitol and Magnesium Stearate

Figure 4-5 shows (a) diffuse-reflectance (DR) NIR spectra and (b) the second derivative spectra of powder of ascorbic acid (AsA), D-mannitol and magnesium stearate in the 950–1700 nm region. Narrow bands of AsA at around 1361 and 1458 nm may be due to the first overtones of stretching vibrations of free and intermolecular hydrogen-bonded OH groups, respectively.[28] A broad absorption in the 1150–1250 nm region of AsA may be assigned to the second overtones of CH stretching vibrations.[28] A broad absorption in the 1490–1590 nm region of D-mannitol may be assigned to the first overtones of OH stretching vibrations.

3.2 Evaluation of Inhomogeneity During Blending Process by In-Line NIR Spectrometer

Figure 4-6 shows a series of second derivative spectra of the blending sample measured during rotation mixing. The inset of Figure 4-6 depicts the enlargement of the

1445–1475 nm region. It is noted that the peak intensity at 1458 nm due to the first overtone of the OH stretching vibration mode of AsA changes with time. The band of 1458 nm is not detected in the initial stage of the mixing. However, this band becomes strong as mixing proceeds. The spectrum measured at 0 s reflects D-mannitol only; the band at 1495 nm arises only from the first overtone of the OH stretching mode. The intensity at 1495 nm becomes weak with mixing.

Figure 4-7 plots a 5-point moving block standard deviation of the peak intensity at 1458 nm in the second-derivative spectra *versus* time. We also prepared similar plot by using the band at 1495 nm due to D-mannitol. The 1495 nm band gave similar result to the 1458 nm band. It is noted in Figure 4-7 that during the initial stage of mixing, the powder sample in the vessel is inhomogeneous, and therefore, the standard deviation (SD) value is high. As mixing proceeds, the sample becomes homogeneous. Then, the spectra of the mixtures of ascorbic acid, D-mannitol and magnesium stearate as the mixing ratio are detected, and thus, the spectral variation decreases, yielding a low SD value. The result in Figure 4-7 shows that the SD gives a constant value around 168 s after the start of rotation mixing. Thus, it is very likely that the sample in the bottle becomes homogeneous after 168 s.

3.3 Evaluation of Inhomogeneity during Blending Process by NIR Imaging

Figures 4-8, 4-9 and 4-10 depict: (a) images for the distribution of AsA and (b) binary images for mixing times of 1, 8, and 15 min. A binary image is the two color image, it usually consists of white and black color. To determine the color in an image, the arbitrary threshold is defined prior to the visualization from the digital numbers and intensities, *etc* of all pixels. Figure 4-8a–c show the second derivative spectra collected at different points in the two-dimensional spectroscopic image of the blend sample at 1 min after the start of blending. In the measurement of two-dimensional spectroscopic image of blend sample NIR spectra acquisition, second differentiation treatment, and absorbance mapping using specific wavelength were carried out at the same time. The ND-NIRs allows the spectral acquisition in 242 s for a measurement area of 5 mm × 5 mm, spatial resolution 0.1 mm in the wavelength region of 934–1713 nm, with the wavelength resolution of 1 nm. In this system the number of data is 2601 pixels × 780 absorbance data = 202,878 data points. Table 4-1 summarizes the measurement times for various measurement conditions. The results in the table demonstrate that ND-NIRs can provide imaging spectra data at a high speed. Second derivative spectra of one pixel (one point) shown in Figure 4-11 demonstrate that they catch clearly the specific absorption wavelength of 1458 nm due to AsA. These results suggest that ND-NIRs has

high signal-to-noise ratio and high wavelength resolution, enabling the correction of baseline deviation and the band separations without the influence of the increase of noise emphasized by the second derivative treatment. Each point spectrum obtained from the binary images corresponds well to the spectrum of AsA, showing that the sample existing in the points is AsA.

Area ratios (pixel ratios) of AsA and non-AsA from the binary images were calculated, and then estimated the temporal change in the relative amount of AsA. The area ratio of AsA in the binary images of imaging spectra at the mixing time of 1, 8, and 15 min was 1.49%, 9.57%, and 8.74%, respectively. The relative amount of AsA at the mixing time of 8 and 15 min was almost the same as that the initial sample throw amount (10%). On the other hand, the relative amount of AsA at the mixing time of 1 min was much smaller, indicating that the mixing is insufficient. From the present result we can conclude that the mixing time of 8 min is enough for homogeneous mixing.

4. Conclusion

A new version of a polychromator-type NIR spectrometer with a high-resolution photo diode array detector was developed, which we built before (D-NIRs). The new version has achieved a high signal-to-noise ratio and a high speed. The noise level of the

new version is 10 times lower than that of the old version, and the measurement speed of the new version is seven times higher than that of the original one. By using the new version we performed an in-line evaluation of inhomogeneity during a blending process and determined the end point for homogeneous mixing. The evaluation of inhomogeneity during the blending process was also carried out by NIR imaging. Imaging spectra of mixing samples were measured at different times. The NIR imaging revealed that the distribution of AsA in the blend sample changes with time. It has turned out that the mixing time of 8 min is sufficient for homogeneous mixing. The present study has demonstrated that NIR imaging is very useful for further understanding of the result of in-line monitoring of blending process.

5. References

1. International Conference on Harmonisation of Technical Requirements for Registration of Pharmaceuticals for Human Use. ICH Harmonized Tripartite Guideline Pharmaceutical Development Q8 (R2). Available online: http://www.ich.org/fileadmin/Public_Web_Site/ICH_Products/Guidelines/Quality/Q8_R1/Step4/Q8_R2_Guideline.pdf (accessed on 15 January 2015).
2. US Food Drug Administration. Guidance for Industry, PAT: A Framework for Innovative Pharmaceutical Development, Manufacturing, and Quality Assurance. Available online: http://www.fda.gov/downloads/Drugs/Guidances/ucm070305.pdf (accessed on 15 January 2015).
3. Bakeev, K.A. Process Analytical Technology, 1st ed.; Blackwell Publishing: Oxford, UK, 2005; pp. 13–38.
4. Ozaki, Y; Amari, T. Near-Infrared Spectroscopy in Chemical Process Analysis; Sheffield Academic Press: Sheffield, UK, 2000; pp. 53–95.
5. Andersson, M.; Folestad, S.; Gottfries, J.; Johansson, M.O.; Josefson, M.; Wahlund, K.G. Quantitative analysis of film coating in a fluidized bed process by in-line NIR spectrometry and multivariate batch calibration. Anal. Chem. 2000, 72, 2099–2108.
6. Kogermann, K.; Aaltonen, J.; Strachan, C.J.; Pollanen, K.; Heinamaki, J.; Yliruusi,

J.; Rantanen, J. Establishing quantitative in-line analysis of multiple solid state transformations during dehydration. J. Pharm. Sci. 2008, 97, 4983–4999.

7. Li, W.; Worosila, G.D.; Wang, W.; Mascaro, T. Determination of polymorph conversion of an active pharmaceutical ingredient in wet granulation using NIR calibration models generated from the premix blends. J. Pharm. Sci. 2005, 94, 2800–2806.
8. Trafford, A.D.; Jee, R.D.; Moffatand, A.C.; Graham, P. A rapid quantitative assay of intact paracetamol tablets by reflectance near-infrared spectroscopy. Analyst 1999, 124, 163–167.
9. Rantanen, J.; Räsänen, E.; Tenhunen, J.; Känsäkoski, M.; Mannermaa, J.P.; Yliruusi, J. In-line moisture measurement during granulation with a four-wavelength near infrared sensor: An evaluation of particle size and binder effect. Eur. J. Pharm. Biopharm. 2000, 50, 271–276.
10. Sekulic, S.S.; Ward, H.W., II; Brannegan, D.R.; Stanley, E.D.; Evans, C.L.; Sciavolino, S.T.; Hailey, P.A.; Aldridge, P.K. On-Line Monitoring of Powder Blend Homogeneity by Near-Infrared Spectroscopy. Anal. Chem. 1996, 68, 509–513.
11. El-Hagrasy, A.S.; Delgado-Lopez, M.; Drennen, J.K., III. A Process Analytical

Technology approach to near-infrared process control of pharmaceutical powder blending: Part II: Qualitative near-infrared models for prediction of blend homogeneity. J. Pharm. Sci. 2006, 95, 407–421.

12. Ozaki, Y. Near-infrared spectroscopy—Its versatility in analytical chemistry. Anal. Sci. 2012, 28, 545–563.
13. Šašić, S.; Ozaki, Y. Raman, Infrared, and Near-Infrared Chemical Imaging; John Wiley & Sons Ltd.: Hoboken, NJ, USA, 2009.
14. Shinzawa, H.; Awa, K.; Ozaki, Y. Compression induced morphological and molecular structural changes of cellulose tablets probed with near infrared imaging. J. Near Infrared Spectrosc. 2011, 19, 15–22.
15. Ishikawa, D.; Murayama, K.; Genkawa, T.; Awa, K.; Komiyama, M.; Ozaki, Y. Development of compact near infrared imaging device with high-speed and portability for pharmaceutical process monitoring. NIR News 2012, 23, 14–17.
16. Unger, M.; Ozaki, Y.; Siesler, H.W. Variable-Temperature Fourier Transform Near-Infrared (FT-NIR) Imaging Spectroscopy of the diffusion process of Butanol (OD) into Polyamide 11. Appl. Spectrosc. 2011, 65, 1051–1055.
17. Neil Lewis, E.; Schoppelrei, J.; Lee, E. Near-infrared Chemical Imaging and the PAT Initiative-NIR-CI adds a completely new dimension to conventional NIR

spectroscopy. Spectroscopy 2004, 19, 26–36.

18. Gao, P.; Meury, R.H. Swelling of hydroxypropyl methylcellulose matrix tablets. 1. Characterization of swelling using a novel optical imaging method. J. Pharm. Sci. 1996, 85, 725–731.
19. Ishikawa, D.; Murayama, K.; Genkawa, T.; Awa, K.; Komiyama, M.; Sergei, K.; Ozaki, Y. Application of a newly developed portable NIR imaging device to dissolution process monitoring of tablets. Anal. Bioanal. Chem. 2013, 405, 9401–9409.
20. Murayama, K.; Genkawa, T.; Ishikawa, D.; Komiyama, M.; Ozaki, Y. A polychromator-type near-infrared spectrometer with a high-sensitivity and high-resolution photodiode array detector for pharmaceutical process monitoring on the millisecond time scale. Rev. Sci. Instrum. 2013, 84, 023104, doi: 10.1063/1.4790413
21. Ishikawa, D.; Genkawa, T.; Murayama, K.; Komiyama, M.; Ozaki, Y. Feasibility study of diffuse reflectance and transmittance near infrared spectroscopy for rapid analysis of ascorbic acid concentration in bilayer tablets using a high-speed polychromator-type spectrometer. J. Near Infrared Spectrosc. 2014, 22, 189–197.
22. Otsuka, M.; Tanabe, H.; Osaki, K.; Otsuka, K.; Ozaki, Y. Chemoinformetrical

Evaluation of Dissolution Property of Indomethacin Tablets by Near-Infrared Spectroscopy. J. Pharm. Sci. 2007, 96, 788–801.

23. Van der Weerd, J.; Kazarian, S.G. Combined approach of FTIR imaging and conventional dissolution tests applied to drug release. J. Control. Release 2004, 98, 295–305.

24. Kazarian, S.G.; van der Weerd, J. Simultaneous FTIR Spectroscopic Imaging and Visible Photography to Monitor Tablet Dissolution and Drug Release. Pharm. Res. 2004, 25, 853–860.

25. Ufret, C.; Morris, K. Modeling of powder blending using on-line near infrared measurements. Drug Dev. Ind. Pharm. 2001, 27, 719–729.

26. Li, W.; Woldu, A.; Kelly, R.; McCool, J.; Bruce, R.; Rasmussen, H.; Cunningham, J.; Winstead, D. Measurement of drug agglomerates in powder blending simulation samples by near infrared chemical imaging. Int. J. Pharm. 2008, 350, 369–373.

27. El-Hagrasy, A.S.; Morris, H.R.; D'amico, F.; Lodder, R.A.; Drennen, J.K., III. Near-Infrared Spectroscopy and Imaging for the Monitoring of Powder Blend Homogeneity. J. Pharm. Sci. 2001, 90, 1298–1307.

28. Cogdill, R.P.; Anderson, C.A.; Delgado-Lopez, M.; Molseed, D.; Chisholm, R.; Bolton, R.; Herkert, T.; Afnan, A.M.; Drennen, J.K., III. Process Analytical

Technology Case Study Part I: Feasibility Studies for Quantitative Near-Infrared Method Development. AASP Pharm. Sci. Tech. 2005, 6, 262–272.

29. Lui, H.; Xiang, B.; Qu, L. Structure analysis of ascorbic acid using near-infrared spectroscopy and generalized two dimensional correlation spectroscopy. J. Mol. Struct. 2006, 794, 12–17.

30. Savitzky, A.; Golay, M.J.E. Smoothing and differentiation of data by simplified least squares procedures. J. Anal. Chem. 1964, 36, 1627–1639.

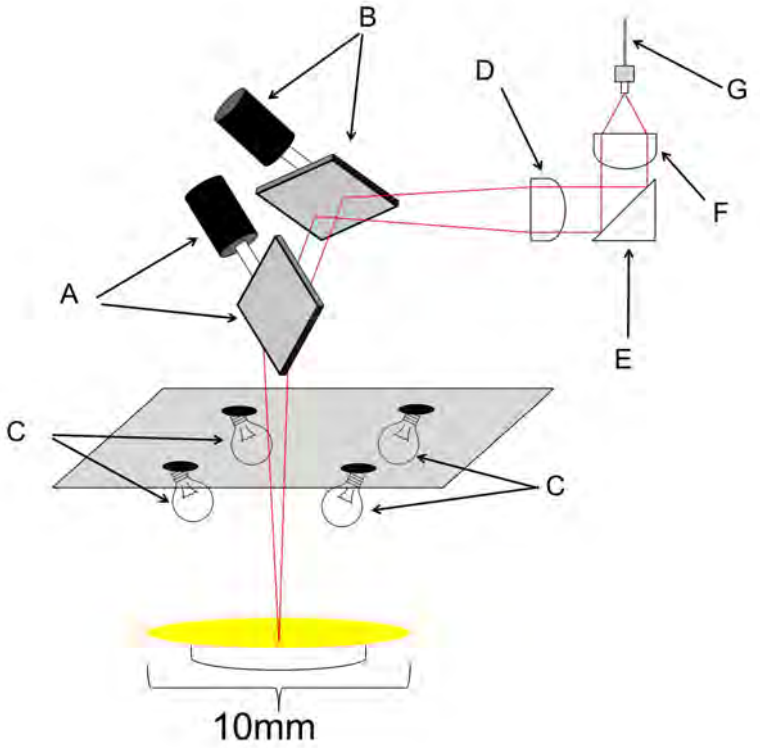

Figure 4-1 Overview of the developed NIR imaging device (ND-NIRs). A: *X* axis galvano mirror, B: *Y* axis galvano mirror, C: 5 W halogen lamp, D: Condensing lens 1, E: Right angle prism mirror, F: Condensing lens 2, G: Optical fiber cable.

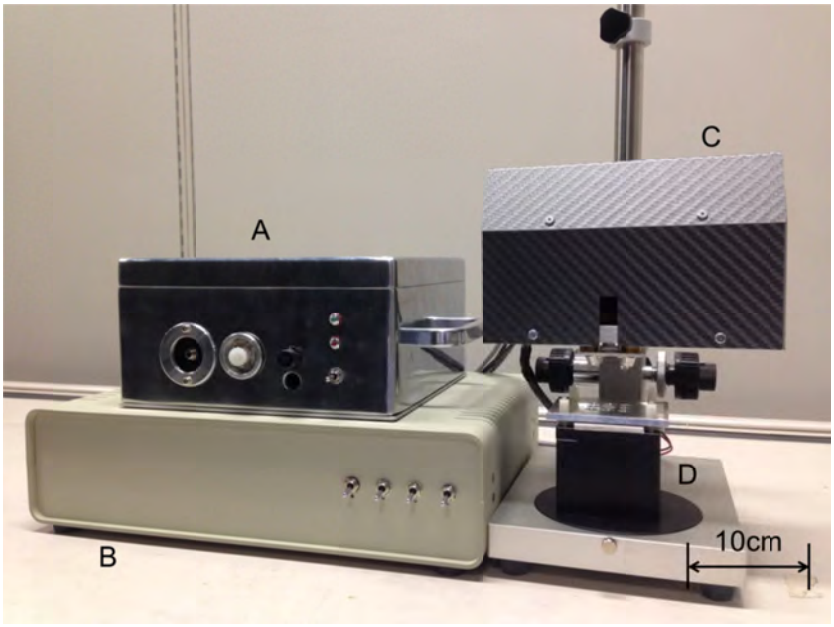

Figure 4-2 Outline of D-NIRs. A: P-NIRs, B: XY scanning unit, C: control unit, D: Sample plinth with temperature control function.

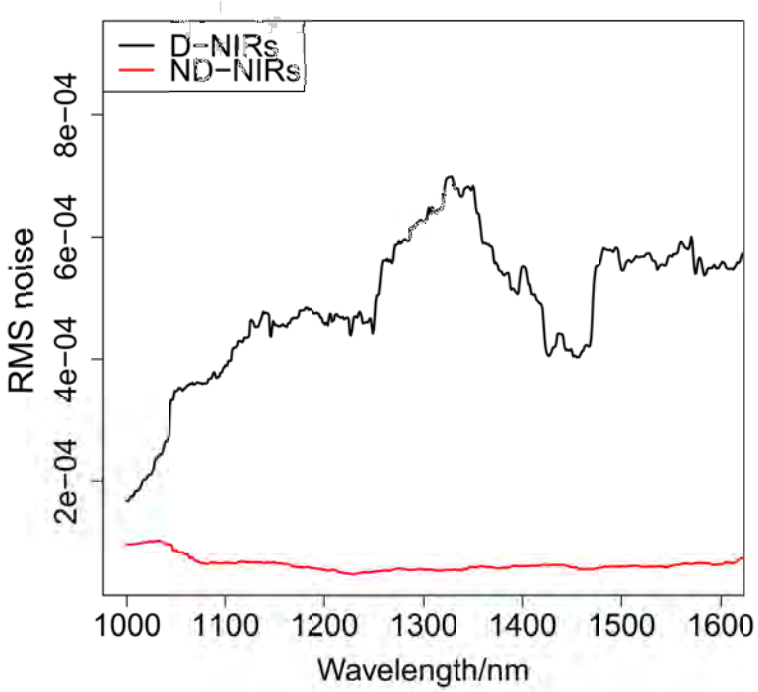

Figure 4-3 A plot for root mean square noise of D-NIRs and ND-NIRs at high-light flux.

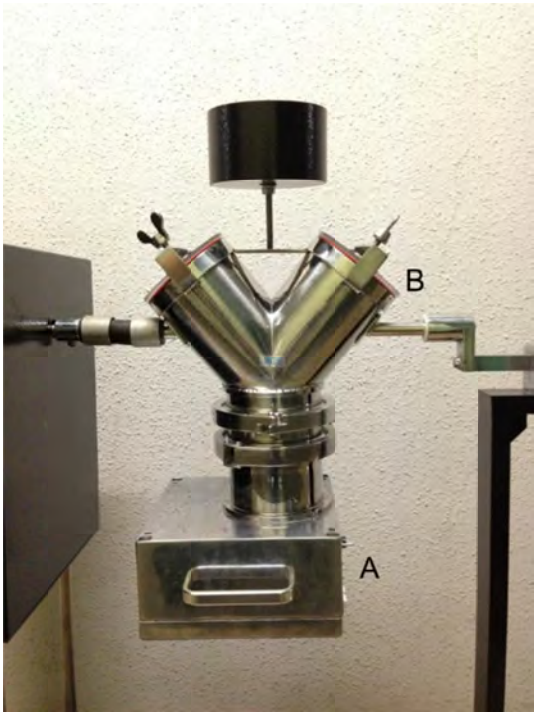

Figure 4-4 Outline of the blending test setup. A: P-NIRs for the in-line blending process monitor, B: Vessel-type blending machine.

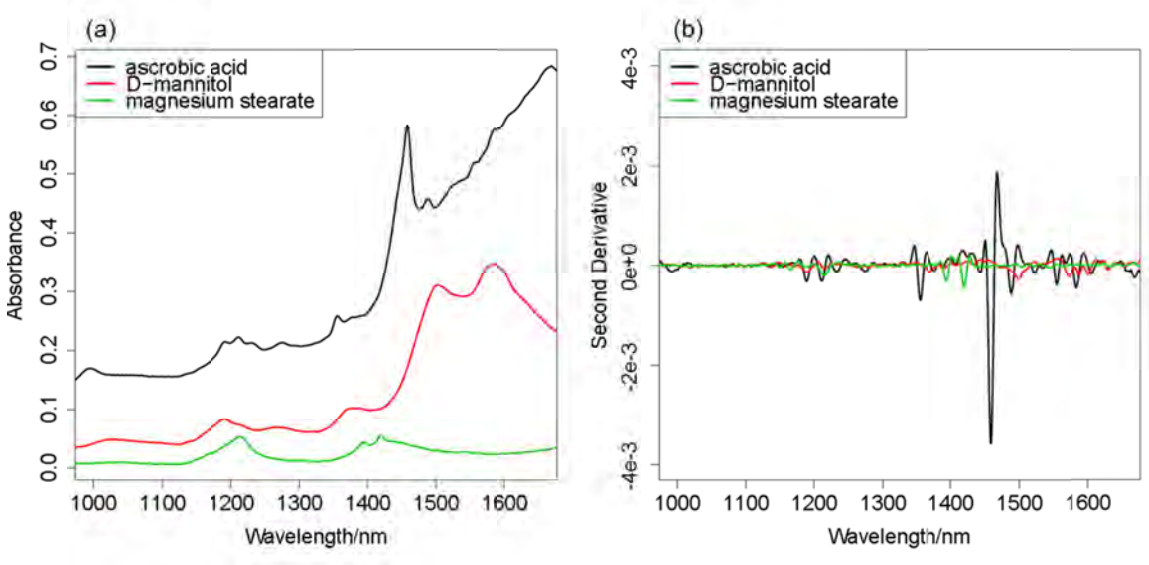

Figure 4-5 (**a**) NIR spectra of ascorbic acid, D-mannitol and magnesium stearate. (**b**) The second derivative of the spectra shown in (**a**).

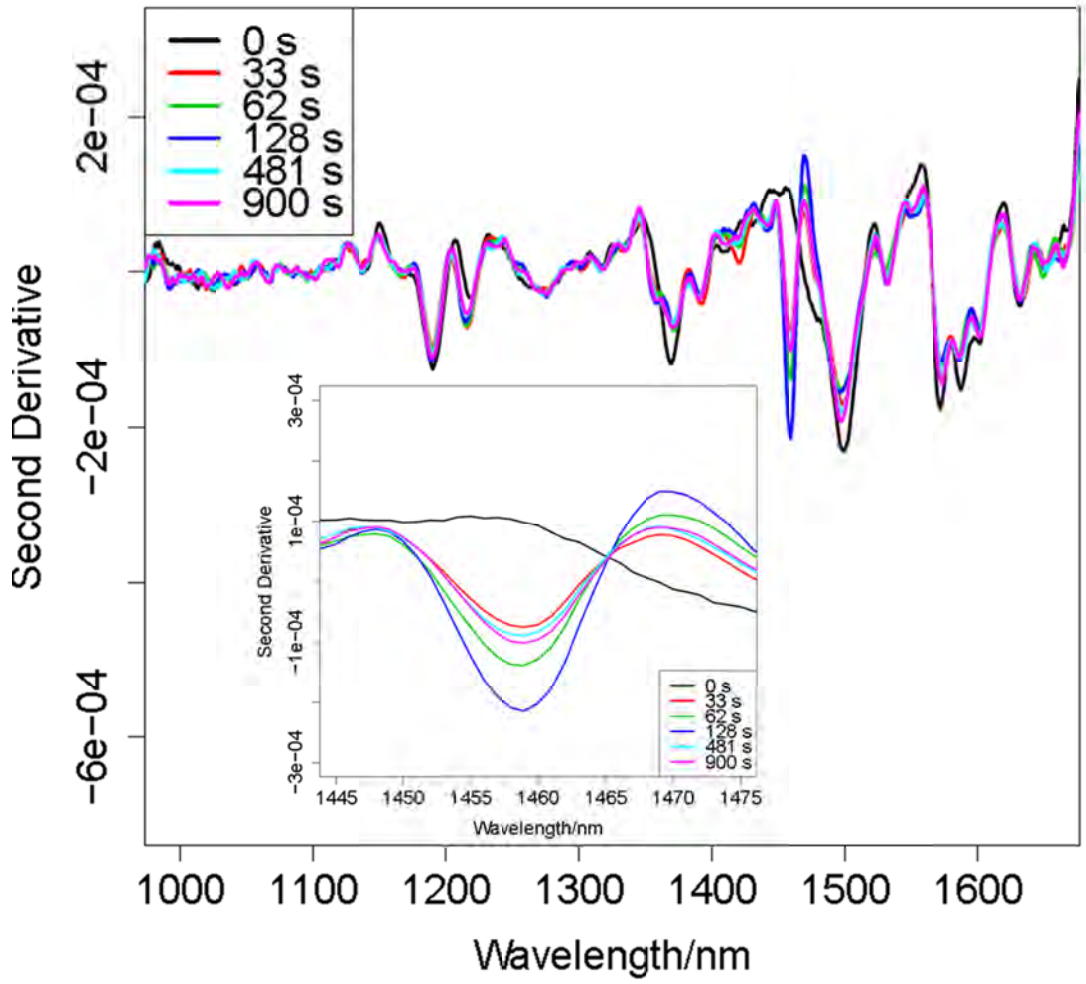

Figure 4-6 The second derivative spectra of mixing sample measured during the blending process.

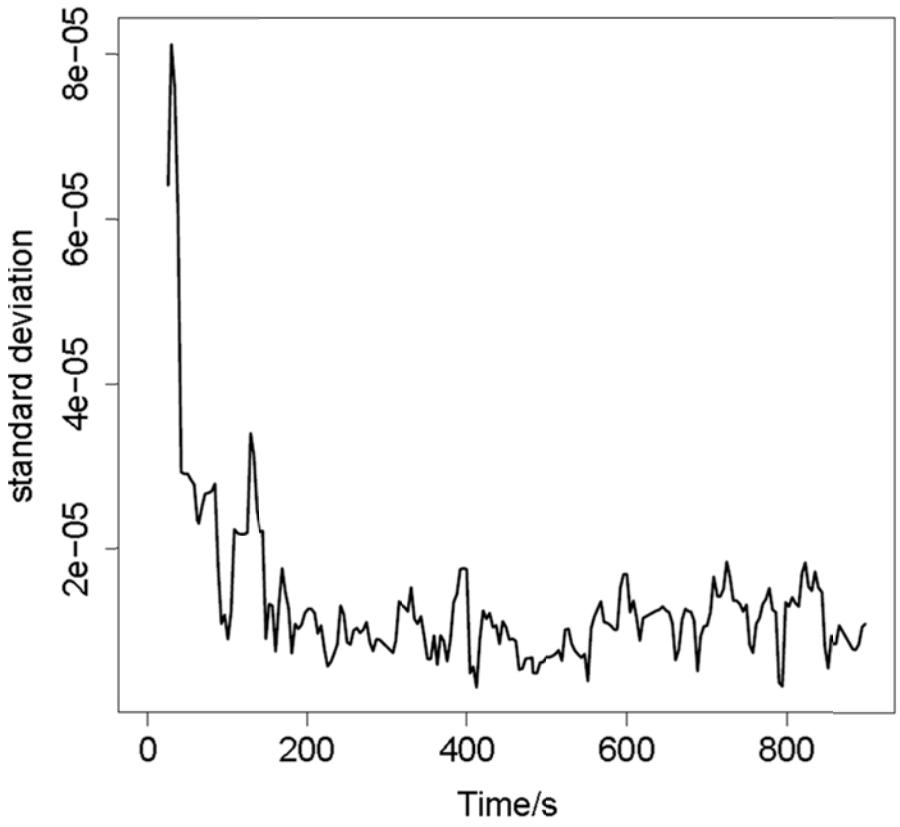

Figure 4-7 A plot for standard deviation of the second derivative intensity at 1,458 nm plotted as a function of time. The DR-NIR spectrum was measured with 4 s intervals.

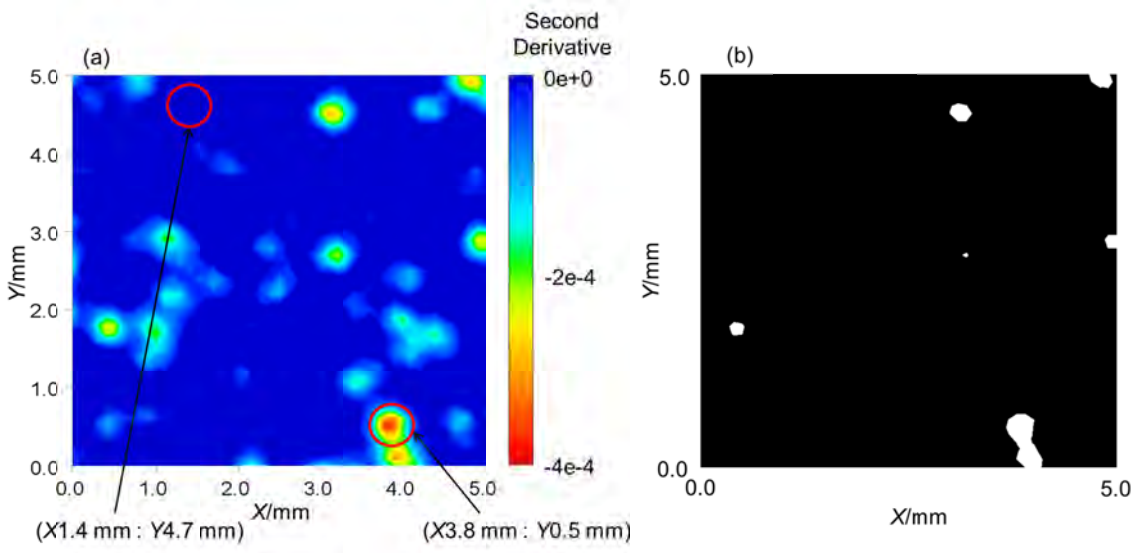

Figure 4-8 (**a**) The second derivative intensity mapping image of the mixing sample at 1 min after the start of the blending. (**b**) A binary image of the sample at 1 min after the start of the blending. A binary image developed by arbitrary threshold value.

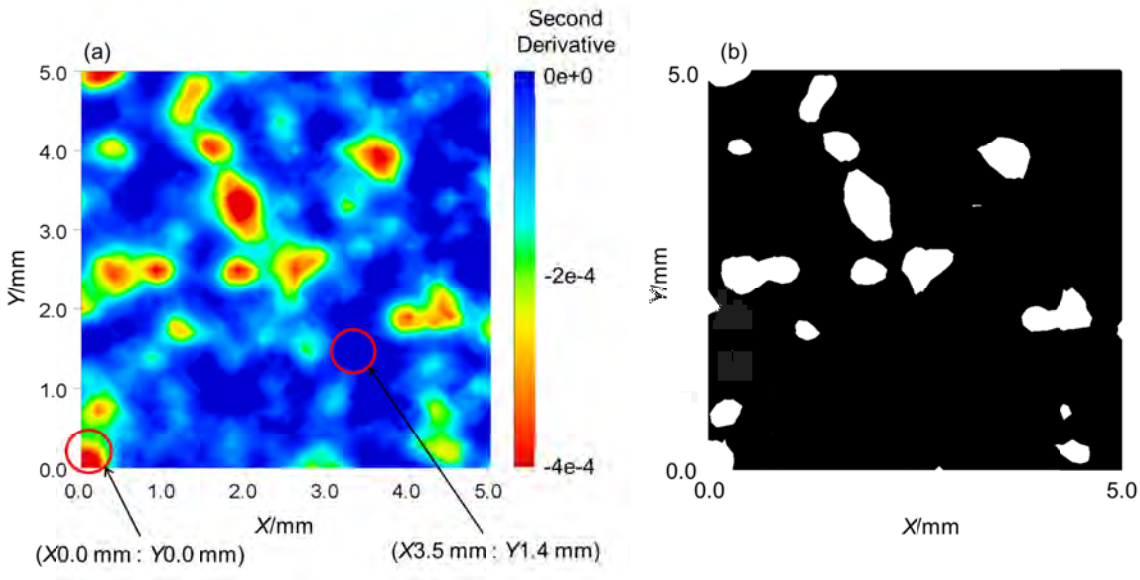

Figure 4-9 (**a**) The second derivative intensity mapping image of the mixing sample at 8 min after the start of the blending. (**b**) A binary image of the sample at 8 min after the start of the blending. A binary image developed by arbitrary threshold value.

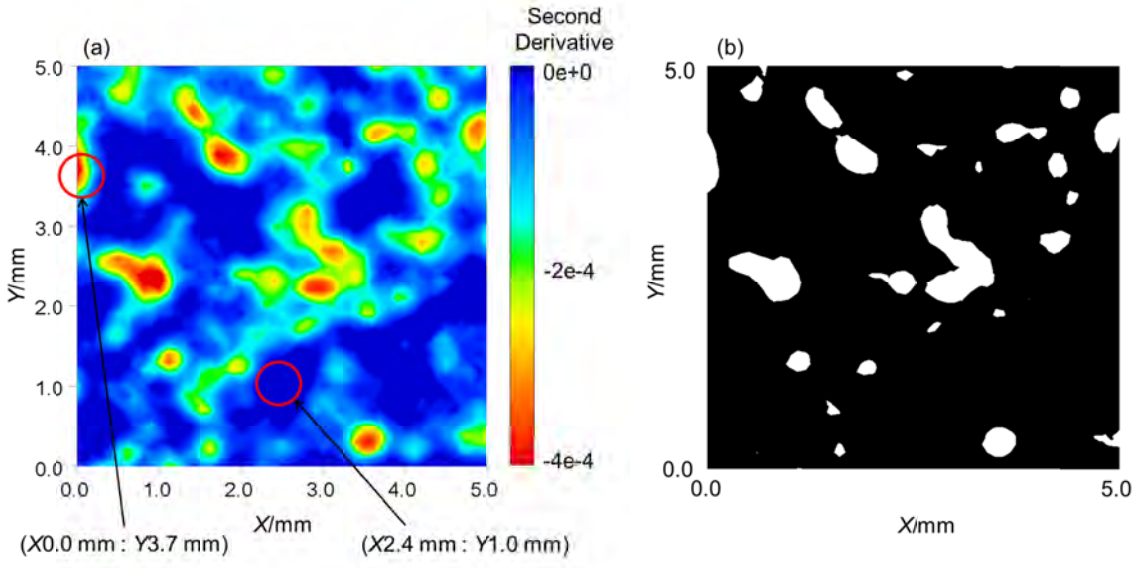

Figure 4-10 (**a**) The second derivative intensity mapping image of the mixing sample at 15 min after the start of the blending. (**b**) A binary image of the sample at 15 min after the start of the blending. A binary image developed by arbitrary threshold value.

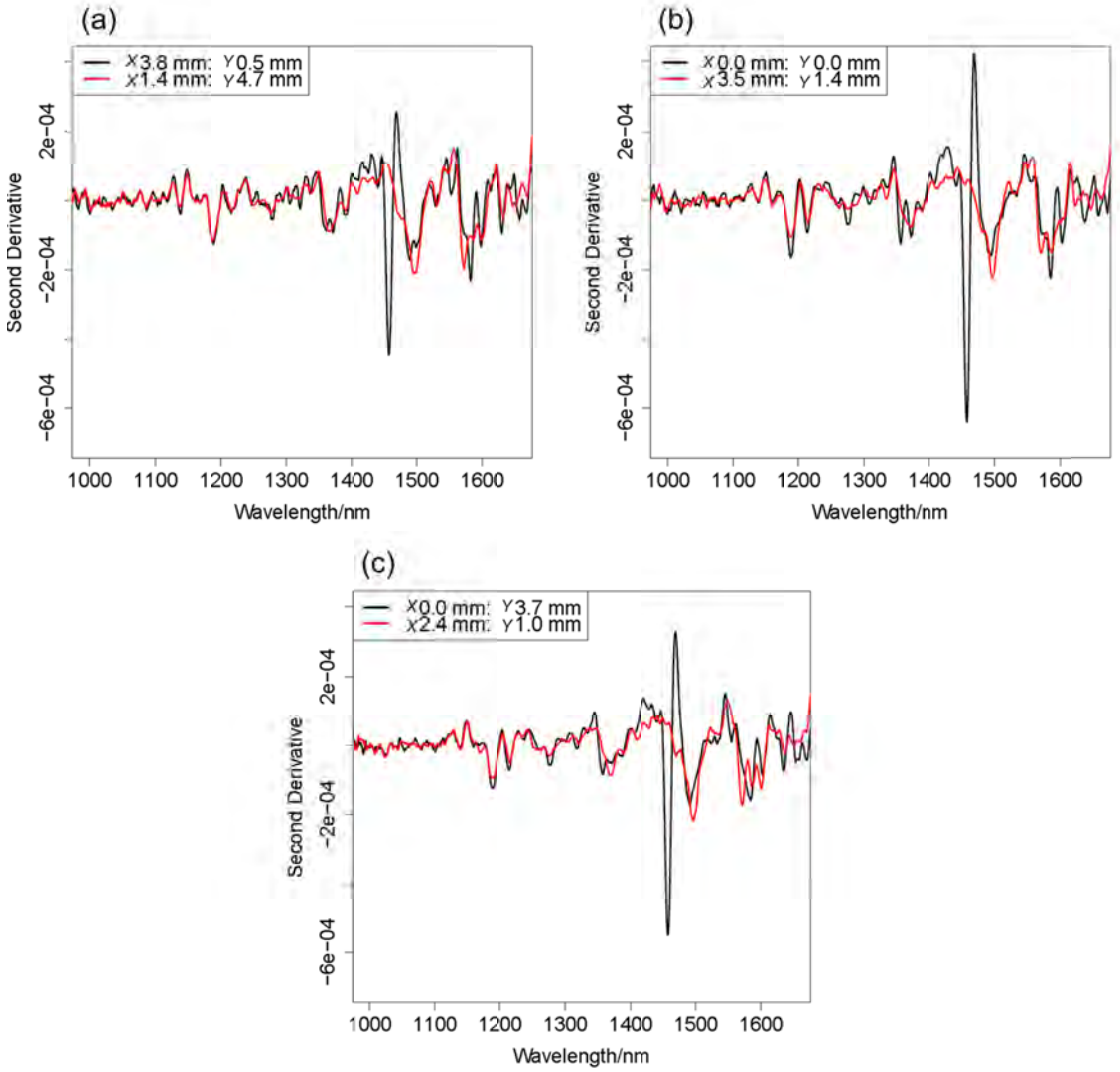

Figure 4-11 (**a**) The second derivative spectra at *X*=3.8 mm, *Y*=0.5 mm and *X*=1.4 mm, *Y*=4.7 mm points of the binary image of the blending at 1 min after the start of the blending. (**b**) Those at *X*=0.0 mm, *Y*=0.0 mm and *X*=3.5 mm, *Y*=1.4 mm points. (**c**) Those at *X*=0.0 mm, *Y*=3.7 mm and *X*=2.4 mm, *Y*=1.0 mm points.

Table 4-1 Measurement time for each condition by ND-NIRs.

Measurement Area	5 mm × 5 mm			
Spatial Resolution	1 mm	0.5 mm	0.2 mm	0.1 mm
Number of Measurement Point (Number of Spectra Data)	36	121	676	2061
Measurement Time	5 s	13 s	64 s	242 s

Chapter 5

An application for the quantitative analysis of pharmaceutical tablets using a rapid switching system between a near-infrared spectrometer and a portable near-infrared imaging system equipped with fiber optics

Abstract

In this study present a rapid switching system between a newly developed near-infrared (NIR) spectrometer and its imaging system to select the spot size of a diffuse reflectance (DR) probe. In a previous study, we developed a portable NIR imaging system, known as D-NIRs, which has significant advantages over other systems. Its high speed, high spectral resolution, and portability are particularly useful in the process of monitoring pharmaceutical tablets. However, the spectral accuracies relating to the changes in the formulation of the pharmaceutical tablets, have not been fully discussed. Therefore, the rapid optical switching system was improved and presented a new model of D-NIRs (ND-NIRs). This system can automatically switch the optical paths of the DR and NIR imaging probes, greatly contributing to the simultaneous measurement of both the imaging and spot.

The NIR spectra of the model tablets, including 0-10 % ascorbic acid, were measured and simultaneous NIR images of the tablets were obtained. The predicted results using spot sizes for the DR probe of ⌀1 and ⌀5 mm, resulted in coefficient of determination R^2 = 0.79 and 0.94, with root-mean-square errors (RMSEs) of 1.78 wt% and 0.89 wt%, respectively. For tablets with a high concentration of ascorbic acid, the NIR imaging results showed inhomogeneity in concentration. However, the predicted values for the

low concentration samples appeared higher than the known concentration of the tablets, although the homogeneity of the concentration was confirmed. In addition, the optimal spot size using NIR imaging data was estimated to be 5 mm to 7 mm. The results obtained in this study show that the spot size of the fiber probe, attached to a spectrometer, is important in developing a highly reliable model to determine the component concentration of a tablet.

1. Introduction

In the past decade, process analytical technology (PAT), a framework developed by the Food and Drug Administration, has been widely applied to the pharmaceutical and food industry fields.[1–5] PAT is a comprehensive control system for pharmaceutical production, and includes production design, process analysis, and management.

It is well known that spectroscopic techniques are one of the most effective methods of PAT in pharmaceutical processes.[1,4] Ultraviolet-visible (UV-Vis) spectroscopy has been used with charge-coupled device detector based instruments. Several research groups have reported UV-Vis techniques that are useful in extracting qualitative and quantitative information regarding the contents of tablets.[6]

Vibrational spectroscopy, for example mid-infrared (mid-IR) and Raman spectroscopy, can be used to obtain the intrinsic characteristics of the molecules in the components. Therefore, mid-IR and Raman spectroscopy have been used to evaluate the physical and chemical properties, such as, the concentration, intra- and inter-molecular interactions, and the crystallinity of the products in pharmaceutical processing.[7–11] Since the mid-IR spectrum enables a clear assignment of bands and has a high quantitative performance, extensive research has been performed in the past decade relating to the concentrations in samples and reaction monitors.[12] Moreover, mid-IR spectroscopy

plays an effective role in the polymeric properties of a sample (e.g., crystallization), to determine the efficiency of downstream operations (e.g., filtration, drying, and formulating) and the product effectiveness.

Raman spectroscopy is a nondestructive analytical method, with minimal influence by water and an easily operatable light fiber. Therefore, Raman spectroscopy is a useful tool in pharmaceutical applications.[8–9] Raman spectroscopy has been used to evaluate the homogeneity of pharmaceutical blending and granulation for in-line process analysis.[9–10] Raman spectroscopy, in combination with chemometrics, has also been utilized as a PAT tool for the in-line and real-time endpoint determinations of several different powder blending processes.[8–10]

Near-infrared (NIR) spectroscopy has several advantages, such as remote and bulk analyses, non-contact, and minimal sample preparation for pharmaceutical process monitoring. Moreover, improvements in the instrument, such as higher speeds and light fiber optics enhances its applicability for implementation in pharmaceutical process monitoring.[1,4–5] However, in general, NIR spectra are more complicated than mid-IR spectra because the NIR bands are produced by overtones and combinations with many overlapping bands. Therefore, the quantitative accuracy is problematic when using spectra in the NIR region for process monitoring.[4–5,11] More recently, remarkable

improvements in NIR imaging instrumentation have enabled the evaluation of pharmaceutical powder blend and tablet uniformities, as well as tablet dissolution with on-line monitoring systems using the standard deviation of the spectra.[13–15]

Generally, the pharmaceutical process is divided into several steps: milling of materials, blending, drying, coating, and tableting. The evaluation of the quality at each step reflects changes in the physical and chemical properties of the components, including the particle size, thickness, moisture content, and inhomogeneity.[16–19] Therefore, to appropriately monitor the target, which changes through various states during the process, the measurement conditions, such as the measurement speed, wavelength resolution, probe type, and signal-to-noise ratio, should all be adjusted according to the changes in the properties of the target.

Recently, an in-line monitoring NIR spectrometer, P-NIRs, and an NIR imaging device, D-NIRs were developed for a pharmaceutical process monitoring.[20–22] P-NIRs can obtain NIR spectra in the 950 – 1700 nm region at a spectral resolution of 1.25 nm. D-NIRs are composed of P-NIRs, an imaging unit, and a light source unit. D-NIRs can measure 900 mm^2 area with a 100 μm spatial resolution. We note that, for an area of 100 mm^2, a spectrum in the 950-1700 nm range can be obtained within less than 10 s.

Another innovative feature of D-NIRs is the portability of the instrument.[21–22]

Although a working space of 25×30×30 cm^3 is required to use D-NIRs, the size of the P-NIRs and the imaging unit of D-NIRs, are only 20×20×10 and 25×20×17 cm^3, respectively. In addition, D-NIRs enable simultaneous quantitative and distribution monitoring using the same spectrometer. This feature is very useful in process monitoring, and it show that D-NIRs can be used to obtain the quantity and distribution of the concentrations of the components of a tablet during process monitoring.[20–23] It also present the determination method for the blending process when using the D-NIRs.[21] Moreover, Ishikawa et al. demonstrated the potential of D-NIRs as an important monitoring tool of the tablet dissolution process.[23] In a previous study also showed that combination of chemometrics with principal component analysis (PCA) and partial least squares regression (PLSR) enabled the application of P-NIRs in highly-accurate and high-speed tablet internal measurements.[19–23]

However, the optimization of NIR spectroscopy for use in process monitoring is still under consideration. One of the problems of NIR spectroscopy is that the differences of the spot sizes in the DR probes, constrains their use in practical applications in the pharmaceutical process as these generate differences in the spectral accuracies. Therefore, this study aims to explore a rapid switching system of P-NIRs and D-NIRs, equipped with fiber optics, to be applied in the process of monitoring pharmaceutical

tablets. NIR spectra using P-NIRs, and NIR imaging using D-NIRs, for the on-line monitoring of the tablets were measured. Also, the application potential of D-NIRs in the on-line monitoring of pharmaceutical tablets through the optimization of the beam size of the fiber probe was evaluated.

2. Instrumentation

A schematic diagram of the spectral measurement system, an imaging probe (D-NIRs), and an in-line type NIR spectrometer with a diffuse reflection (DR) probe are shown in Figure 5-1. The spectral measurement system can switch between the DR probe and imaging probe optical paths automatically, using an optical switching device. A sample tablet was placed on a tablet holder of the D-NIRs system. The DR light reached the DR optical fiber probe connected with the P-NIRs, and the NIR spectra in the 950 - 1700 nm region was obtained at various points in the tablet. The spectral resolution was 1.25 nm, and the integration time was 1 s. Other details of the D-NIRs system were described in previous studies.[12,21] The DR optical fiber probe consisted of a condenser lens and an optical fiber bundle. The detection and incident fibers were bundled into the new probe at a high density. Consequently, the newly developed optical fiber probe achieved mechanical strength with a sufficient light intensity.[20] In the

present study, the optimum spot size of the DR probe was investigated, by developing ⌀1 and ⌀5 mm beam size probes which were connected to the P-NIRs.

The DR light reaches the imaging unit, consisting of an area scan mirror unit and an irradiation light unit. The two-dimensional measurement in the 950 - 1700 nm region was obtained though the DR optical fiber. The spatial resolution of the imaging was 0.1 mm. Note that the one-spot and two-dimensional spectra were obtained only at 1 and 900 s by the system, respectively. In the newly developed system, the measurements of the one-spot and two-dimensional spectra were obtained by easily switching the optic fiber connection. The optical switch module AQ2200-412 (Yokogawa Electric Corp., Tokyo, Japan) was used. AQ2200-412 performed the switching of the optical paths with high accuracy. Therefore, the optical switching module mechanically operated the optical ports using a high positioning accuracy stepping motor and rotary switching mechanism.[24] The spectral noise of the switching system was evaluated. Figure 5-2 shows the spectral noise of the DR and imaging probes measured by the optical switch. The DR and imaging probes have a high signal-to-noise ratio (SNR) of 0.0001 in an absorbance unit.

3. Material and Methods

3.1 Sample preparation

The sample tablets were prepared using a powder of 0-10 wt% ascorbic acid (Kanto Chemical Co. Inc., Tokyo, Japan), 35-45 wt% lactose, 20 wt% corn starch, 30 wt% cellulose, and 5 wt% talc, which were placed in a plastic bag, mixed for 5 minutes, and the obtained mixture was pressed at 10 kN by a tableting machine (Handtab-100, Ichihashi Seiki Co. Ltd., Kyoto, Japan). Eleven sample tablets were obtained, with different concentrations of ascorbic acid and lactose, and the diameter and thickness of each tablet were ⌀8 mm and 1.0 mm, respectively. The shape of the sample tablets were flat. Five samples were prepared for each concentration to ensure adequate accuracy, and consequently, 55 samples were used in the quantitative analysis.

3.2 Spectral collection

For the point measurements, the DR spectra in the 950 - 1700 nm region were obtained from the central part of a tablet. The DR probe was inclined 15° with respect to the tablet samples. A 5 W halogen lamp was used, with an integration time of 1 s. Two-dimensional simultaneous spectra measurements were obtained by switching the optical probe. The field of view of an image was 10×10 mm^2, with a spatial resolution

of 100 μm. The measurement procedure was then performed. First, the point measurements were obtained by the DR probe. Then, the imaging measurements were obtained by the imaging probe, after switching the optical path using the optical switching module.

3.3 Spectral analysis

The spectra obtained from the D-NIRs were transferred to text format and analyzed by Unscrambler Ver. 10.3. The spectra were subjected to a second derivative procedure with 21 points, including Savitzky-Golay smoothing.[25] A partial least squares (PLS) regression was applied to these spectra to determine the concentration of the ascorbic acid. The data from the 55 samples were used to build the calibration model with PLS regression. The accuracy of the models were determined using full cross validation.

4. Results and Discussion

4.1 NIR spectra of ascorbic acid, lactose, corn starch, cellulose, and talc

Figure 5-3 shows the DR spectra and their second derivative spectra in the 950 - 1700 nm region of ascorbic acid, lactose, corn starch, cellulose, and talc. The bands around 1354 and 1458 nm of ascorbic acid were due to the first overtones of the stretching

vibrations of the free and intermolecularly hydrogen-bonded OH groups, respectively.[26] The bands in the 1150 - 1250 nm region of ascorbic acid are due to CH stretching vibrations. The peak at 1391 nm for talc was associated with the first overtone of the OH stretching mode.[27] Cellulose, starch, and lactose also contain numerous OH groups, with similar corresponding bands.

4.2 Determination of the accuracy of the concentration

Figures 5-4 and 5-5 display the DR spectra and their second derivative spectra in the 950 - 1700 nm region of the tablet samples measured by the DR probes with 1 and 5 mm spot sizes. In the NIR spectra obtained by the DR probe with the 1 mm spot, the band intensity for the 1400 - 1600 nm region varied largely compared to that obtained with the 5 mm spot. Moreover, the variations in the second derivative spectra collected by the DR probe with the 1 mm spot were also more prominent than those obtained by the DR probe with the 5 mm spot, over the whole region. The difference between the maximum and minimum values of the secondary differential intensity of 1458 nm (AsA absorption band peak) of the spectrum obtained with the ⌀1 mm spot size was 0.00025. Moreover, the difference between the maximum and minimum values of the secondary differential intensity of 1458 nm of the spectrum obtained with the ⌀5 mm spot size was

0.00012. In particular, for the probe with the ⌀5 mm spot, the average spectra obtained from the wider area of the tablet contributed to a reduction in the variations. These variations may have arisen from the differences in the particle sizes between ascorbic acid and the other excipients. The area dependence of the spectrum is more prominent in the absorption band region of ascorbic acid, 1400 - 1600 nm, for the probe with the 1 mm spot.

Therefore, the spectra collected by the (smallest) ⌀1 mm spot probe restricted the quantitative analysis results of the concentrations due to the area dependence. The analysis conditions, results of the PLS, and the predicted concentration of ascorbic acid are listed in Table 5-1. The determination accuracies of the ⌀1 and ⌀5 mm spot size probes were described by the determination coefficients of 0.79 and 0.94, with RMSE of 1.79 wt% and 0.86 wt%, respectively. As expected, the improvement of the determination accuracy was dependent on changes in the spot size.

Figure 5-6 shows the average values in the concentrations predicted by PLS regression. In addition, Table 5-2 shows the standard error of concentrations predicted by PLS regression. In the whole region, the error values obtained by the ⌀1 mm spot probe were higher than those obtained by the ⌀5 mm spot probe. The spectral noise did not differ between the point and imaging measurements using the switching system.

Therefore, the switching system was useful to utilize the same spectrometer for both the point and imaging measurements. In Figure 5-7, panels (A), (B), and (C) show the NIR images obtained by mapping the predicted values of the ascorbic acid concentration using the PLS prediction models, for the data collected using the ⌀5 mm spot size probe. In the tablet sample of Figure 5-7 (A), the predicted concentration value of AsA obtained by the ⌀1 mm spot probe was 7.8 wt%. In the tablet sample of Figure 5-7 (B), the predicted concentration value of AsA obtained by the ⌀1 mm spot probe was 14.8 wt%. Conversely, in the tablet sample of Figure 5-7 (C), the predicted concentration value of AsA obtained by the ⌀1 mm spot probe was 9.1 wt%. The concentration value of AsA was low in the central area of the NIR imaging data of Figure 5-7 (A). Therefore, the AsA concentration was low in the area measured by the ⌀1 mm spot probe. The high concentration area of the NIR imaging data of Figure 5-7 (B) was clearly observed in the area measured by the ⌀1 mm spot probe. The concentration value of AsA was dispersed in the whole area of the NIR imaging data of Figure 5-7 (C). Therefore, the concentration value of AsA was the average concentration in the area measured by the ⌀1 mm spot probe. In the case of the ⌀1 mm sample spot, the data strongly reflected the inhomogeneity of the tablet. Therefore, these results revealed that the particle size and/or blending time may be used to determine high concentrations. In addition, the

⌀1–9 mm circular spot average AsA concentration values of each sample's NIR imaging data were calculated, and a plot of the difference between each circular spot average AsA concentration value with the ⌀5 mm spot average reference value is shown in Figure 5-8. The spot average AsA concentration values for ⌀1–3 mm were higher than the ⌀5 mm spot average AsA concentration value. Conversely, the spot average AsA concentration values for ⌀5–7 mm were almost the same as the ⌀5 mm spot average AsA concentration value, which is a plateau region for the ⌀5–7 mm range. Moreover, the spot average AsA concentration values for ⌀8–9 mm were lower than the ⌀5 mm spot average AsA concentration value. Therefore, the optimal spot size for measuring the AsA concentration was estimated to be between ⌀5–7 mm by the dispersibility and average AsA concentration values obtained from the NIR imaging data. Furthermore, the DR spectra of the tablet samples were collected using the ⌀9 mm spot probe, and a PLSR analysis was performed. The determination accuracy of the ⌀9 mm spot probe is described by the determination coefficient of 0.37 with a RMSE of 2.61 wt%. This result is lower than the determination accuracy for the ⌀5 mm spot size due to the fact that background light noise from around the tablet sample is collected because the spot size is larger than the tablet sample. Therefore, the quantitative analysis of the AsA concentration in the tablet samples with a ⌀5 mm spot size is more appropriate.

Conversely, the value obtained by the ⌀1 mm spot probe implied a large dispersion in the known concentration in the tablet. The homogeneity of the NIR imaging obtained from the high ascorbic acid concentration tablet was similar to the predicted concentration of ascorbic acid obtained by the ⌀5 mm probe. The spectra measured by the ⌀1 mm spot probe may have contained a relatively high level of noise due to contaminants, although the distribution of ascorbic acid was homogeneous. To avoid overestimation, not only improvements in the band separation of the spectral pre-treatment are needed, but also the acquisition of a sufficient signal for process monitoring. In NIR spectroscopy-based monitoring, these are the obstacles faced in cases of low concentrations. However, the results obtained by the probes with different spot sizes successfully demonstrated that an optimized spot size can improve and contribute to the prediction accuracy of the concentration of tablets.

5. Conclusion

In order to simplify the probe design and the development of in-line type NIR spectrometers, we have developed an optical fiber switching system using a DR probe and an NIR imaging device (D-NIRs), which can change the spot size. This switching system acquired DR spectra and NIR imaging data with one polychromator type NIR

spectrometer (P-NIRs). Therefore, it was possible to evaluate the dispersibility and uniformity of a sample by NIR imaging and to evaluate the quality of the spectral data obtained by the DR probe. The model tablets, containing 0-10% ascorbic acid as active pharmaceutical ingredient (API), were prepared, and NIR spectra in the 950 - 1700 nm region were measured using P-NIRs. The optical switching system with D-NIRs and P-NIRs was able to collect the DR spectra and NIR imaging data with rapid, high-precision, and automatic performance, with a rotary mechanical component optical fiber type switching module. The predicted error results for the ⌀1 mm spectra were substantially greater than those of the ⌀5 mm spectra. The results showed that the ⌀5 mm spot size DR probe was superior to the ⌀1 mm spot size DR probe. In addition, the optimum spot size for quantifying AsA concentration was estimated to 5–7 mm spot size by the NIR imaging data. Moreover, the predicted error results for the ⌀9 mm spectra were substantially greater than those of the ⌀5 mm spectra. The results showed that the estimation result of the optimum spot size based on the NIR imaging data almost agreed with the prediction error results of ⌀1, ⌀5 and ⌀ 9 mm spot size probes.

An image of the high concentration of ascorbic acid resulted in an inhomogeneous distribution. Therefore, the quantitative accuracy depends mainly on the inhomogeneity due to the insufficient particle size and blending time. However, the predicted value for

the low concentration was higher than the measured value. Therefore, in cases of low concentrations, the quantitative accuracy may be determined by using the spectra accurately, rather than the inhomogeneity of the component. This study suggested the possibility of selecting a more suitable optical fiber probe by using a system that can switch between the one-point measurement type optical fiber probe and NIR imaging measurement.

6. References

1. K.A. Bakeev. "Process Analytical Technology". Oxford, UK: Blackwell Publishing, 2005. 1st ed. Pp. 13–38.
2. International Conference on Harmonisation of Technical Requirements for Registration of Pharmaceuticals for Human Use. ICH Harmonized Tripartite Guideline Pharmaceutical Development Q8 (R2). http://www.ich.org/fileadmin/Public_Web_Site/ICH_Products/Guidelines/Quality/Q8_R1/Step4/Q8_R2_Guideline.pdf [accessed January 15 2015].
3. U.S. Food and Drug Administration (Maryland), Guidance for Industry, PAT: A Framework for Innovative Pharmaceutical Development, Manufacturing, and Quality Assurance, 2004.
4. Y. Ozaki, T. Amari. Near-Infrared Spectroscopy in Chemical Process Analysis. Sheffield, UK: Sheffield Academic Press, 2000. Pp. 53–95.
5. Y. Ozaki. “Near-infrared Spectroscopy. Its Versatility in Analytical Chemistry”. Anal. Sci. 2012. 28: 545–563.
6. S. Behera, S. Ghanty, F. Ahmad, S. Santra, S. Banerjee. “UV-Visible Spectrophotometric Method Development and Validation of Assay of Paracetamol Tablet Formulation”. J. Anal. Bioanal. Techniques. 2012. 3: 151.

7. S. Wartewig, R.H.H. Neubert. “Pharmaceutical Applications of Mid-IR and Raman Spectroscopy”. Adv. Drug Deliv. Rev. 2005. 57: 1144–1170.

8. T.R.M De Beer, C. Bodsonb, B. Dejaegher, B. Walczak, P. Vercruyssea, A. Burggraevea, A. Lemos, L. Delattre, Y. Vander Heyden, J.P. Remone, C. Vervaet, W.R.G. Baeyens. “A Raman Spectroscopy as a Process Analytical Technology (PAT) Tool for the In-line Monitoring and Understanding of a Powder Blending Process”. J. Pharm. Biomed. Anal. 2008. 48: 772–779.

9. G.J. Vergote, T.R.M. De Beer, C. Vervaet, J.P. Remon, W.R.G. Baeyens, N. Diericx, F. Verpoort. “In-line Monitoring of a Pharmaceutical Blending Process using FT-Raman Spectroscopy”. Eur. J. Pharm. Sci. 2004. 21: 479–485.

10. H. Wikström, P.J. Marsac, L.S. Taylor. “In-line Monitoring of Hydrate Formation During Wet Granulation using Raman Spectroscopy”. J. Pharm. Sci. 2005. 94: 209–219.

11. T.R.M. De Beer, P. Vercruysse, A. Burggraeve1, T. Quinten, J. Ouyang, X. Zhang, C. Vervaet, J.P. Remon, W.R.G. Baeyens. “In-line and Real-time Process Monitoring of a Freeze Drying Process using Raman and NIR Spectroscopy as Complementary Process Analytical Technology (PAT) Tools”. J. Pharm. Sci. 2009. 98(9): 3430–3446.

12. S. G. Kazarian, A. V. Ewing. “Applications of Fourier transform infrared spectroscopic imaging to tablet dissolution and drug release”. Expert Opin. Drug Deliv. 2013. 10.9: 1207-1221.

13. D. Ishikawa, H. Shinzawa, T. Genkawa, G.S. Kazarian, Y. Ozaki. “Recent Progress of Near-Infrared (NIR) Imaging Development of Novel Instruments and Their Applicability for Practical Situations”. Anal. Sci. 2014. 30: 143–150.

14. S. Šašić, Y. Ozaki. Raman, Infrared, and Near-Infrared Chemical Imaging. Hoboken, NJ, USA: John Wiley & Sons Inc., 2009.

15. H. Shinzawa, K. Awa, Y. Ozaki. “Compression Induced Morphological and Molecular Structural Changes of Cellulose Tablets Probed with Near Infrared Imaging”. J. Near Infrared Spectrosc. 2011. 19: 15–22.

16. I. Jedvert, M. Josefson, F.W. Langkilde. “Quantification of an Active Substance in a Tablet by NIR and Raman spectroscopy”. J. Near Infrared Spectrosc. 1998. 6: 279.

17. N.W. Broad, R.D. Jee, A.C. Moffat, M.R. Smith. “Application of Transmission Near-infrared Spectroscopy to Uniformity of Content Testing of Intact Steroid Tablets”. Analyst. 2001.126: 2207.

18. M. Otsuka, H. Tanabe, K. Osaki, K. Otsuka, Y. Ozaki. “Chemoinformetrical

Evaluation of Dissolution Property of Indomethacin Tablets by Near-Infrared Spectroscopy". J. Pharm. Sci. 2007. 96: 788–801.

19. D. Ishikawa, T. Genkawa, K. Murayama, M. Komiyama, Y. Ozaki. "Feasibility Study of Diffuse Reflectance and Transmittance Near Infrared Spectroscopy for Rapid Analysis of Ascorbic Acid Concentration in Bilayer Tablets using a High-speed Polychromator-type Spectrometer". J. Near Infrared Spectrosc. 2014. 22: 189–197.
20. K. Murayama, T. Genkawa, D. Ishikawa, M. Komiyama, Y. Ozaki. "A Polychromator-type Near-infrared Spectrometer with a High-sensitivity and High-resolution Photodiode Array Detector for Pharmaceutical Process Monitoring on the Millisecond Time Scale". Rev. Sci. Instrum. 2013. 84(2): 023104.
21. K. Murayama, D. Ishikawa, T. Genkawa, H. Sugino, M. Komiyama, O. Yukihiro. "Image Monitoring of Pharmaceutical Blending Processes and the Determination of an End Point by Using a Portable Near-Infrared Imaging Device Based on a Polychromator-Type Near-Infrared Spectrometer with a High-speed and High-Resolution Photo Diode Array Detector". Molecules. 2015. 20: 4007–4019.
22. D. Ishikawa, K. Murayama, T. Genkawa, K. Awa, M. Komiyama, Y. Ozaki. "Development of Compact Near Infrared Imaging Device with High-speed and

Portability for Pharmaceutical Process Monitoring". NIR News. 2012. 23: 14–17.

23. D. Ishikawa, K. Murayama, T. Genkawa, K. Awa, M. Komiyama, K. Sergei, Y. Ozaki. "Application of a Newly Developed Portable NIR Imaging Device to Dissolution Process Monitoring of Tablets". Anal. Bioanal. Chem. 2013. 405: 9401–9409.
24. Yokogawa Electric Corporation, AQ2200 series Multi Application Test System Data sheet. printed Japan. 2012.
25. A. Savitzky, M.J.E. Golay. "Smoothing and Differentiation of Data by Simplified Least Squares Procedures". J. Anal. Chem. 1964. 36: 1627–1639.
26. S. Petit, A. Decarreau, F. Martin, R. Buchet. "Refined Relationship between the Position of the Fundamental OH Stretching and the First Overtones for Clays." Phys. Chem. Miner. 2004. 31: 585.
27. H. Lui, B. Xiang, L. Qu. "Structure Analysis of Ascorbic Acid using Near-infrared Spectroscopy and Generalized Two-dimensional Correlation Spectroscopy". J. Mol. Struct. 2006. 794: 12–17.

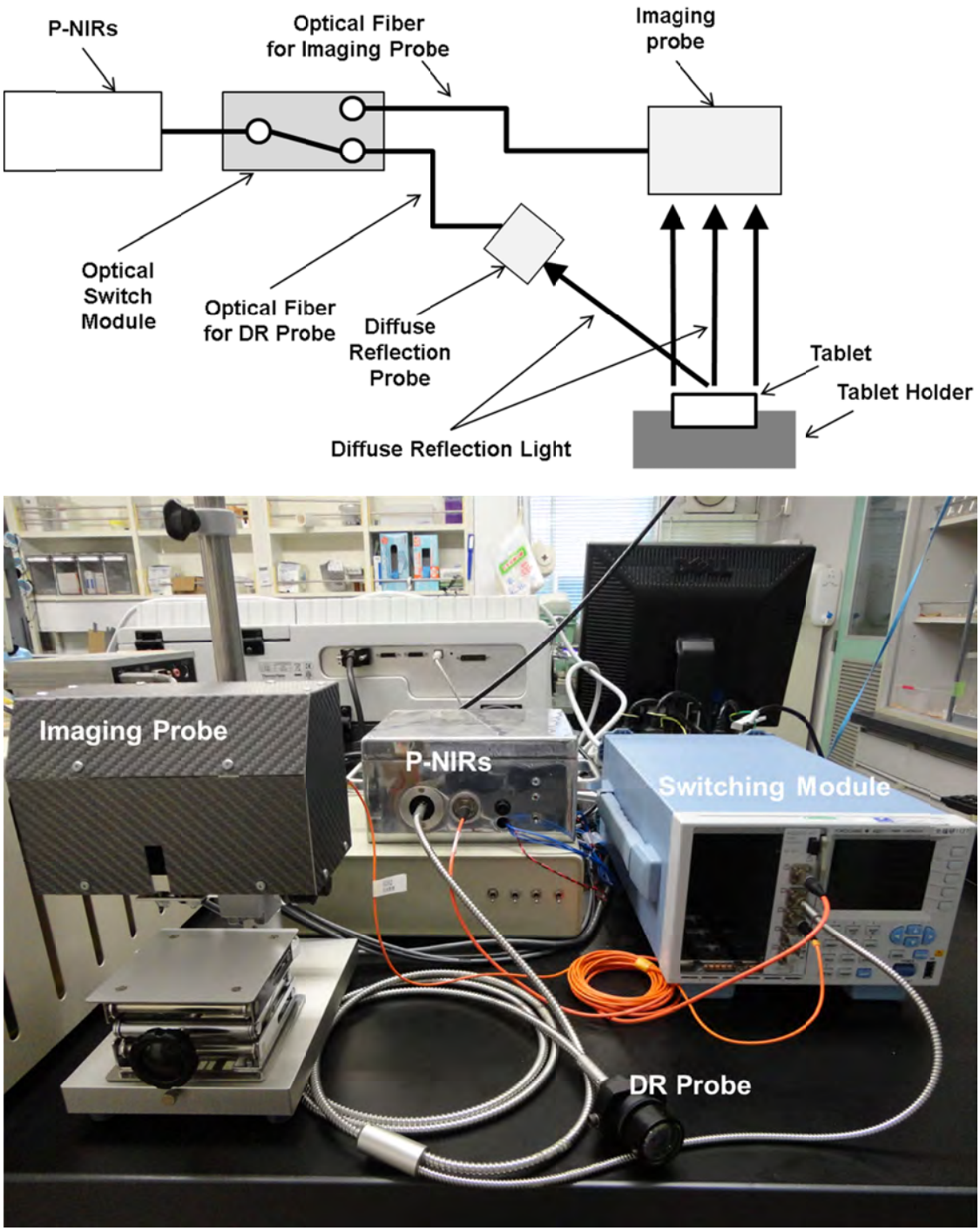

Figure 5-1 A schematic diagram of a NIR spectrometer and related optical system, and a photograph of the same.

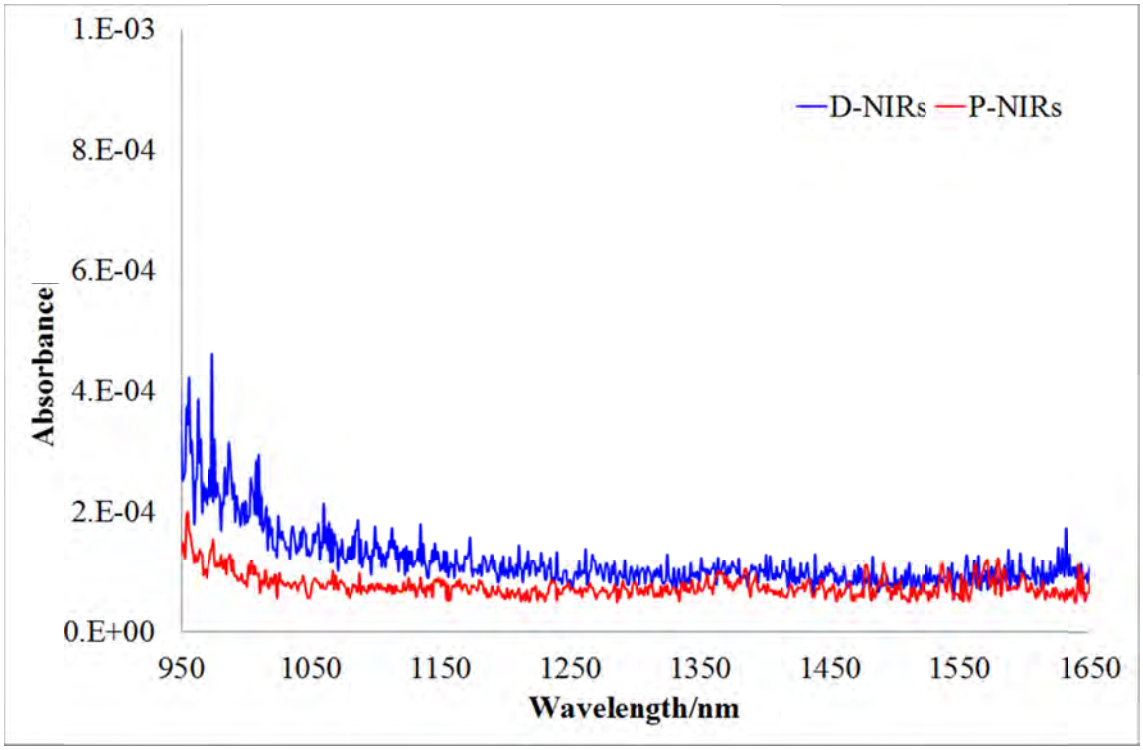

Figure 5-2 NIR imaging spectrum noise (blue) and NIR DR spectrum noise (red) plotted by the optical fiber-type switching module.

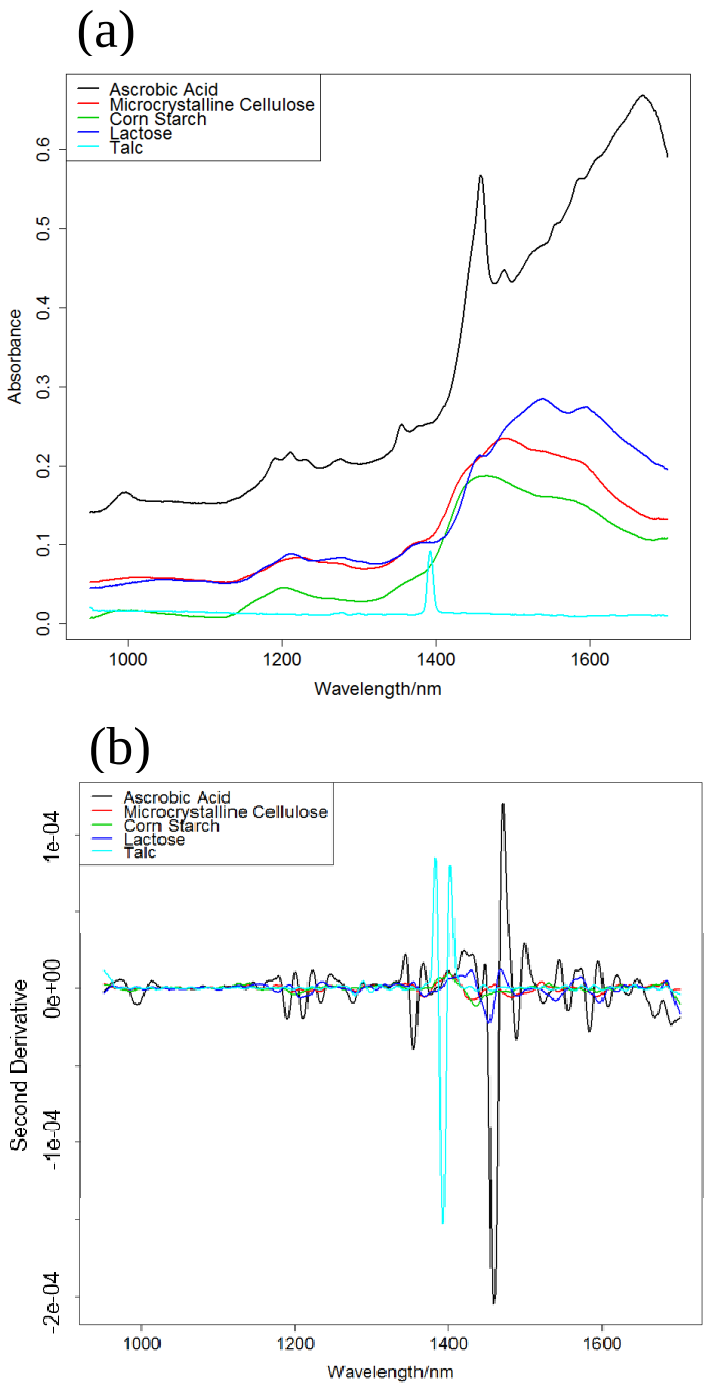

Figure 5-3 (a) DR spectra and (b) their 2nd derivative spectra in the 950-1700 nm region for ascorbic acid, lactose, microcrystal cellulose, starch, and talc

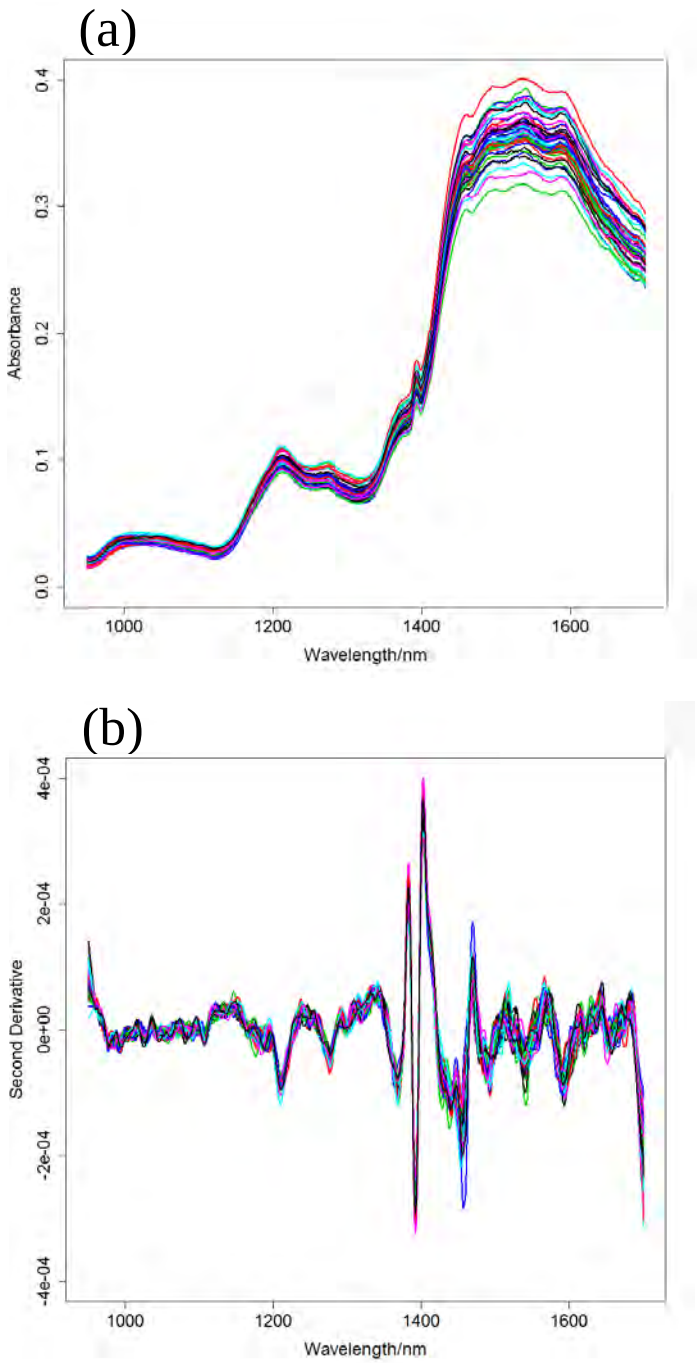

Figure 5-4 (a)DR spectra and (b) their 2nd derivative spectra in the 950-1700 nm region of tablet samples measured by a 1 mm spot size DR probe.

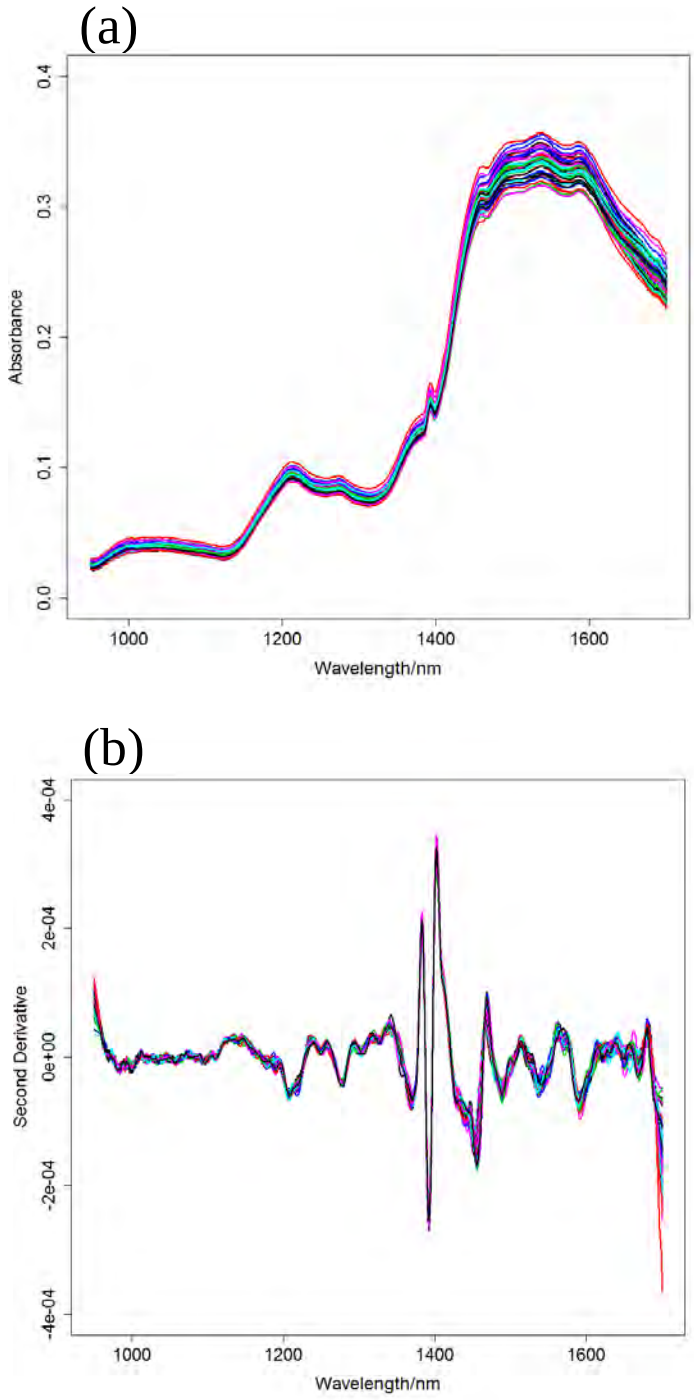

Figure 5-5 (a)DR spectra and (b) their 2nd derivative spectra in the 950-1700 nm region of tablet samples measured by the 5 mm spot size DR probe.

Table 5-1 Analysis conditions and results of PLS.

Model	Wavelength Region [nm]	R^2	RMSE of Calibration [%]
Spot Size 1mm	950-1700	0.73	1.79
Spot Size 5mm	950-1700	0.94	0.86

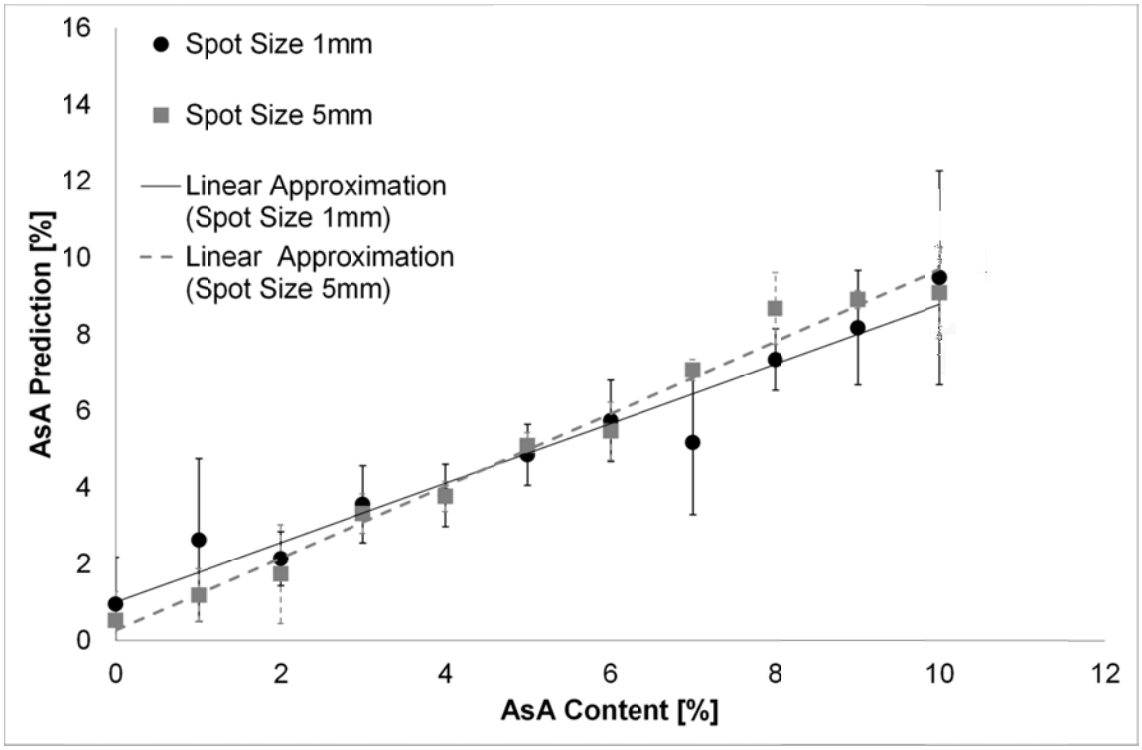

Figure 5-6 The average of the concentrations predicted by PLS regression.

Table 5-2 The standard error of concentration predicted by PLS regression.

	Average Standard Error[%]	
AsA Content [%]	**Spot Size 1mm**	**Spot Size 5mm**
0	1.23	0.76
1	2.13	0.70
2	0.71	1.29
3	1.01	0.51
4	0.82	0.39
5	0.79	0.34
6	1.06	0.76
7	1.88	0.28
8	0.80	0.93
9	1.49	0.23
10	2.79	1.18

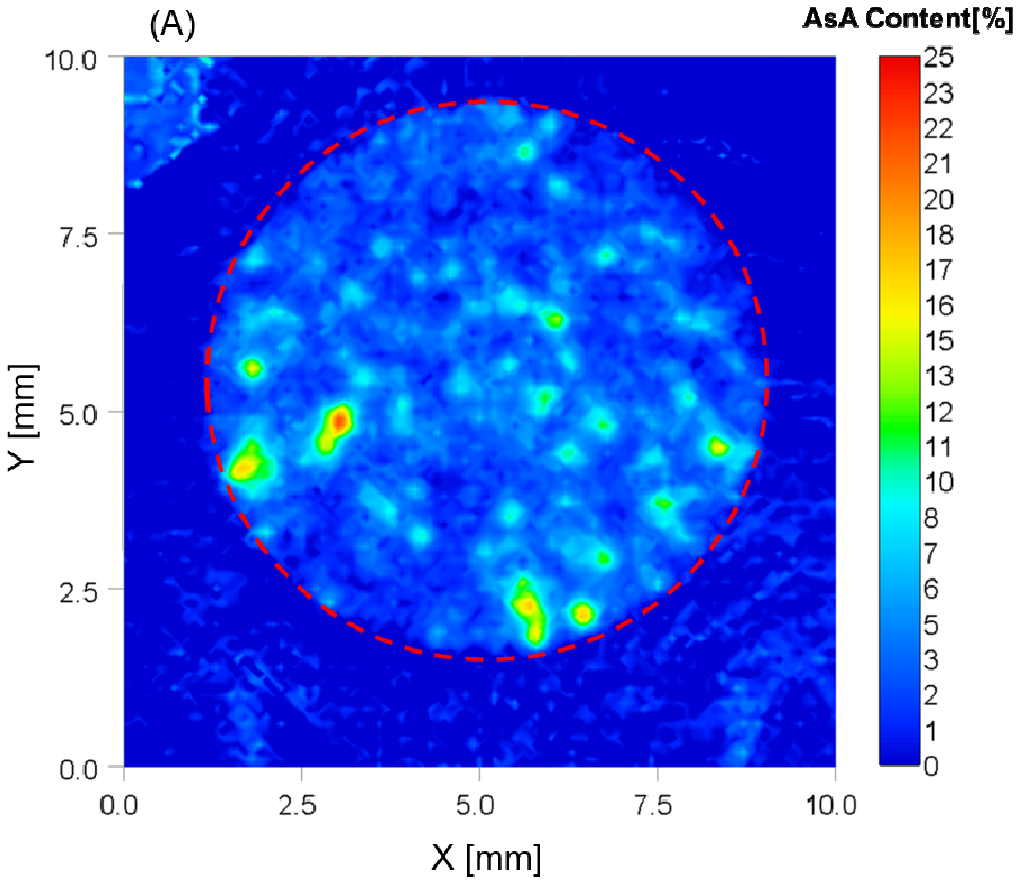
(A)
AsA Content[%]
25
23
22
21
20
18
17
16
15
13
12
11
10
8
7
6
5
3
2
1
0
10.0
7.5
5.0
2.5
0.0
Y [mm]
0.0
2.5
5.0
7.5
10.0
X [mm]

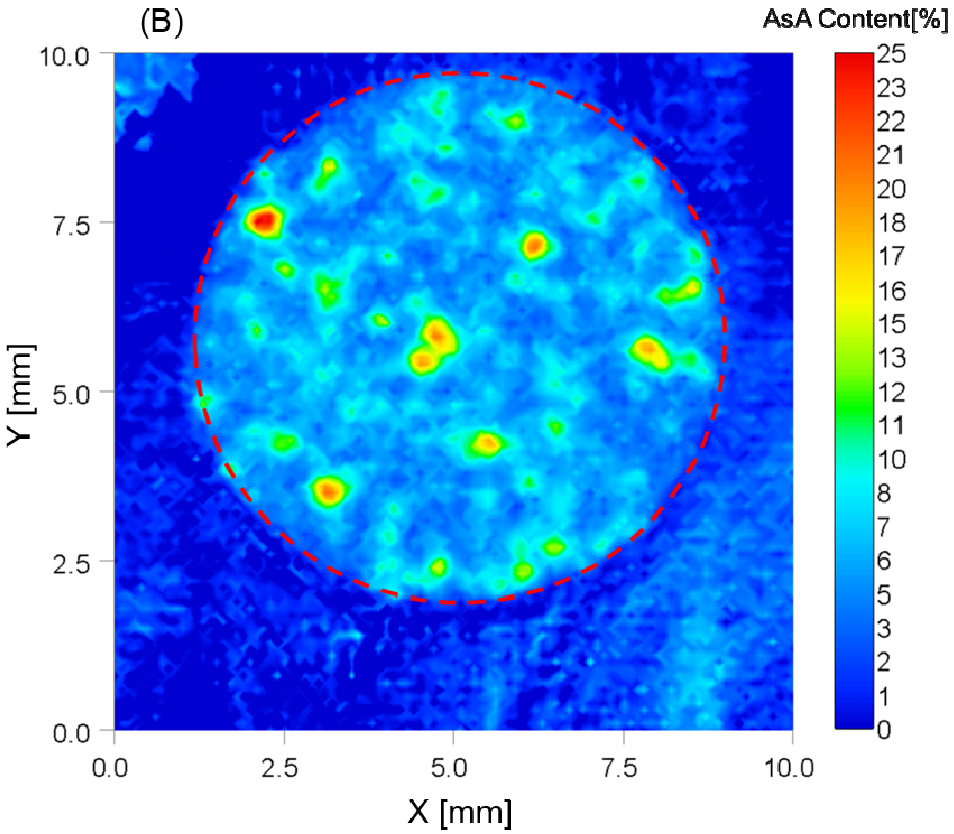
(B)
AsA Content[%]
25
23
22
21
20
18
17
16
15
13
12
11
10
8
7
6
5
3
2
1
0
10.0
7.5
5.0
2.5
0.0
Y [mm]
0.0
2.5
5.0
7.5
10.0
X [mm]

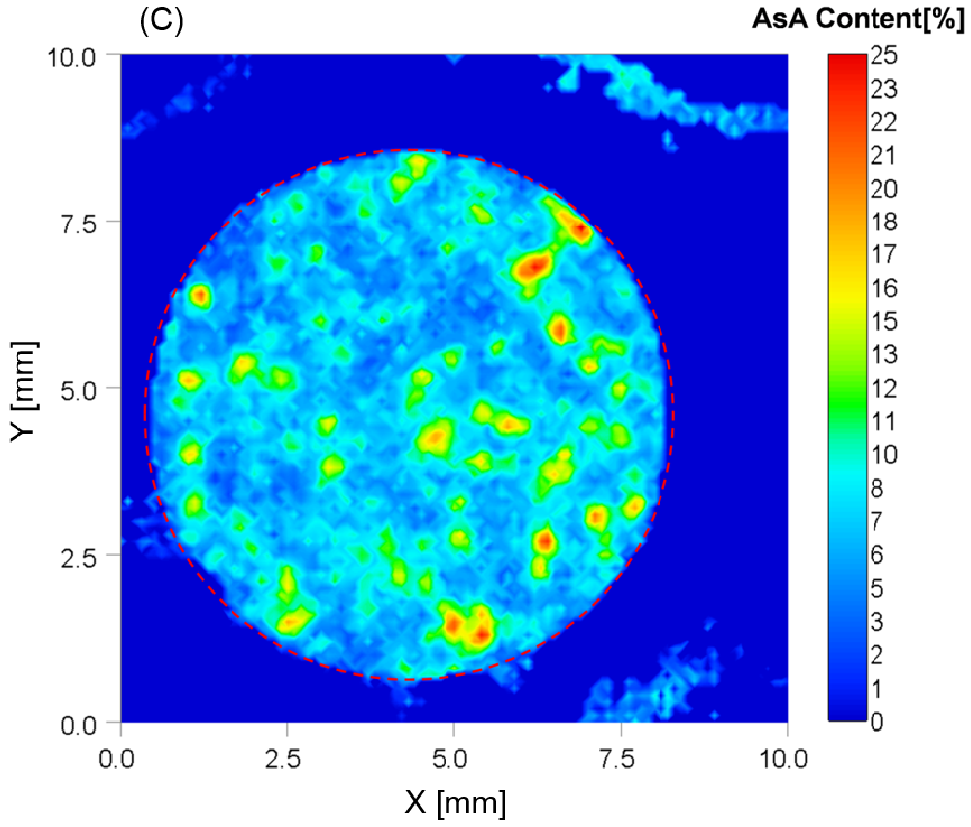

Figure 5-7 NIR images developed by the PLS models using data collected by the spot size 5 mm probe of 10% ascorbic acid. (A) NIR imaging of the AsA 10 wt% tablet; sample 1, (B) NIR imaging of AsA 10 wt% tablet; sample 2, and (C) NIR imaging of AsA 10 wt% tablet; sample 3.

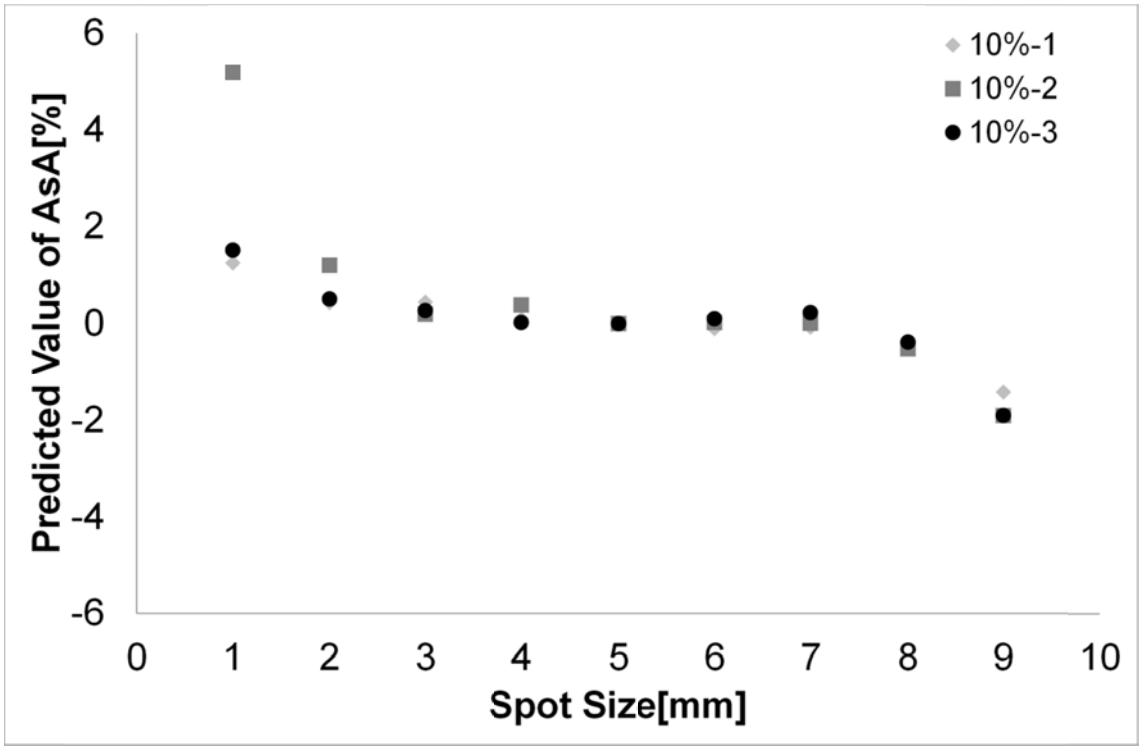

Figure 5-8 The circle spot average AsA concentration value of 1 - 9 mm of the NIR imaging data of each sample was calculated and the difference from each circle spot average AsA concentration value with 5 mm spot average value as a reference plotted.

Conclusion

In this paper, the development of an inline NIR analyzer and portable NIR imaging device having high speed and high wavelength resolution characteristics were described and clarified the fact that these inline analyzers and NIR imaging devices are powerful tools for monitoring the pharmaceutical manufacturing process and for evaluating the quality analysis of pharmaceutical products.

In Chapter 1, by realizing the real-time monitoring of the mixing process using an inline NIR analyzer featuring high speed and high wavelength resolution, equipped with high density and high sensitivity PDA detector developed, the usefulness of the NIR analyzer was demonstrated. In Chapter 2, using the developed NIR analyzer, the possibility of acquiring the tablet transmitted light was proved, an ultra-weak light, in 1 second or less and showed the possibility of realizing the real-time release testing. In Chapters 3 and 4, by developing a portable NIR imaging device, these showed that the temporal change monitoring of the tablet dissolution process and the evaluation of the heterogeneity of mixed samples can be done in two dimensions and prompted the understanding of the physical properties of tablets and powders. In Chapter 5, in order to design the diffuse reflective probe of the inline NIR analyzer appropriately, a

switching system for the diffuse reflective probe and the NIR imaging device was developed, and showed the possibility of optimizing the spot size of the diffuse reflective probe to improve the accuracy of the quantitative analysis of the tablet.

The researches have shown that the developed inline NIR analyzer and the portable NIR imaging device promote scientific understanding of the pharmaceutical manufacturing processes and formulations and in addition, they are tools for realizing adequate quality assurance. Further, the developed NIR analyzer and NIR imaging device have functions such as high speed, high sensitivity, high wavelength resolution, portability and so on that are useful for onsite analysis and hence their applicability to many applications is shown.

Acknowledgements

During the course of the study, I have received a number of fruitful discussion, enlightening comments, and hearty encouragement from many people.

First of all, I wish to express my sincere gratitude to Professor Yukihiro Ozaki (Kwansei Gakuin University) for his continuous instruction, really sincere discussion, helpful advices and encouragements in carrying out this study. I am deeply indebted to Assistant Professor Takuma Genkawa (University of Tsukuba) and Assistant Professor Daitaro Ishikawa (Tohoku University) for precious advices, valuable discussion, and cordial encouragements.

I am very much grateful to Mr. Makoto Komiyama and Mr. Hiroyuki Sugino (Former Yokogawa Electric Corporation), Dr. Mitsuhiro Iga and Mr. Yuma Kitagawa (Yokogawa Electric Corporation) for technical supports and warm encouragement during my work. I am deeply grateful to Dr. Tsuyoshi Abe, Mr. Tsuyoshi Yakihara, Mr. Satoshi Kato, Dr. Hitoshi Hara and Mr. Yoshiaki Tanaka (Yokogawa Electric Corporation) for having given me the chance that I do study vibrational spectroscopy in Yokogawa Electric Corporation.

I would like to thank many other colleagues in Ozaki group of Kwansei Gakuin University and Yokogawa Electric Corporation.

Finally, special thanks are due to Megumi, Haru, Yo and my parents for their support and encouragement.

List of Publications

Original Papers:

[1] K. Murayama, T. Genkawa, D. Ishikawa, M. Komiyama, Y. Ozaki ‘‘A polychoromator-type near-infrared spectrometer with a high-sensitivity and high-resolution photodiode array detector for pharmaceutical process monitoring on the millisecond time scale’’ *Review of Scientific Instruments*, 2013, 84, 023104.

[2] D. Ishikawa, K. Murayama, K. Awa, T. Genkawa, M. Komiyama, S.G. Kazarian, Y. Ozaki ‘‘Application of a newly developed portable NIR imaging device to monitor the dissolution process of tablets’’ *Analytical and Bioanalytical Chemistry*, 2013, 405, 9401-9409.

[3] D. Ishikawa, T. Genkawa, K. Murayama, M. Komiyama, Y. Ozaki ‘‘Feasibility study of diffuse reflectance and transmittance near-infrared spectroscopy for rapid analysis of ascorbic-acid concentration in bilayer tablets using high-speed polychromator-type spectrometer’’ *Journal of Near infrared Spectroscopy*, 2014, 22, 189-197.

[4] K. Murayama, D. Ishikawa, T. Genkawa, H. Sugino, M. Komiyama, Y. Ozaki ‘‘Image Monitoring of Pharmaceutical Blending Processes and the Determination of an End Point by Using a Portable Near-Infrared Imaging Device Based on a Polychromator-Type Near-Infrared Spectrometer with a High-speed and High-Resolution Photo Diode Array Detector’’ *Molecules*, 2015, 20, 4007-4019.

[5] K. Murayama, D. Ishikawa, T. Genkawa, Y. Ozaki ‘‘An application for spot size selection for diffuse-reflectance probe using a rapid switching system between a near-infrared spectrometer and a portable near-infrared imaging system equipped with fiber optics’’ submitted to *Applied Spectroscopy.*

Related Papers:

[1] T. Genkawa, H. Shinzawa, H. Kato, D. Ishikawa, K. Murayama, M. Komiyama, Y. Ozaki, H. Sato ‘‘Baseline Correction of Diffuse Reflection Near-Infrared Spectra Using Searching Region Standard Normal Variate (SRSNV)’’ *Applied Spectroscopy*, 2015, 69, 1432-1441.

[2] 坂本知昭，村山広大，藤巻康人，小金井誠司，北川雅博，小宮山誠，檜山行雄，香取典子，奥田晴宏『高速・高感度分散形近赤外分光器を用いた錠剤中主薬成分の定量と工程内導入への適用性』医薬品医療機器レギュラトリーサイエンス，2014，45，4

[3] 坂本知昭，村山広大，藤巻康人，小金井誠司，北川雅博，小宮山誠，香取典子, 合田幸広『高速 NIR 分光器を活用した錠剤含量分析法』Pharm Tech Japan, 2014, 30, 3, 417-424.

[4] 村山広大，村上譲司『近赤外分光によるイメージング技術』製剤機械技術学会，2016, 25,424-426.

[5] 村山広大，村上譲司『製剤工程のためのインライン分析ツール』製剤機械技術学会，2016, 25,427-432.

Presentation:

[1] K. Murayama, M. Komiyama, T. Genkawa, M. Konta, Y. Ozaki ‘‘Development of a High-speed and High-sensitivity Near-Infrared Spectrometer and short-time transmission measurement of tablets by using it’’ October 17-21, 2010, The 37th Federation of Analytical Chemistry and Spectroscopy Societies, Raleigh, NC, USA.

[2] K. Murayama, M. Komiyama, T. Genkawa, M. Konta, Y. Ozaki ‘‘Comparison of the transmission measurement and the diffuse reflection measurement of tablets by using the high-speed and high-sensitivity Near-Infrared Photo-diode array Spectrometer’’ May 24-26, 2011, International Congress on Analytical Sciences 2011, Kyoto, Japan.

[3] 石川大太郎，村山広大，源川拓磨，小宮山誠，尾崎幸洋『可搬型高速イメージング装置を用いた錠剤の成分分布の解析』日本分析化学会第 60 年会, 2011 年 9 月 16-17 日（名古屋大学，愛知）.

[4] K. Murayama, M. Komiyama, T. Genkawa, M. Konta, Y. Ozaki ‘‘Transmittance and diffuse reflectance measurement of the bi-layered tablets by using the high-speed and high-sensitivity Near-Infrared Photo-diode array Spectrometer’’ October 2-7, 2011, The 38th Federation of Analytical Chemistry and Spectroscopy Societies, Reno, NV, USA.

[5] 村山広大，杉野弘幸，小宮山誠，源川拓磨，石川大太郎，今田三樹子，尾崎

幸洋『高速・高感度近赤外分光分析計を用いた 2 層錠の透過測定』第 27 回近赤外フォーラム，2011 年 11 月 9-11 日（文部科学省研究交流センター，茨城）.

[6] K. Murayama, M. Komiyama, T. Genkawa, D. Ishikawa, Y. Ozaki ‘‘On-line moisture monitoring of the fluidized bed granulation process by using high-speed and highly sensitive Near Infrared Spectrometer’’ January 22-25, 2012, The 26th International Forum and Exhibition Process Analysis and Control, Baltimore, ML, USA.

[7] 村山広大，石川大太郎，源川拓磨，鳥越洋子，小宮山誠，尾崎幸洋『高速・高感度近赤外分光分析計による流動層造粒プロセスのリアルタイムモニタリング』第 72 回分析化学討論会，2012 年 5 月 19-20 日（鹿児島大学，鹿児島）.

[8] 石川大太郎，村山広大，源川拓磨，鳥越洋子，小宮山誠，尾崎幸洋『ポータブル高速近赤外イメージング装置を用いた錠剤のコーティング成分定量と分布解析』第 72 回分析化学討論会，2012 年 5 月 19-20 日（鹿児島大学，鹿児島）.

[9] 石川大太郎，村山広大，源川拓磨，阿波君枝，鳥越洋子，小宮山誠，尾崎幸洋『可搬型高速近赤外イメージングを用いた錠剤の成分分布評価法の提案』日本分析化学会第 61 年会，2012 年 9 月 19-21 日（金沢大学，石川）.

[10] K. Murayama, D. Ishikawa, T. Genkawa, Y. Torigoe, M. Komiyama, Y. Ozaki ‘‘A Study on Penetration depth of Near-Infrared diffuse-reflectance light at bilayer tablets by using a high-spec. NIR photo-diode array spectrometer’’ September 30 - October 5, 2012, SCIX2012, MO, United States.

[11] K. Murayama, T. Nagato, T. Genkawa, D. Ishikawa, H. Sugino, Y. Kitagawa, M. Komiyama, Y. Ozaki ‘‘On-line moisture monitoring of the fluidized bed granulation process by using high-speed and highly sensitive Near Infrared Spectrometer’’ January 22-25, 2013, The 27th International Forum and Exhibition Process Analysis and Control, Baltimore, ML, USA.

[12] 村山広大，源川拓磨，石川大太郎，杉野弘幸，北川雄真，小宮山誠，鳥越洋子，尾崎幸洋『高速・高感度 NIR 分析計を用いた医薬品混合均一性の解析』第 28 回近赤外フォーラム，2013 年 3 月 6-9 日（沖縄県男女共同参画センターてぃるる，沖縄）.

[13] K. Murayama, T. Sakamoto, Y. Fujimaki, M. Kitagawa, M. Komiyama, S. Koganei, Y. Hiyama, N. Katori, H. Okuda ‘‘Transmission measurement of tablet in very short-time by using high-speed and high-sensitive Near Infrared spectrometer’’ June 2-7, 2013, ICNIRS, La Grande-Motte, France.

[14] K. Murayama, T. Genkawa, D. Ishikawa, H. Sugino, M. Komiyama, Y. Ozaki ‘‘On-line measurement of pharmaceutical blending process using high-speed, high-sensitivity and compact Near Infrared spectrometer’’ August 25-30, 2013, The 7h International Conference on Advanced Vibrational Spectroscopy, Kobe, Japan.

[15] K. Murayama, T. Genkawa, D. Ishikawa, H. Sugino, M. Komiyama, Y. Ozaki ‘‘Process control and endpoint detection of a fluid bed granulation process using high-speed, high-sensitivity and compact Near Infrared spectrometer’’ August 25-30, 2013, The 7h International Conference on Advanced Vibrational Spectroscopy, Kobe, Japan.

[16] 石川大太郎，村山広大，源川拓磨，杉野弘幸，北川雄真，小宮山誠，尾崎幸洋『可搬型高速イメージング装置(D-NIRs)を用いた混合過程における錠剤成分の分布解析』日本分析化学会第 62 年会, 2013 年 9 月 10-12 日（近畿大学, 大阪）.

[17] 石川大太郎，村山広大，源川拓磨，杉野弘幸，小宮山誠，尾崎幸洋『近赤外イメージングによる錠剤成分の不均一性評価の研究』第 29 回近赤外フォーラム，2013 年 11 月 27-29 日（文部科学省研究交流センター，茨城）.

[18] 加藤秀明，源川拓磨，石川大太郎，トファエルアハマド，野口良造，瀧川具弘，村山広大，杉野弘幸，小宮山誠，尾崎幸洋『近赤外分光法用いたアイスクリーム融解プロセスにおける微細構造の推定』第 29 回近赤外フォーラム，2013 年 11 月 27-29 日（文部科学省研究交流センター，茨城）.

[19] 源川拓磨，森下美咲，石川大太郎，トファエルアハマド，野口良造，瀧川具弘，村山広大，杉野弘幸，小宮山誠，尾崎幸洋『近赤外分光法を用いたプレミックス粉の混合モニタリングと混合挙動の解析』第 73 回農業食料工学会年次大会，2014 年 5 月 16-19 日（琉球大学，沖縄）.

[20] 石川大太郎，村山広大，源川拓磨，小宮山誠，尾崎幸洋『可搬型近赤外イメージング装置による錠剤成分不均一性評価法開発に関する研究』第 74 回分析化学討論会，2014 年 5 月 24-25 日（日本大学，福島）.

[21] T. Genkawa, D. Ishikawa, K. Murayama, T. Ahamed, R. Noguchi, T. Takigawa, H.

Sugino, M Komiyama, Y. Ozaki ‘‘Mixing behavior of flour and sucrose in a cutter mixer monitored with a high-speed NIR spectrometer’’ June 17-20, 2014, The 4th Asian NIR Symposium, Daegu, Korea.

[22] K. Murayama, D. Ishikawa, T. Genkawa, Y. Ozaki ‘‘Optimization of analytical tools for the pharmaceutical tablets by NIR Probe and NIR imaging switching system’’ December 4-6, 2016, The 4th Japan-Taiwan Medical Spectroscopy International Symposium 2016, Awaji, Japan.

[23] 村山広大『近赤外分光法・イメージング装置の開発と産業プロセス応用の研究』第 33 回近赤外フォーラム，2017 年 11 月 15-17 日（筑波大学，茨城）. 発表予定

Patents:

[1] 分光分析装置, 横河電機株式会社, 2014 年 11 月 6 日，特願 2013-085847, 2013 年 4 月 16 日，特開 2014-209063, G01N 21/05

[2] 分光装置, 横河電機株式会社, 2012 年 8 月 23 日，特願 2011-018170, 2011 年 1 月 31 日，特開 2012-159353, G01J 3/36

[3] 分光器, 横河電機株式会社, 2012 年 1 月 5 日，特願 2010-135014, 2010 年 6 月 14 日，特開 2012-002529, G01J 3/18

[4] 光分析装置, 横河電機株式会社, 2011 年 5 月 6 日，特願 2009-241018, 2009 年 10 月 20 日，特開 2011-089772, G01N 21/27

[5] 光検出器, 横河電機株式会社, 2011 年 4 月 14 日，特願 2009-226851, 2009 年 9 月 30 日，特開 2011-075399, G01J 1/02

[6] 分光分析装置, 横河電機株式会社, 2011 年 3 月 17 日，特願 2009-199939, 2009 年 8 月 31 日，特開 2011-052996, G01N 21/35

[7] 光照射検出器, 横河電機株式会社, 2010 年 10 月 7 日，特願 2009-071633, 2009 年 3 月 24 日，特開 2010-223773, G01N 21/27

[8] 光検出装置, 横河電機株式会社, 2010 年 5 月 27 日，特願 2008-288525, 2008 年 11 月 11 日，特開 2010-117146, G01N 21/27

[9] 電源制御装置, 横河電機株式会社, 2009 年 10 月 15 日，特願 2008-083616, 2008 年 3 月 27 日，特開 2009-240078, H02J 7/00

[10]センサアレイ読み出し回路, 横河電機株式会社, 2009 年 7 月 30 日, 特願 2008-007216, 2008 年 1 月 16 日, 特開 2009-171241, H04N 5/335

[11]分光器, 横河電機株式会社, 2009 年 6 月 18 日, 特願 2007-308135, 2007 年 11 月 29 日, 特開 2009-133650, G01J 3/36

[12]近赤外分析計, 横河電機株式会社, 2009 年 6 月 11 日, 特願 2007-303237, 2007 年 11 月 22 日, 特開 2009-128175, G01N 21/35

[13]回折格子及びこれを用いた分光装置, 横河電機株式会社, 2009 年 4 月 30 日, 特願 2007-260023, 2007 年 10 月 3 日, 特開 2009-092680, G02B 5/18

[14]照射集光装置, 横河電機株式会社, 2009 年 3 月 26 日, 特願 2007-231223, 2007 年 9 月 6 日, 特開 2009-063407, G01N 21/27

[15]照射集光装置, 横河電機株式会社, 2009 年 3 月 26 日, 特願 2007-231222, 2007 年 9 月 6 日, 特開 2009-063406, G01K 11/12

[16]光スイッチ装置, 横河電機株式会社, 2008 年 6 月 26 日, 特願 2006-328927, 2006 年 12 月 6 日, 特開 2008-145459, G02B 26/08

[17]回折光学素子及び光スペクトラムアナライザ, 横河電機株式会社, 2008 年 5 月 29 日, 特願 2006-307786, 2006 年 11 月 14 日, 特開 2008-122770, G02B 5/18

Awards:

[1] K. Murayama, M. Komiyama, T. Genkawa, M. Konta, Y. Ozaki ‘‘Comparison of the transmission measurement and the diffuse reflection measurement of tablets by using the high-speed and high-sensitivity Near-Infrared Photo-diode array Spectrometer’’ May 24-26, 2011, International Congress on Analytical Sciences 2011, Kyoto, Japan., Wiley Psoter Presentation Award

[2] 村山広大『近赤外分光法・イメージング装置の開発と産業プロセス応用の研究』第 33 回近赤外フォーラム，2017 年 11 月 15-17 日（筑波大学，茨城）. NIR Advance Award